

**Coupling between opioid receptors and potassium channels
in pain reduction: relevance for species differences
and efficacy**

Dissertation zur Erlangung des akademischen Grades des
Doktors der Naturwissenschaft (Dr. rer. nat.)

eingereicht im Fachbereich der Biologie, Chemie, Pharmazie
der Freien Universität Berlin

vorgelegt von
Dinah Nockemann
aus Hattingen

März 2012

Die vorliegende Arbeit wurde in der Forschungsabteilung für Anästhesiologie und operative Intensivmedizin an der Charité, Campus Benjamin Franklin, Berlin durchgeführt. Die Dissertation wurde von Juli 2007 bis März 2012 unter Leitung von Prof. Dr. Christoph Stein angefertigt.

1. Gutachter: Prof. Dr. med. Christoph Stein; Charité Berlin, Klinik für Anästhesiologie mit Schwerpunkt operative Intensivmedizin
2. Gutachter: Prof. Dr. Petra Knaus; Freie Universität Berlin, Institut für Chemie und Biochemie

Disputation am 12.04.2013

Danksagung

Ich möchte mich ganz herzlich bei Herrn Prof. Dr. Christoph Stein und Dr. Paul Heppenstall für das interessante Thema und die tolle Betreuung bedanken. Die regelmäßigen Gespräche mit Prof. Stein sowie Pauls Ideen und Optimismus waren stets hilfreich und motivierend. Beide haben mich während meiner Promotion immer unterstützt und sind mir mit Rat und Tat zur Seite gestanden. Zusätzlich möchte ich mich besonders bei Prof. Dr. Petra Knaus bedanken, zum einen für die Übernahme des Gutachtens und zum anderen für die regelmäßige Organisation der externen Doktoranden-Symposien, die einem die Möglichkeit boten, sich auch fächerübergreifend mit anderen Studenten auszutauschen.

Unterstützt wurde meine Doktorarbeit durch ein Stipendium im Rahmen des Graduiertenkollegs „The impact of inflammation on nervous system function“ (GRK 1258).

Ein großes Dankeschön geht an die Mitarbeiter der AG Stein und insbesondere an das „upper office“, das sich dann nach dem Umzug leider etwas verkleinert hat. Ich hatte eine tolle Zeit. Es war eine Freude mit euch zu arbeiten. Besonders danke ich Viola, Yvonne, Melli, Morgane und Julia für eure nie endende Hilfsbereitschaft und die tollen wissenschaftlichen und privaten Gespräche. Ich möchte mich außerdem bei Dominika Labuz für die geduldige und ausgezeichnete Einführung in die Verhaltensexperimente bedanken, sowie für ihre Hilfe bei der Durchführung von einem Teil der Verhaltensexperimente. Sandra, vielen Dank für deine Unterstützung und Gesellschaft bei meinen Laborbesuchen in Monterotondo und deine geduldige Hilfe mit den römischen öffentlichen Verkehrsmitteln.

Für die emotionale Unterstützung waren in erster Linie Steffen und meine tollen Freunde zuständig. Danke für euren aufmunternden Optimismus. Und nicht zuletzt danke ich meiner Familie, die in jeglicher Hinsicht die Grundsteine für meinen Weg gelegt haben. Danke für Eure nie endende Unterstützung und den bestärkenden Zuspruch.

Table of contents	I
Abbreviations	V
1 Introduction	1
1.1 Pain and nociception	1
1.1.1 Primary sensory afferents	2
1.1.2 Molecular characteristics of nociceptors	3
1.1.3 Plasticity of nociceptors	5
1.2 Inhibition of pain by opioids	6
1.2.1 Opioid receptors in the central and peripheral nervous system	6
1.2.2 Molecular mechanisms of opioid-induced antinociception	7
1.3 The K_{ir} channel family	9
1.3.1 Structure and function of GIRK channels	10
1.3.2 The role of GIRK channels in opioid antinociception	12
1.4 Species differences in opioid antinociception-a possible role of GIRK channels	13
1.5 Objectives	14
2 Materials and methods	16
2.1 Animals	16
2.2 Materials	16
2.2.1 Bacteria and cell lines	16
2.2.2 Antibiotics	17
2.2.3 Oligonucleotides	17
2.2.4 Plasmids and constructs	18
2.2.5 Enzymes	19
2.2.6 Antibodies	19
2.2.7 Pharmacological agents	20
2.2.8 Chemicals, reagents and media	20
2.2.9 Kits and reaction systems	22
2.2.10 Buffers and solutions	22
2.2.11 Consumable materials	24
2.2.12 Technical equipment	25
2.2.13 Software	27

2.3 Methods	28
2.3.1 Molecular biology	28
2.3.1.1 DNA restriction	28
2.3.1.2 Vector dephosphorylation	28
2.3.1.3 Ligation	29
2.3.1.4 Transformation	29
2.3.1.5 Isolation of plasmids from bacteria	30
2.3.1.6 Determination of nucleic acid concentration	30
2.3.1.7 Amplification of DNA fragments	30
2.3.1.8 PCR product purification and analysis	31
2.3.1.9 Total RNA preparation	32
2.3.1.10 Reverse-transcription polymerase chain reaction (RT-PCR)	32
2.3.1.11 Quantitative real time PCR (qRT-PCR)	32
2.3.2 Generation of BAC transgenic mice	34
2.3.2.1 BAC DNA purification for transgenesis	35
2.3.2.2 Extraction of genomic DNA from mouse tails	35
2.3.2.3 Genotyping of transgenic mice	36
2.3.2.4 Determination of transgenic copy number	37
2.3.2.5 Southern blot	37
2.3.3 Tissue preparation for immunohistochemistry and DRG culture	38
2.3.4 Cell culture methods	39
2.3.4.1 Transfection	39
2.3.4.2 AAV infection of DRG neurons	40
2.3.4.3 Primary mouse DRG culture	40
2.3.4.4 Primary rat DRG culture	40
2.3.5 Immunohistochemistry	41
2.3.6 Immunocytochemistry	43
2.3.7 Western blot	43
2.3.8 Electrophysiology	44
2.3.9 FluxOR™ potassium ion channel assay	45
2.3.10 Behavior	46
2.3.10.1 Thermal nociception	46
2.3.10.2 Mechanical nociception	47

2.3.10.3 Induction of inflammation	47
2.3.11 Statistical data analysis	48
3 Results	49
3.1 GIRK channel expression in peripheral sensory neurons	49
3.1.1 GIRK channel mRNA expression in DRG neurons of mice and rats	49
3.1.2 GIRK channel protein expression in mouse and rat	51
3.2 Coupling of GIRK channels and mu-opioid receptors in rat and mouse	54
DRG neurons	
3.2.1 Establishment of GIRK channel whole cell patch-clamp recordings in DRG Neurons	54
3.2.2 No functional coupling of GIRK channels and mu-opioid receptors in normal mouse DRG neurons	56
3.2.3 GIRK channels are coupled to mu-opioid receptors in rat DRG neurons	59
3.3 Generation of BAC transgenic GIRK2 mice	60
3.3.1 Expression of GIRK2 in Na _v 1.8-GIRK2 mice	63
3.3.2 Functional characterization of Na _v 1.8-GIRK2 mice	67
3.3.2.1 Analysis of opioid receptor and GIRK channel coupling in Na _v 1.8-GIRK2 mice	67
3.3.3 Behavioral analysis of Na _v 1.8-GIRK2 mice	70
4 Discussion	75
4.1 Functional GIRK channel expression in peripheral sensory neurons of rats indicates a role of GIRK channels in peripheral opioid antinociception in rats but not in mice	76
4.2 A genetic approach to target the nociceptive pathway by using BAC transgenesis	79
4.2.1 Inflammation enhanced DAMGO induced antinociception in Na _v 1.8-GIRK mice	81
4.2.2 Unidirectional protein transport of Flag-GIRK2 in peripheral sensory neurons of Na _v 1.8-GIRK2 mice	83
4.3 Do GIRK channels play a role in human peripheral opioid analgesia?	84
4.4 The choice of species for preclinical studies	85
4.5 GIRK channels as a possible therapeutic target	86

4.6 Conclusion and outlook	87
5 Summary/ Zusammenfassung	89
6 References	92
7 Appendix	104
7.1 Negative controls of immunostaining	104
8 Curriculum Vitae	106
9 Publications and conferences	107
10 Erklärung	108

Abbreviations

AAV	adeno-associated virus
AM	acetoxymethyl
AMV	avian myeloblastosis virus
ANOVA	analysis of variance
ATP	adenosine triphosphate
bp	base pairs
Ba ²⁺	barium
BAC	bacterial artificial chromosome
BSA	bovine serum albumin
cAMP	cyclic adenosine monophosphate
<i>C. elegans</i>	<i>Caenorhabditis elegans</i>
cDNA	complementary desoxyribonucleic acid
CFA	Complete Freund's Adjuvant
CGRP	calcitonin gene-related peptide
CNS	central nervous system
C-terminus	carboxy-terminus
DAB	3,3'-Diaminobenzidine
DAMGO	D-Ala ² , N-MePhe ⁴ , Gly-ol-enkephalin
DEG/ENaC	degenerin/epithelial sodium channel
ddH ₂ O	double distilled water
DMEM	Dulbecco's Modified Eagle's Medium
DMSO	dimethyl sulfoxide
DNA	desoxyribonucleic acid
dNTP	desoxyribonucleosidtriphosphate
DPDPE	D-Pen ² ,d-Pen ⁵ -enkephalin
DRG	dorsal root ganglion
Ds	double-stranded
ECL	enhanced chemiluminescence
<i>E. coli</i>	<i>Escherichia coli</i>
EDTA	ethylene-diamine-tetra-acetic acid
EGTA	ethylene glycol-bis (2-amino-ethyl ether)N,N,N',N'-tetra acetic acid
ER	endoplasmic reticulum

ET	endothelin
FBS	fetal bovine serum
FITC	fluorescein isothiocyanate
FRT	flippase recognition target
Fw	forward
GABA _B	gamma-aminobutyric acid B receptor
GAPDH	Glycerinaldehyd-3-phosphat-Dehydrogenase
GDP	guanosine diphosphate
GIRK	g protein-gated inwardly rectifying K ⁺
GPCR	G-protein coupled receptor
GTP	guanosine triphosphate
HEK293	human embryonic kidney cells 293
HEPES	4-2-hydroxyethyl-1-piperazineethanesulfonic acid
HSV	herpes simplex virus
I	current
I _A	fast inactivating K ⁺ current
I _D	slow inactivating K ⁺ current
I _K	dominant sustained K ⁺ current
IB4	isolectin B4
K _{2P}	two-pore K ⁺ channels
kb	kilo base pairs
kDA	kilo Dalton
K _{ir}	inward rectifier K ⁺ channels
K _v	voltage-gated K ⁺ channels
LB	Luria-Bertani
mRNA	messenger RNA
n	number
Na _v	voltage-gated sodium channels
Neo	neomycin
NF	neurofilaments
NGF	nerve growth factor
NK	neurokinin
NLXM	naloxone methiodide
NMDA	<i>N</i> -Methyl-D-aspartic acid

N-terminus	amino-terminus
P ₂ X	purinergic receptors
PAG	periaqueductal gray
PB	phosphate buffer
PBS	phosphate buffered saline
PCR	polymerase chain reaction
PENK	preproenkephalin
PFA	paraformaldehyde
PNS	peripheral nervous system
qRT-PCR	quantitative real time PCR
RNA	ribonucleic acid
rpm	revolutions per minute
RT	room temperature
RT-PCR	reverse transcription PCR
Rv	reverse
SDS	sodium dodecyl sulphate
s.e.m	standard error of the mean
TG	trigeminal ganglion
TM	transmembrane (domain)
TNF α	tumor necrosis factor alpha
TRIS	tris (hydroxymethyl) amino-methane
TrkA	tyrosine kinase receptor, type 1
TRPA1	transient receptor potential ankyrin 1
TRPV1	transient receptor potential vanilloid 1
TTX	tetrodotoxin
Tween®	polyoxyethylene-sorbitan monolaurate
UV	ultraviolet
U-50488	<i>trans</i> -(-)-3,4-Dichloro- <i>N</i> -methyl- <i>N</i> -[2-(1-pyrrolidinyl) cyclohexyl] benzeneacetamide
YFP	yellow fluorescent protein
X-Gal	5-Brom-4-chlor-3-indoxyl- β -D-galactopyranosid
5HT1A	5-hydroxytryptamine (serotonin) receptor 1A

1 Introduction

1.1 Pain and nociception

The International Association for the Study of Pain (IASP) defines pain as “an unpleasant sensory and emotional experience associated with actual or potential tissue damage or described in terms of such damage”. Pain serves normally as a warning system which protects our body from severe tissue damage (Loeser and Treede, 2008). If pain transforms to a chronic state it loses its protective role and leads to allodynia or hyperalgesia (among other somatic and non-somatic consequences), where a usually innocuous stimulus (warmth or light touch) or a lowered threshold to a painful stimulus causes severe pain (Basbaum et al., 2009). The detection of pain-producing stimuli is a process called nociception and can be regarded as a sensory system like vision or olfaction. A subpopulation of peripheral nerve fibers is thought to be responsible for the detection of painful stimuli and their transformation into an electrical signal. These so-called nociceptors can be distinguished from other sensory nerve fibers based on their activation threshold and sensitivity (Julius and Basbaum, 2001). They innervate skin, muscle, joints and internal organs and transmit sensory information from free nerve endings to the spinal cord (illustrated in figure 1). From there, nociceptive signals travel to the brain via secondary neurons. Nociception and temperature sensation is thought to be captured by sensory neurons with free nerve endings, whereas touch and proprioception are transmitted by sensory neurons with encapsulated terminals (Lumpkin and Caterina, 2007; Scholz and Woolf, 2002). Primary sensory neurons are polymodal. They are excited by several distinct stimuli like intense pressure, noxious heat or irritant chemicals (Julius and Basbaum, 2001). Nociceptors are pseudounipolar, which means they have a peripheral terminal that innervates the target organ and a central axonal branch that projects to the dorsal horn laminae I, II and V of the spinal cord (or to the brainstem in case of trigeminal neurons). The somata of nociceptors innervating skin, muscle and viscera of the body are located in the dorsal root ganglia (DRG). Somata of nociceptors innervating the face are located in the trigeminal ganglia (TG). Peripheral sensory neurons can transport proteins (synthesized in the DRG or TG) to both central and peripheral terminals (Basbaum et al., 2009).

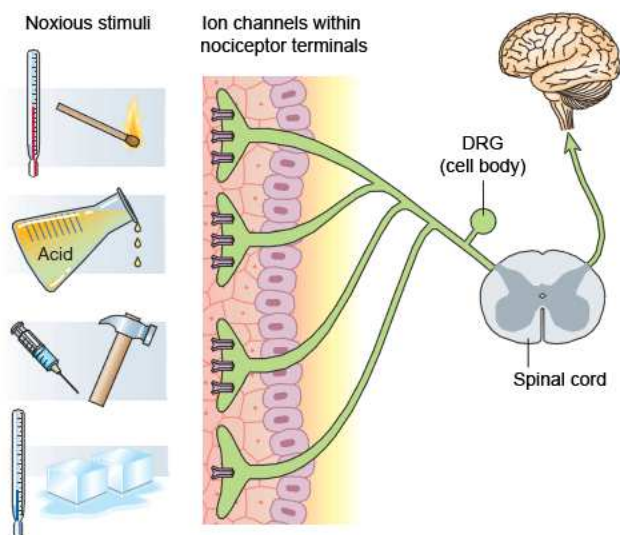


Figure 1 Peripheral terminals of nociceptors innervate the skin. Noxious stimuli such as temperature, chemicals or mechanical force activate nociceptors which transduce the noxious stimulus into an electrical signal through ion channels located in the peripheral terminals. The signal is conducted along the axon to the cell body, within the DRG, and then to the central terminal located in the dorsal horn of the spinal cord. After transmission along the central pathways by secondary neurons to higher brain regions and integration of other functions or processes (e.g. memory, emotions) the signal is perceived as pain (modified from Scholz and Woolf, 2002).

1.1.1 Primary sensory afferents

Cutaneous primary sensory neurons in normal (healthy) tissue can be categorized into three main groups, A α/β -, A δ -, and C-fibers, based on their degree of myelination, conduction velocity and sensory modality (Lumpkin and Caterina, 2007; Millan, 1999). A β -fibers (mechanoreceptors) transmit innocuous stimuli like light touch and pressure whereas A α -fibers provide information about limb positions (proprioception). Both fiber types are highly myelinated, conduct stimuli with >10 m/s in mice and do not normally contribute to nociception (Koltzenburg et al., 1997). Nociceptive information is normally received and transduced by two groups of primary sensory neurons, the unmyelinated and slowly conducting C-fibers (<1 m/s) and the thinly myelinated and more rapidly conducting A δ -fibers (1-10 m/s) (Julius and Basbaum, 2001; Koltzenburg et al., 1997). The cell soma size of primary sensory neurons correlates with the degree of myelination. Thickly myelinated, fast

conducting A α /B-fibers have a large soma diameter (30-50 μm) whereas nociceptors are smaller with a diameter of 15-30 μm (Harper and Lawson, 1985; Lawson and Waddell, 1991). All C-fibers are nociceptors and respond to noxious thermal and mechanical stimuli as well as to cooling. Another population of C-fibers is normally mechanically insensitive and solely responsive to noxious heat. They are called “silent” nociceptors and can only be activated when sensitized by tissue injury (Basbaum et al., 2009; Julius and Basbaum, 2001).

1.1.2 Molecular characteristics of nociceptors

Based on the expression of different markers, ion channels and receptors we can divide unmyelinated C-fibers into two broad classes, the so-called peptidergic and non-peptidergic nociceptors. The non-peptidergic population expresses proteins and lipids with α -D-galactosyl-residues which are recognized by the IsolectinB4. This group also expresses the c-Ret neurotrophin receptor as well as a subtype of ATP-gated ion channels (P2X₃ receptors). The second group is mostly designated as IB4-. This population produces peptide neurotransmitters like substance P, and calcitonin-gene related peptide (CGRP) and expresses the high-affinity tyrosine kinase receptor TrkA, the receptor for nerve growth factor (NGF) (Basbaum et al., 2009; Julius and Basbaum, 2001; Stucky and Lewin, 1999). Other markers are available to define additional subgroups.

The activation of nociceptors and the transduction of noxious stimuli requires depolarization of the peripheral terminals to generate action potentials which are then conducted along the axon to synapses in the dorsal horn. A variety of voltage-gated ion channels are responsible for these actions (see figure 2). To cause a shift of the membrane potential in the more positive direction (depolarization) sodium (Na^+) and calcium (Ca^{2+}) ions need to flow into the cell along their electrochemical gradient. In contrast, potassium (K^+) channels close during depolarization because the electrochemical gradient for potassium is more negative than the resting potential (Dubin and Patapoutian, 2010).

Two tetrodotoxin (TTX)-insensitive voltage-gated sodium channels ($\text{Na}_v1.8$ and $\text{Na}_v1.9$) mainly contribute to action potential generation in a subpopulation of sensory neurons and are involved in nociception. Deletion of the *Scn10a* gene encoding for $\text{Na}_v1.8$ in mice changed the sensitivity to innocuous or noxious heat, to mechanical stimuli (Akopian et al., 1999) and altered the sensitivity to cold (Zimmermann et al., 2007). Peripheral sensory neurons also express voltage-gated sodium channels that can be blocked by nanomolar concentrations of

TTX. One of these channels ($\text{Na}_v1.7$) has been linked to different pain syndromes in humans. Patients with a loss-of function mutation within its gene claimed to feel less pain while gain-of-function mutations led to severe pain (Basbaum et al., 2009; Cox et al., 2006; Dib-Hajj et al., 2008).

A variety of voltage-gated calcium channels contribute to the excitability of nociceptors. The activation of L-, N-, and P/Q-type Ca^{2+} channels also causes the release of the pronociceptive and proinflammatory peptides substance P and CGRP at the central and peripheral terminals. N- and P/Q-type Ca^{2+} channels can be inhibited by activation of co-expressed opioid receptors. This reduces both the Ca^{2+} influx and the release of the neuropeptides, leading to an attenuation of the excitability of the peripheral sensory neurons and to reduced neurotransmission at the central terminals (Busch-Dienstfertig and Stein, 2010; Heinke et al., 2011).

In contrast to the central nervous system (CNS), the role of potassium channels in peripheral sensory neurons is not well understood. Basically three classes of K^+ currents can be recorded from DRG neurons: fast inactivating (I_A), slow inactivating (I_D) and dominant sustained (I_K). DRG neurons express a variety of voltage-gated K^+ channels (K_v channels). The expression of some is decreased in injured tissue (inflammation), leading to increased excitability of the cell since K^+ channel activation hyperpolarizes the membrane (Lee et al., 2005; Takeda et al., 2011).

Ligand-gated ion channels also contribute to transmission of heat-, cold-, chemical-, and mechanical stimuli (see figure 2). The respective composition of ion channels together with a number of receptors and molecular markers leads to the unique phenotype of peripheral sensory neurons.

Since it is rather difficult to gain experimental access to the nociceptor terminals, the function of peripheral sensory neurons has been studied mostly at the cell body using neuronal cultures. Different morphology and electrical characteristics makes it possible to distinguish between A- and C-fibers. Nociceptors have a small cell body and typically exhibit a shoulder or inflection on the falling phase of action potentials. Besides some minor differences in protein expression, cultured peripheral sensory neurons show the same electrophysiological properties *in vitro* and *in vivo* (Gold et al., 1996).

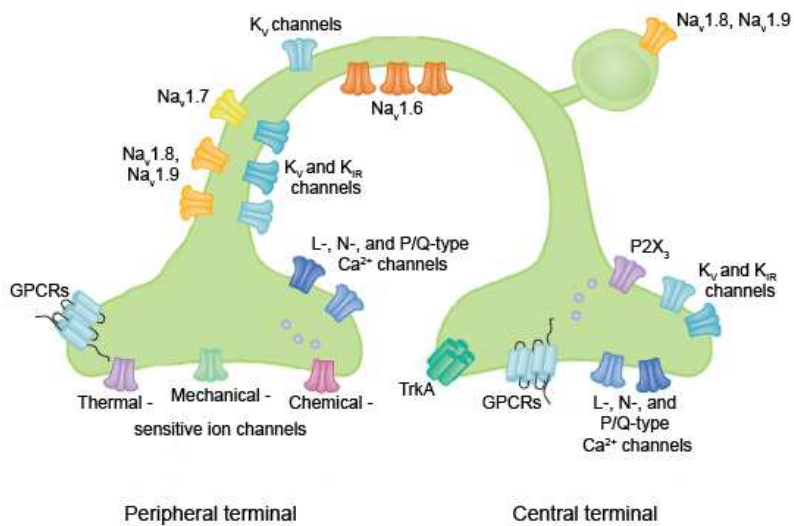


Figure 2 Illustration of a polymodal nociceptor expressing different ion channels and receptors leading to the heterogeneous and unique nature of peripheral sensory neurons (modified from Gold and Gebhart, 2010).

1.1.3 Plasticity of nociceptors

Tissue damage, irritation and inflammation can cause an increased excitability of primary sensory afferents leading to sensitization, an important property of nociceptors. Following tissue injury, nociceptors and infiltrating cells (for example mast cells, macrophages and neutrophils) produce and release mediators, referred to as “inflammatory soup”, that target different receptors and ion channels and cause a reduction in the neuronal threshold to noxious stimuli. This enhances the sensitivity to chemicals, touch and temperature. Peptides such as substance P and CGRP contribute to vasodilation and edema. Following activation of TrkA receptors on C fibers, neurotrophic factors (e.g. NGF) produce hypersensitivity to heat and mechanical stimuli through induction of downstream signaling pathways. In addition, NGF is transported to the nucleus of nociceptors to provoke enhanced expression of substance P, TRPV1 (a nonselective ion channel sensing heat and chemicals), Na_v1.8 and opioid receptors (Mousa et al., 2007). All these changes together with the release of cytokines and alterations in the activity and sensitivity of ion channels lead to nociceptive hypersensitivity during inflammation (Basbaum et al., 2009; Gold and Gebhart, 2010; Julius and Basbaum, 2001). Mechanisms counteracting nociception and inflammation are activated concomitantly. They involve the production and release of endogenous opioid peptides from immune cells infiltrating the injured tissue, as well as an enhanced expression and axonal transport of

opioid receptors in nociceptors. Inflammation also causes a disruption of the perineurial barrier, thus facilitating the access of opioids to their receptors on peripheral nerve terminals and leading to an enhanced analgesic effect of peripherally acting opioids (Stein et al., 2003).

1.2 Inhibition of pain by opioids

Opioids such as morphine are the most powerful pain relieving (analgesic) drugs but their use is limited due to severe side effects such as respiratory depression, nausea, constipation, addiction and tolerance. These side effects are mediated by activation of opioid receptors in the CNS. The development of opioids without these side effects has always been a major goal in pain research (Stein and Zollner, 2009).

In the 1970s three main types of opioid receptors were identified and named mu-, delta- and kappa after the first letter of the ligand binding to each receptor (e.g. morphine bound to the mu-opioid receptor) (Martin et al., 1976; Pert and Snyder, 1973; Simon et al., 1973). About 20 years later the respective genes *Oprm1*, *Oprd1* and *Oprk1* (encoding for mu-, delta- and kappa receptors respectively) were cloned (Chen et al., 1993; Evans et al., 1992; Kieffer et al., 1992; Thompson et al., 1993; Yasuda et al., 1993). The three genes show high homology in humans and mice, which might indicate that they derive from a common ancestor (Kieffer and Evans, 2009). Opioid-receptors belong to the superfamily of G protein coupled receptors (GPCRs). These are seven transmembrane proteins with an extracellular N-terminal domain and an intracellular C-terminal tail (Hollmann et al., 2005). All three receptors are highly conserved (86-100%) in their transmembrane region but they differ in the sequence of the N- and C-terminal domains (Kieffer and Evans, 2009).

Besides exogenous opioid-receptor agonists such as morphine, endogenous opioid peptides have been isolated from different tissues and shown to act selectively and with high affinity as mu-, delta- and kappa opioid-receptor agonists (Akil et al., 1998; Hughes et al., 1975).

1.2.1 Opioid receptors in the central and peripheral nervous system

The distribution of mu-, delta- and kappa-receptors in the CNS is broad. Nociceptive responses can be abolished by activating opioid receptors in the spinal cord and in brain regions such as the sensory cortex, the amygdala and the thalamus. The mu opioid-receptor is

expressed in all these CNS regions (Fields, 2004; Hunt and Mantyh, 2001). Furthermore, stimulation of the periaqueductal gray (PAG) controls nociceptive transmission through endogenous opioids acting on mu opioid-receptors on neurons projecting to the spinal cord dorsal horn (Roychowdhury and Fields, 1996).

Activation of opioid-receptors on terminals of peripheral sensory neurons directly decreases sensitization and hyperexcitability of C- and A-fibers. Binding studies and immunohistochemistry illustrated that about 70% of spinal opioid receptors are found on the central presynaptic terminals of C- and A δ -fibers projecting to laminae I and II of the dorsal horn. This indicates that a major part of spinal opioid antinociception is mediated by presynaptic opioid receptors (Besse et al., 1990).

In the peripheral nervous system (PNS), opioid-receptors are mainly synthesized by small and medium-diameter DRG neurons and are intraaxonally transported from the cell body to central and peripheral nerve terminals (Hassan et al., 1993; Li et al., 1998). Peripherally active opioids are often ineffective or provoke only weak antinociception if applied to normal tissues. In contrast, activation of peripheral mu-, delta- and kappa opioid-receptors in injured or inflamed tissue elicits pronounced analgesic effects (Joris et al., 1987; Stein et al., 2003; Stein and Zollner, 2009). Studies investigating the role of mu-receptors in inflammation have shown an up-regulation of mu opioid-receptor mRNA transcripts and higher protein content in DRG neurons as well as an increase in the number of peripheral sensory neurons expressing the mu opioid-receptor (Hassan et al., 1993; Puehler et al., 2004). Furthermore, G-protein coupling of opioid-receptors is enhanced during inflammation (Antonijevic et al., 1995; Zollner et al., 2003) and opioids have been shown to act as anti-inflammatory agents, e.g. by reducing the release of substance P from peripheral terminals (Stein et al., 2001). All of these mechanisms contribute to enhanced antinociception and anti-inflammatory action of opioids in inflamed tissue.

1.2.2 Molecular mechanisms of opioid-induced antinociception

Intracellularly, opioid receptors couple to heterotrimeric G proteins of the G $_{i/o}$ type which modulate several ion channels and signaling molecules upon activation. This prevents neurons from excitation and nociceptive transmission by hyperpolarizing the cell (Stein and Zollner, 2009). Inactivated G proteins are comprised of a G α subunit that binds guanosine diphosphate (GDP), and a G $\beta\gamma$ subunit. The binding of an opioid to its receptor leads to conformational

changes resulting in the binding of G_{i/o} proteins to the receptor's C-terminus, followed by an exchange of GDP by GTP at G_α. This leads to dissociation of the G protein complex into its G_α and G_{βγ} subunits. Both are now able to interact with different effector proteins and thereby activate distinct signaling cascades (Clapham and Neer, 1997).

The G_α subunit inhibits adenylyl cyclase which results in a reduction of intracellular cyclic adenosine monophosphate (cAMP). This modulates ion channels and indirectly decreases the release of neuropeptides, e.g. substance P and CGRP. In the spinal cord, this results in a reduced excitation of postsynaptic neurons (Law et al., 2000; Sharma et al., 1977).

The G_{βγ} subunit directly inactivates P/Q- and N-type voltage-gated calcium channels and thereby prevents the influx of Ca²⁺ ions. Furthermore, in the CNS voltage-gated K⁺ and G protein-gated inwardly rectifying K⁺ (GIRK) channels can be activated through the binding of the G_{βγ} subunit. This causes a potassium outflow and finally a hyperpolarization of the cell (see figure 3). Together these processes reduce neuronal excitability which finally leads to diminished nociceptive perception (Hescheler et al., 1987; North et al., 1987; Rhim and Miller, 1994; Yoshimura and North, 1983).

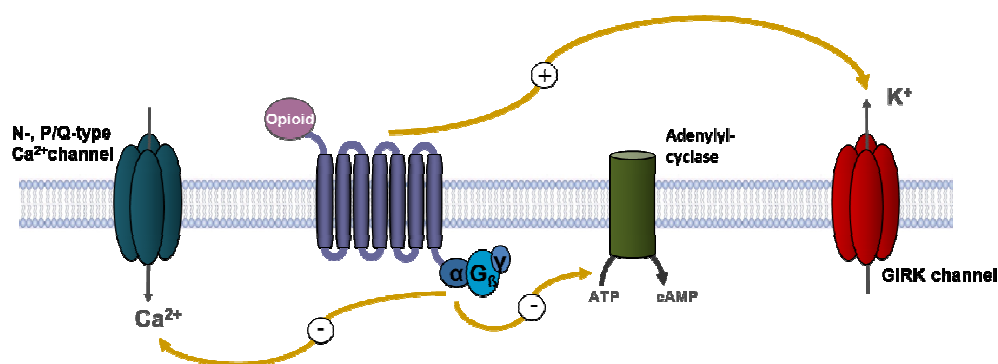


Figure 3 Intracellular signaling cascade of opioid receptors in the CNS. Activation of an opioid receptor leads to binding of the trimeric G protein and to an exchange of the GDP with GTP, followed by G protein dissociation into G_α and G_{βγ} subunits. G_α reduces cAMP levels in the cell by inhibiting adenylyl cyclases. G_{βγ} activates GIRK channels and inhibits Ca²⁺ channels, both reduce neuronal excitability.

The reduction of adenylyl cyclase activity as well as the inhibition of voltage-gated calcium channels contribute to opioid antinociception in both the CNS and PNS. To date it is not known whether the modulation of K⁺ channels is involved in opioid-induced inhibition of peripheral sensory neurons, whereas the activation of GIRK channels has been demonstrated conclusively in the CNS (see 1.3.2.). The question whether GIRK channels are expressed and

functionally coupled to opioid receptors in the PNS is still under debate (Akins and McCleskey, 1993; Moises et al., 1994; Schroeder et al., 1991). This will be subject of the present thesis.

1.3 The K_{ir} channel family

The opening of K^+ channels leads to a K^+ flow down its electrochemical gradient and thereby stabilizes the membrane potential of the cell (Ocana et al., 2004). Based on structure and phylogenetic homologies K^+ channels have been classified into four groups known as voltage-gated (K_v), two-pore (K_{2P}), calcium-activated (K_{Ca}) and inward rectifier (K_{ir}) K^+ channels. These groups can be further separated into different families. K^+ channels are the most diverse group among ion channels (Gutman et al., 2003).

Particularly the inwardly rectifying K^+ channels have been implicated in nociception and antinociception. This class consists of seven distinct families ($K_{ir}1-K_{ir}7$) and can be further divided into four groups based on their function (Fig. 4). These subfamilies comprise classical K_{ir} channels ($K_{ir}2.x$), K^+ -transport channels ($K_{ir}1.x$, $K_{ir}4.x$, $K_{ir}5.x$ and $K_{ir}7.x$), ATP-sensitive K^+ channels ($K_{ir}6.x$) and G protein-gated K_{ir} channels ($K_{ir}3.x$) (Hibino et al., 2010).

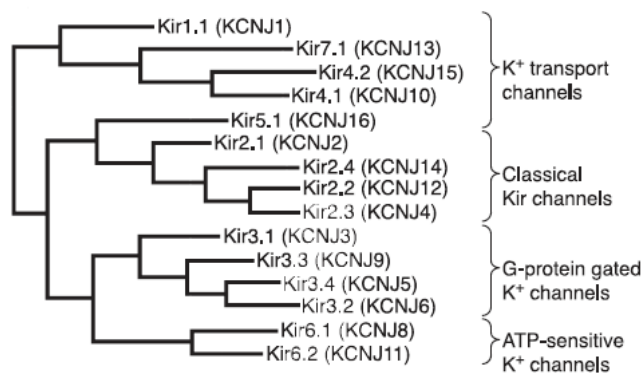


Figure 4 Phylogenetic tree of K^+ channels showing the relation of human K_{ir} channel subunits. Based on their function the subunits can be classified into four different groups (obtained from Hibino et al., 2010).

K_{ir} channels are characterized by their “inwardly rectifying” behavior. This means that these channels allow K^+ ions to flow more easily into the cell than out of the cell. If the membrane of a typical neuron is hyperpolarized K_{ir} channels produce large inward currents. If the membrane is depolarized activation of K_{ir} channels give rise to a small outward current which hyperpolarizes the membrane and decreases the excitability of the cell. Cytoplasmic ions such as Mg^{2+} and polyamines are responsible for the small outward current during depolarization. They occlude the channel and prevent K^+ outflow, thus causing inward rectification (Hibino et al., 2010; Luscher and Slesinger, 2010; Ocana et al., 2004). The inward rectification differs between the K_{ir} channel subfamilies. $K_{ir}2.x$ and $K_{ir}3.x$ are strong inward rectifiers, $K_{ir}4.x$ exhibit intermediate inward rectifying behavior whereas $K_{ir}1.1$ and $K_{ir}6.x$ show weak inward rectification (Hibino et al., 2010).

Two subfamilies of K_{ir} channels are involved in nociception, the ATP-sensitive channel (K_{ATP} or $K_{ir}6$) and GIRK ($K_{ir}3$) channels. Several studies demonstrated that activation of opioid receptors opens both GIRQ and K_{ATP} channels. GIRQ channels are directly coupled to opioid receptors and can be activated by binding of the $G_{\beta\gamma}$ subunit whereas K_{ATP} channels are activated through a cascade of intracellular signaling events (Cunha et al., 2010; Hibino et al., 2010; North et al., 1987; Ocana et al., 2004).

1.3.1 Structure and function of GIRQ channels

Four distinct GIRQ channel subunits (GIRQ1-GIRQ4) can be localized in different tissues of mammals including mice, rats and humans. GIRQ1, GIRQ2 and GIRQ3 are highly expressed throughout the brain while GIRQ4 is primarily present in pancreas and heart. The predominant channels in the brain are built of GIRQ1 and GIRQ2 and both can be found pre- and postsynaptically (Grosse et al., 2003; Hibino et al., 2010; Koyrakh et al., 2005; Ponce et al., 1996). Studies in GIRQ2 knock-out mice demonstrated that in different brain regions such as the hippocampus or the cerebellum GIRQ currents are mainly generated by GIRQ2 (Luscher and Slesinger, 2010).

Functional GIRQ channels are composed of four subunits. Except for GIRQ2 (and theoretically GIRQ4) all subunits exclusively assemble to heterotetramers. Transportation of the subunit to the plasma membrane is due to an endoplasmic reticulum (ER) export signal in the N-terminus of GIRQ2 and GIRQ4, and to a post-ER trafficking signal in their C-terminal tail. GIRQ1 lacks both signals and, thus, is not transported to the plasma membrane if

expressed alone. Co-expression with GIRQ2 or GIRQ4 assures transportation of GIRQ1 to the membrane by forming heterotetramers. GIRQ2 is unique among the four $K_{ir}3$ subunits as it forms functional homotetramers, but it also assembles with other subunits to form heterotetramers such as GIRQ1-GIRQ2 or GIRQ2-GIRQ3. Channels composed of GIRQ1 or GIRQ3 alone are not functional but heterotetramers (GIRQ1-GIRQ3) can be found on the cell surface (Ma et al., 2002).

Each GIRQ channel subunit comprises two membrane-spanning domains (M1 and M2) connected by an extracellular pore-forming motif (P-loop). The N- and C-termini are located in the cytoplasm (illustrated in figure 5) (Ocana et al., 2004). The selectivity for K^+ ions is given by the sequence T-X-G-Y(F)-G within the pore-forming region. This is a common motif in all K^+ -selective ion channels (Bichet et al., 2003; Heginbotham et al., 1994). A point mutation within the selectivity filter of GIRQ2 in *weaver* mice results in a loss of K^+ ion selectivity leading to a nonselective cation channel insensitive to G protein activation. The phenotype of *weaver* mice shows severe locomotor defects, a dopamine deficiency in the midbrain and a depletion of cerebellar granule cells resulting in reduced size of the cerebellum (Navarro et al., 1996; Patil et al., 1995; Schmidt et al., 1982). This illustrates the relevance of K^+ -selectivity and GIRQ2 channel function in the nervous system.

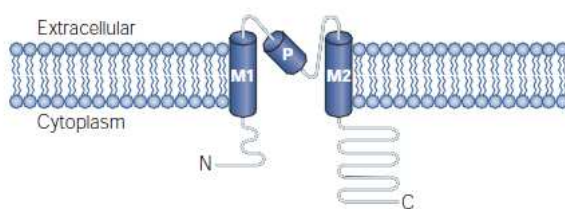


Figure 5 Schematic structure of a single GIRQ subunit. The two transmembrane domains (M1 and M2) are connected by a pore-forming region (P). N- and C-termini are located in the cytoplasm (obtained from Bichet et al., 2003).

Activation of GIRQ channels involves direct binding of the $G_{\beta\gamma}$ subunit to regions in the N- and C-termini of the channel (Huang et al., 1995; Kunkel and Peralta, 1995). Each subunit of a GIRQ channel binds one $G_{\beta\gamma}$ complex resulting in four $G_{\beta\gamma}$ binding sites per channel tetramer (Corey and Clapham, 2001; Sadja et al., 2002). In addition, some studies demonstrated a direct interaction of the GIRQ N- and C-terminus with the G_α subunit (Clancy

et al., 2005; Huang et al., 1995). Thereby, G_{α} seems to be involved in GIRK channel activity by forming a macromolecular signaling complex of GDP-bound G_{α} , $G_{\beta\gamma}$ and GIRK channels. It is proposed that this complex is involved in fast activation of GIRK channels upon agonist binding (Peleg et al., 2002; Riven et al., 2006).

1.3.2 The role of GIRK channels in opioid antinociception

Many studies revealed an involvement of CNS GIRK channels in opioid-induced reduction of nociception. This was first observed in *weaver* mice where morphine (a mu opioid receptor agonist) and U-50488 (a kappa opioid receptor agonist) failed to induce antinociception (Ikeda et al., 2000). Subsequently a lot of studies were performed using GIRK channel knock-out mice to determine the contribution of GIRK channels to opioid-induced antinociception. GIRK2-null mice also showed a complete loss of postsynaptic outward currents evoked by other $G_{i/o}$ - protein coupled receptors (GABA_B, adenosine A1, 5HT1A) in hippocampal neurons (Luscher et al., 1997). The global deletion of GIRK2 significantly decreased spinal mu-opioid receptor dependent antinociception but a residual effect of morphine was maintained. This indicated that opioid receptor signaling pathways independent of GIRK2 contribute to this preserved antinociception (Mitrovic et al., 2003). Since it is known that GIRK2 is expressed postsynaptically in excitatory interneurons of lamina II of the spinal cord and no GIRK2 immunostaining was observed in DRG sections, one can assume that this preserved antinociception in global GIRK2 knock-out mice was caused by presynaptic opioid receptors (Marker et al., 2006; Mitrovic et al., 2003).

Deletion of GIRK1 or GIRK2 led to decreased analgesic responses after spinal administration of higher but not of lower doses of morphine. The reduced antinociceptive effect in these mutant mice was related to a dramatic reduction of GIRK1 and GIRK2 expression in the dorsal horn of the spinal cord of both GIRK1 and GIRK2 knock-out mice (Marker et al., 2004). Furthermore, the analgesic effect of spinally administered mu- and delta-opioid receptor agonists was attenuated in mice lacking GIRK1 or GIRK2 (Marker et al., 2005). Another study reported a decreased antinociceptive potency but a preserved maximal response to morphine in GIRK2-GIRK3 double knock-out mice (Cruz et al., 2008). Interestingly, GIRK2 knock-out animals showed decreased antinociception induced by morphine in tests for acute (physiologic) (hot plate and tail flick tests) but not in inflammatory nociception (formalin test) (Mitrovic et al., 2003).

Together, CNS GIRK channel activation significantly contributes to mu-opioid receptor induced antinociception. The involvement of GIRK channels in antinociception mediated by delta- and kappa-opioid receptors has not been fully evaluated. All of these studies (performed in mice) implicated a postsynaptic contribution of GIRK channels to antinociception induced by systemically or spinally administered opioids. In addition, the inhibition of presynaptic voltage-gated Ca^{2+} channels and the reduction of neurotransmitter release are important mechanisms. The presence and function of GIRK channels in DRG neurons and their involvement in peripherally mediated opioid antinociception has not been studied yet.

1.4 Species differences in opioid antinociception-a possible role of GIRK channels

Animal models are essential for our understanding of the pathophysiology of clinical, e.g. neuropathic and inflammatory pain. Historically, the typical non-human research subject has been the rat. Mice have been used as models for an increasing number of pain studies, partly because of relatively inexpensive maintenance and ease of breeding, but mostly because of the advent of genetic models (Wilson and Mogil, 2001). However, evolutionarily mice and rats have been dispersed over 10 million years ago (Mogil, 2009) which might explain the widely variable responses to opioids between them (Le Bars et al., 2001). Our group also observed large differences concerning the dose of opioids required to evoke peripherally mediated antinociception in mice versus rats. Much lower opioid doses are needed in rats and even high doses are often without any effects in mice if applied peripherally. Since analgesic drugs which seemed to be effective in animal models often failed in humans, it is important to consider species differences in opioid antinociception (Le Bars et al., 2001; Whiteside et al., 2008).

Studies on peripheral GIRK channel expression and function in rats differ from those done in mice. In rats GIRK channels functionally coupled to GABA_B receptors were detected on peripheral terminals of small and medium diameter DRG neurons. Furthermore, indirect evidence suggested a role of GIRK channels in peripheral antinociception elicited by the activation of mu-opioid receptors (Gao et al., 2007; Khodorova et al., 2003). However, studies performed in mice neither showed expression nor a functional role of GIRK channels in the peripheral nervous system (Kanjhan et al., 2005; Mitrovic et al., 2003). Such species differences will be subject of this thesis.

1.5 Objectives

The **overall hypothesis** of this thesis is that GIRQ channels in DRG neurons are required for the generation of significant peripheral opioid antinociception.

Until now, it has only been shown that GIRQ channels are involved in opioid antinociception in the CNS (Marker et al., 2005; Marker et al., 2004). Whether GIRQ channels contribute to opioid antinociception in the PNS is not known. Indeed, the presence and function of GIRQ channels in peripheral sensory neurons is controversially discussed in the literature (Gao et al., 2007; Kanjhan et al., 2005; Karschin and Karschin, 1997; Khodorova et al., 2003; Mitrović et al., 2003; Werz and MacDonald, 1983a). Furthermore, pronounced antinociceptive responses by peripherally acting opioids are detectable in rats but only weak effects in mice (Cunha et al., 2010; Stein et al., 1989). Peripheral mu-opioid receptors are the most extensively studied and prominent receptor types (Stein and Machelska, 2011). Studies on the function of GIRQ channels in peripheral sensory neurons point to a role of GIRQ channels in rats but not of mice. However, none of these studies examined species differences directly (Gao et al., 2007; Kanjhan et al., 2005; Karschin and Karschin, 1997; Khodorova et al., 2003; Mitrović et al., 2003; Werz and MacDonald, 1983a).

Thus, this project sought to determine GIRQ channel expression and function in peripheral sensory neurons by using quantitative real time PCR, whole-cell patch clamping, immunohistochemistry and in vivo behavioral analysis. In addition, we generated a transgenic mouse line overexpressing GIRQ2 in DRG neurons. This was achieved by using the promoter of the voltage dependent sodium channel $\text{Na}_v1.8$ which is known to be selectively expressed in such neurons (Akopian et al., 1996; Djouhri et al., 2003; Stirling et al., 2005).

The following main hypotheses were put forth:

Hypothesis 1: A lack of GIRQ channel expression in peripheral sensory neurons of mice underlies the observed weak peripheral opioid antinociception. In contrast, rats express GIRQ channels in peripheral sensory neurons and they are functionally coupled to mu-opioid receptors.

Hypothesis 2: Expression of GIRK channels in peripheral sensory neurons of transgenic mice leads to coupling of the channels to mu-opioid receptors and to an increased antinociceptive response to peripherally applied mu-opioids.

2 Materials and methods

2.1 Animals

Wild-type c57/BL6-J mice, Na_v1.8-GIRK2 mice and male Wistar rats were bred in the Forschungseinrichtung für experimentelle Medizin (FEM) Berlin and were housed in cages lined with ground corncob bedding. Standard laboratory rodent chow and tap water were available *ad libitum*. Rooms were maintained at 22°C and at a relative humidity between 40% and 60%. A 12/12 h (8 a.m./8 p.m.) light/dark cycle was used. Experiments were approved by the animal care committee of the State of Berlin and strictly followed the guidelines of the *International Association for the Study of Pain* (IASP) (Zimmermann, 1983).

Na_v1.8-GIRK2 mice were generated in collaboration with Jeanette Rientjes from the European Molecular Biology Laboratory (EMBL) Gene expression Service in Monterotondo, Italy.

2.2 Materials

2.2.1 Bacteria and cell lines

Table 1

Name	Genotype	Company
<i>Escherichia coli</i> (<i>E. coli</i>)	FΦ80lacZΔM15Δ(<i>lacZYA-argF</i>)	Invitrogen
MAX Efficiency® DH5αTM	U169 <i>recA1 endA1 hsdR17</i> (r _k -,	
Competent cells	m _k +) <i>phoA supE44 λ⁻ thi⁻¹ gyrA96</i> <i>relA1</i>	
<i>Escherichia coli</i> (<i>E. coli</i>)	Tet ^r Δ(<i>mcrA</i>)183; Δ(<i>mcrCB-hsdSMR-mrr</i>)173 <i>endA1supE44 thi-1 recA1</i>	Stratagene
XL10-Gold® Ultracompetent Cells	<i>gyrA96 relA1 lac Hte</i> [F' <i>proAB lacI^qZΔM15 Tn10</i> (Tet ^r) Amy Cam ^r]	
HEK293 cell line (human embryonic kidney cells 293)		Deutsche Sammlung von Mikroorganismen und Zellkulturen (DSMZ)

2.2.2 Antibiotics

Ampicillin	Sigma-Aldrich
Kanamycin	Sigma-Aldrich
Penicillin (10.000U)/Streptomycin (10.000 µg/ml)	Biochrom AG

2.2.3 Oligonucleotides

The primers used for polymerase chain reaction (PCR), qRT-PCR and quantitative analysis of transgene copy number are listed in table 2 All primers were custom made by TIB MOLBIOL.

Table 2

Name	5'- 3' sequence	Application
GIRK1 mouse / rat fw	acc tga aca aag ccc atg tc	Quantitative RT-PCR
GIRK1 mouse / rat rv	gtt gat cgg ccc ctg tac ta	
GIRK2 mouse fw	gat tcc atg gac cag gat gt	Quantitative RT-PCR
GIRK2 mouse rv	cca taa ccg atg gtg gtt tc	
GIRK3 mouse / rat fw	gag aag gac ggt cgc tgt aa	Quantitative RT-PCR
GIRK3 mouse / rat rv	tgc gag gag aag ac gaga gt	
GIRK4 mouse / rat fw	cgg ctt tgt atc tgc ttt cc	Quantitative RT-PCR
GIRK4 mouse / rat rv	ggc tct tct cgt tga tct cg	
GIRK2 rat fw	tgc ctg atg ttc cgg gta ggg g	Quantitative RT-PCR
GIRK2 rat rv	gct ctg ccc ggt tag cca gc	
GAPDH upper	aca gtc aag gct gaa aat gg	Genotyping of Na _v 1.8-GIRK2 mice
GAPDH lower	cat gag ccc ttc tac aat gc	
Na _v 1.8-GIRK2-FLAG fw	tac aaa gac gat gac gac aa	Genotyping, sequencing and analysis of transgene copy number
Na _v 1.8-GIRK2-FLAG rv	ggt ggt ttc tgt ctc tat gg	

<i>NcoI</i> -Probe fw	acc acc atc ggt tat ggc ta	Southern blot probe
<i>NcoI</i> -Probe rv	ccc cac aag atc tca ctg gt	
GIRK1-FLAG fw	aat agc ggc cgc gtc tgc act ccg aag gaa att	Cloning of pFLAG-CMV-2-GIRK1
GIRK1-FLAG rv	gca tgg atc cat cct atg tga aac ggt cag agt t	
GIRK2-FLAG fw	aat agc ggc cgc gac aat ggc caa gtt aac tga atc c	Cloning of pFLAG-CMV-2-GIRK2
GIRK2-FLAG rv	gca tgg atc cac cca gct ggg cct ata ctt tg	
AAV-FLAG-GIRK2 fw	agc tcg ggc tct aga atg gac tac aaa gac gat gac gac	rAAV-2-GIRK2 targeting vector
AAV-FLAG-GIRK2 rv	gca tgt cga cac cca gct ggg cct ata ctt tg	
Na _v 1.8-GIRK2 rv	cag ctg ggc cta tac ttt gg	Sequencing of Na _v 1.8-GIRK2 mice

2.2.4 Plasmids and constructs

pFLAG-CMV-2	Sigma-Aldrich
pEYFP-C1	Clontech
pD-M203S rAAV-2	Gift from Dr. Stefan Weger
pFLAG-GIRK1	cloned
pFLAG-GIRK2	cloned
rAAV-2-GIRK2	cloned
Na _v 1.8-GIRK2 BAC	cloned by Dr. Jeanette Rientjes
pCR-BluntII-TOPO-GIRK1	RZPD
pCR-TOPO-GIRK2	RZPD
pYX-Asc-GIRK3	RZPD
pCR-BluntII-TOPO-GIRK4	RZPD

2.2.5 Enzymes

AMV Reverse transcriptase	Roche
Collagenase II and IV	Sigma-Aldrich
Phusion® Polymerase	Finnzymes
Proteinase K	Sigma-Aldrich
Restriction enzymes	Invitrogen, Promega, NEB
RNAse-free DNase I	Qiagen
RNase inhibitor	Roche
Shrimp alkaline phosphatase (SAP)	Sigma-Aldrich
Trypsin I	Sigma-Aldrich
Trypsin	Biochrom

2.2.6 Antibodies

Anti-K _i r3.1 and Anti-K _i r3.2	Alomone labs
Anti-GIRK2	Chemicon
Anti GIRK2 guinea pig serum	Gift from Dr. Florian Lesage
Anti-FLAG® M2 Monoclonal Antibody	Sigma-Aldrich
Anti-FLAG	Sigma-Aldrich
Anti-NF200	Chemicon
Anti-CGRP	Biomol
Anti-Mu opioid receptor	Abcam
Fluorescein-Isolectin-B ₄	Vector Laboratories
Anti-GIRK1	Sigma-Aldrich
Anti-GIRK2	Sigma-Aldrich
Fluorescein anti-chicken IgG (H+L) made in goat	Vector Laboratories
Texas red anti-rabbit IgG (H+L) made in goat	Vector Laboratories
Fluorescein anti-mouse IgG (H+L) made in horse	Vector Laboratories
Biotinylated anti-rabbit IgG (H+L) made in goat	Vector Laboratories
Peroxidase-conjugated Goat Anti-Rabbit IgG (H+L)	Jackson Immuno Research

2.2.7 Pharmacological agents

(D-Ala ² ,N-Me-Phe ⁴ ,Glycinol ⁵)-Enkephalin	Bachem
(D-Pen ^{2,5})-Enkephalin	Bachem
Glibenclamide	Sigma-Aldrich
Tetraethylammonium chloride	Sigma-Aldrich
Naloxone Hydrochloride	Sigma-Aldrich
Barium chloride	Sigma-Aldrich

2.2.8 Chemicals, reagents and media

[α- ³² P]dGTP	Perkin Elmer
10x ligase buffer	Promega
100x BSA	New England Biolabs
Adenosine 5'-triphosphate (ATP) magnesium salt	Sigma-Aldrich
Agarose LE	Roche
Albumin from bovine serum (BSA)	Sigma-Aldrich
Albumin solution from bovine serum, 30 %	Sigma-Aldrich
AMV RT buffer	Roche
Bromophenol blue	Sigma-Aldrich
Calcium chloride (CaCl ₂)	Sigma-Aldrich
Complete Freund's Adjuvant (CFA)	Calbiochem
Coverslips	Carl Roth GmbH
D-(+)-glucose	Sigma-Aldrich
Deoxy-nucleotide triphosphate mix (dNTP)	Roche
Dimethyl sulphoxide (DMSO)	Sigma-Aldrich
DNA molecular weight marker (XVII, 500 bp)	Roche
DNA molecular weight marker (XIV, 100 bp)	Roche
DMEM/Hams-F12	GIBCO
Ethanol 99.9%	J.T. Baker
Ethidium bromide	Sigma-Aldrich
Ethyleneglycol tetraacetic acid (EGTA)	Sigma-Aldrich
Fetal bovine serum (FBS)	Biochrom AG
Frozen section medium	Thermo Fisher Scientific

FuGENE HD Transfection Reagent	Roche
Glucose	Sigma-Aldrich
Glycerol	Sigma-Aldrich
Glycine	Roth
Guanosine 5'-triphosphate (GTP) sodium salt	Sigma-Aldrich
Heat-inactivated horse serum	Biochrom AG
HEPES	Sigma-Aldrich
Hydrochloride (HCL) 25%	Merck AG
Forene (Isofluran)	Abbott
Isopropanol	Sigma-Aldrich
Luria Bertani (LB) AGAR Lennox L AGAR	Invitrogen
Luria Bertani (LB) Broth Base (Lennox L Broth Base)	Invitrogen
Magnesium chloride ($MgCl_2$)	Sigma-Aldrich
MEM EARLE	Biochrom
Methanol	J.T. Baker
2-methylbutane	Sigma-Aldrich
Mowiol 4-88®	Calbiochem
NEB buffers 1, 2, 3, 4	New England Biolabs
Normal goat serum	Vector Laboratories
Normal horse serum	Vector Laboratories
OptiMEM®	Invitrogen
Orto-phosphoric acid solution (85 wt. % in H_2O)	Sigma-Aldrich
Paraformaldehyde	Sigma-Aldrich
Phosphate buffered saline (PBS) tablets	GIBCO
PBS Dulbecco	Biochrom AG
Phusion® High-Fidelity PCR Mastermix	Finnzymes
Poly-L-lysine hydrobromide	Sigma-Aldrich
Polylysin microscope slides	Menzel GmbH
Potassium chloride (KCl)	Sigma-Aldrich
Primer dT for cDNA synthesis (oligo dT)	Roche
S.O.C. medium	Invitrogen
Sodium chloride	Carl Roth GmbH
Sodium hydroxide (NaOH)	Sigma-Aldrich
Sodiumhydrogenphosphat ($NaH_2PO_4 \cdot H_2O$)	Merck

Sodium phosphate dibasic dehydrate (Na ₂ HPO ₄ .2H ₂ O)	Sigma-Aldrich
Sucrose	Carl Roth GmbH
Trizma®-Base	Sigma-Aldrich
Tris-hydroxymethyl- aminomethane (TRIS)	Carl Roth GmbH
Triton X 100	Sigma-Aldrich
Trypsin (0.05%)/EDTA(0.02%) Solution	Biochrom AG
Tween®-20 (Polyoxyethylene sorbitan monolaureate)	Sigma-Aldrich
VectaMount	Vector
Xylene	J.T. Baker

2.2.9 Kits and reaction systems

DAB (3,3'-Diaminobenzidine) peroxidase substrate kit	Vector Laboratories
Elite ABC kit (rabbit IgG)	Vector Laboratories
Fast Start DNA Master SYBR Green I Kit	Roche
FluxOR™ Potassium Ion Channel Assay	Invitrogen
High Pure PCR Product Purification Kit	Roche
MinElute Gel Extraction Kit	Qiagen
QIAfilter Plasmid Maxi Kit	Qiagen
QIAprep Spin Miniprep Kit	Qiagen
QIAquick Gel Extraction Kit	Qiagen
Large-construct Kit	Qiagen
Random Primers DNA labeling system	Invitrogen
RNeasy mini kit	Qiagen
XL10-Gold® Ultracompetent Cells	Stratagene

2.2.10 Buffers and solutions

Table 3

Name	Content
Agarose gel	1-2% agarose, 0.0001% ethidium bromide in TAE

Alkaline solution	0.4 M NaOH, 1.5 M NaCl
Blocking solution (Western blot)	5% milk powder in TBS-T
Blotting buffer (Western blot)	10% Western Blot buffer, 15% Methanol in ddH ₂ O
DRG medium (mouse)	10% Horse Serum, 1 mM glutamine, 100 u penicillin / 100 µg/ml streptomycin, 0.8% glucose, in DMEM/HAM'S F12 without glutamine
DRG medium (rats)	10% Horse Serum, 100 u penicillin / 100 µg/ml streptomycin in MEM EARLE 1x
Extracellular solution for whole-cell patch clamping, pH 7.4	150 mM NaCl, 5 mM KCl, 1 mM CaCl ₂ , 1 mM MgCl ₂ , 10 mM HEPES, 10 mM D-Glucose, pH 7.4
Extracellular low K ⁺ solution for whole-cell patch clamping pH 7.4	140 mM NaCl, 5.6 mM KCl, 2.6 mM CaCl ₂ , 1.2 mM MgCl ₂ , 10 mM HEPES, 2.6 mM D-Glucose, pH 7.4
Extracellular high K ⁺ solution for whole-cell patch clamping pH 7.4	140 mM KCl, 2.6 mM CaCl ₂ , 1.2 mM MgCl ₂ , 5 mM HEPES, pH 7.4
Fixation buffer	4 % PFA in 1x PBS or 0.1 M PB, pH 7.4
Gel loading buffer	0.25 % bromphenol blue, 50 mM Tris pH 7.6, 60 % glicerol
Intracellular (pipette) solution for whole cell patch clamping pH 7.2	122 mM KCl, 11 mM EGTA, 1 mM CaCl ₂ , 2 mM MgCl ₂ , 10 mM HEPES, 4 mM MgATP, 0.25 mM NaGTP, 5 mM NaCl, pH 7.25 with KOH
LB agar	32 g of LB AGAR (Lennox L AGAR) in 1 l of ddH ₂ O, autoclaved, supplemented with the appropriate antibiotic, distributed on 10 cm cell culture dishes, stored at 4°C
LB medium	20 g of LB Broth Base (Lennox L Broth Base) in 1 l of ddH ₂ O, autoclaved in 100 ml volumes, appropriate antibiotic added prior to inoculation with bacterial clone
Lysis buffer for protein extraction	50 mM Tris (pH 7.4), 5 mM EDTA, 150 mM NaCl, 0.5% NP40, 0.5% Na desoxycholate
Mowiol embedding solution	12 g glycerine and 4.8 g Mowiol 4-88 in 24 ml 0.2 M Tris/HCl solution (pH 8.5). Stir at 50°C for 30-40 minutes. Clarify by centrifugation at 4000-5000 rpm for 20 min and store the supernatant at 4°C
PB	0.1 M Na ₂ HPO ₄ , 0.1 M NaH ₂ PO ₄ , pH 7.4
PBS ⁺	1x PBS, 0.3 % Triton X-100, 1 % BSA
PBS (1x)	Made from PBS tablets. 0.14 M NaCl, 0.01 M PO ₄ buffer, 0.003 M KCl

Phosphate buffer	1 mM Na ₂ HPO ₄ .2H ₂ O, 40 mM Orto-phosphoric acid
Running buffer for SDS-PAGE	10% Western Blot buffer, 0.1% SDS in dH ₂ O
Separating gel (Western blot)	375mM Tris (pH8.8), 0.1% SDS, 12% Acrylamide, 0.05% APS, 0.07% TEMED in ddH ₂ O
Shrimp alkaline phosphatase (SAP) buffer	50 mM Tris, 5 mM MgCl ₂ , pH 8.5
Southern blot hybridization buffer	0.5 M Phosphate buffer, 1 mM EDTA, 3 % BSA, 5 % SDS
Stacking gel (Western blot)	125mM Tris (pH6.8), 0.1% SDS, 4% Acrylamide, 0.05% APS, 0.1% TEMED in ddH ₂ O
Sucrose solution	30 % sucrose in 1x PBS, pH 7.4
TAE (1x)	40 mM Tris, 20 mM acetic acid, 1 mM EDTA, pH 8.3
Tail lysis buffer	50 mM TRIS, 100 mM EDTA, 100 mM NaCl, 1 % SDS
TBS-T	10% TBS, 0.1% Tween®-20
Wash solution	40 mM Phosphate, 1 mM EDTA, 5 % SDS
Western Blot buffer	250 mM Tris, 1.92 M glycine in ddH ₂ O

2.2.11 Consumable materials

3M paper	Whatman
50ml plastic tubes	Sarstedt AG & Co.
BAS-IP SR2040	Fujifilm
Borosilicat glass capillaries with filament	Hilgenberg
Cell culture bottles	BD Biosciences
Cell culture dishes	TPP AG
Cell culture plates	Sigma-Aldrich
Cell scraper	Sigma-Aldrich
Cell strainer (40µm) Nylon	BD Biosciences
Cellular Incubator 6000	Heraeus
Coverslips	Carl Roth GmbH

Cryo tubes (1.5ml)	Nunc GmbH
Cylinder	TECHNE FHB11
Frozen section medium	Richard Allan Scientific
Hybond-XL membrane	Amersham
LightCycler® Capillaries (20 µl)	Roche
Needles	Becton-Dickinson GmbH
Nylon N ⁺ membrane	Amersham
Parafilm	Pechiney
PCR tubes and caps	Applied Biosystems
Pipettes (1-25ml, one-way)	Sarstedt AG & Co.
Polysin microscope slides	Menzel GmbH
Reaction tubes 0.5, 1.5ml and 2ml	Eppendorf
Real-time tube strips	Eppendorf
Saran wrap	Dow Chemical Company
Silver wire 0.25mm	WPI Inc.
Sterile filters	Millipore
Sterile filters FP 30/0.2 CA-S	Whatman
Syringes	Braun
Tubes (15 and 50ml)	Falcon

2.2.12 Technical equipment

AxioCam MRC	Carl Zeiss Mikroskopie
Bacterial shaker	GFL GmbH
Beckman Avanti J.25 centrifuge	Beckmann Instruments GmbH
CCD Imago camera	Till Photonics GmbH
CO ₂ incubator	Heraeus
Concentrator 5301	Eppendorf
Crosslinker VILBER LOURMAT BLX-E312	Marne La Vallee
Cryostat (Microm HM560)	MICROM International
Electronic timer	IITC Inc/Life Science
EPC-10 patch-clamp amplifier	HEKA Electronic
Flaming/Brown Micropipette Puller Model P-97	Sutter Instruments Co.

Fluorescence microscope (Axioskop 2)	Carl Zeiss Mikroskopie
Fluorescence microscope Hal100	Carl Zeiss Mikroskopie
GeneAmp PCR System 9700	Applied Biosystems
High Precision Multichannel Dispenser	ISMATEC
HS18 laminar airflow	Heraeus
Hybridiser	TECHNE HB-1D
Inverted microscope (Axiovert 200)	Carl Zeiss Mikroskopie
Light-microscope Axiovert 25	Carl Zeiss Mikroskopie
Micromanipulator 5171	Eppendorf
Microscope Eclipse TE 2000-S	Nikon
Microwave	Galanz Inc.
Mini centrifuge Galaxy mini	VWR International GmbH
Minispin table top centrifuge	Eppendorf
Monitor (CDM 1003)	MONOCAR Int. GmbH
Multifuge 4KR	Heraeus
Nanodrop ND-2000	Peqlab
Objective “A-Plan” 10x/0.25 Ph1	Zeiss
Objective “LD Achromplan” 63x/0.75 Korr. Ph2	Zeiss
Objective Plan-Neofluar 5x/0.15	Zeiss
Objective Plan-Neofluar 10x/0.30	Zeiss
Objective Plan-Neofluar 20x/0.75	Zeiss
Objective Plan-Neofluar 40x/0.75	Zeiss
Objective Plan Fluor 20x/0.50 Ph1 DLL	Nikon
Perfusion Fast-Step System (VC-77SP)	Warner Instruments
pH-Meter (MP220)	Mettler-Toledo
Phosphoimager	Fujifilm FLA-5100
Photometer Gene Quant II RNA/DNA Calculator	Pharmacia Biotech
Polychrome manual control	TILL Photonics GmbH
Polychrome V monochromator	TILL Photonics GmbH
Power PAC 300 for electrophoreses	BIO-RAD
Realplex ² Mastercycler	Eppendorf
SensiCam	PCO
SPECTRAmax® Spectrophotometer	Molecular Devices
Table top centrifuge Biofuge fresco	Heraeus

Thermoblock	Eppendorf
Thermocycler (LightCycler 1.5 Instrument)	Roche
Thermocycler (Mastercycler personal) for PCR	Eppendorf
Thermomixer comfort	Eppendorf
Transilluminator RH-2	Herolab
Ultrapure Water Systems (Direct-QTM 5)	Millipore
UV Light (Macro Vue UV=25)	Hoefer Inc.
UV-1601 spectrophotometer	Molecular Devices
VC-6 six channel valve controller	Warner Instrument Corporation
Video copy processor (PSI)	Mitsubishi
Vortexmixer (2TM Mixer 7-2020)	Neolab
Water bath SUB14 Grant	Instruments

2.2.13 Software

AxioVision 4.4	Carl Zeiss Vision GmbH
Endnote X5	Thomson Reuters
Illustrator CS5	Adobe
Photoshop CS3	Adobe
LightCycler® 3.5.3 Software	Roche
Microsoft Office 2010	Microsoft
Pulse software	HEKA Electronic
Realplex 2.2	Eppendorf
Sigmaplot 10 software	Systat Software Inc.
Sigmastat 3.5 software	Systat Software Inc.
Tillvision software	TILL Photonics GmbH

2.3 Methods

2.3.1 Molecular biology

Standard methods of molecular cloning were performed in accordance with (Sambrook, 2001) and will not be described in detail. Sequencing of DNA fragments was conducted by the company AGOWA.

2.3.1.1 DNA restriction

Cleaving of vectors and PCR products was performed in the appropriate buffers delivered with the restriction enzymes. For complete digestion 10 units of enzymes were used for 1 µg of DNA. The reaction was incubated at the temperature required for the restriction enzyme. For preparative digestions (for cloning purposes) 1-5 µg of DNA were set up in 50 µl and incubated overnight. Analytic digestions were set up in 20 µl (0,5-1 µg of DNA) and incubated for 1-2 h.

2.3.1.2 Vector dephosphorylation

Linearized plasmid DNA was treated with alkaline shrimp phosphatase to prevent recirculation. Dephosphorylation was carried out in a total volume of 25 µl using 10x buffer and 1 unit of shrimp alkaline phosphatase for 1 pmol of 3'- or 5' dsDNA ends. The calculation of pmol of 3'- or 5'ends of dsDNA was determined according to the following formula:

$$\frac{2 \cdot 10^6 \mu\text{g (of ds DNA)}}{N_{bp} \times 660 \text{ Da}} = \text{pmol}$$

The reaction was incubated for 1 h at 37°C and afterwards inactivated by warming to 60°C for 15 min.

2.3.1.3 Ligation

DNA fragments were reassembled by ligation. The reaction (10 µl final volume) was prepared on ice and incubated over night (16 h) at 4°C.

The standard ligation solution contained:

Table 4

Reaction mix	Concentration
Insert	300 ng
Linearized plasmid vector	100 ng
10x ligation buffer	1 µl
T4 DNA ligase	1 µl
ddH ₂ O	to 10 µl

The amount of inserted DNA was determined according to the following formula:

$$\text{ng of insert} = \frac{\text{ng of vector} \times \text{size of insert}}{\text{size of vector}} \times \frac{3}{1}$$

2.3.1.4 Transformation

Ultracompetent XL10-Gold® cells (25 µl) were thawed on ice. To increase the transformation efficiency, 1 µl of β-Mercaptoethanol was added to the cells. After 10 min incubation on ice, the DNA (5-10 ng) of interest was mixed with the cells and the reaction was incubated on ice for 30 min. The tube was heat-pulsed at 42°C for 30 s followed by an incubation on ice for 2 min. 225 µl preheated S.O.C. medium was added to the cells and incubated for 1 h at 37°C while shaking. The transformation mixture was plated on LB agar plates containing the appropriate antibiotic and colonies were grown over night at 37°C.

2.3.1.5 Isolation of plasmids from bacteria

For isolation of small amounts of plasmid DNA 5 ml LB medium containing the appropriate antibiotic was inoculated with one bacterial colony and incubated overnight at 37°C while shaking. The plasmid DNA was extracted using “*QIAprep Spin Miniprep Kit*” according to the manufacturer’s instructions. To extract large amount of plasmid DNA (up to 500 µg), 500 µl of the small scale cell suspension was used to inoculate 100 ml LB medium containing the appropriate antibiotic. After shaking overnight at 37°C the plasmid DNA was isolated using the Qiagen “*QIAfilter Plasmid Maxi Kit*” according to the manual provided. All DNA constructs were stored at -20°C.

2.3.1.6 Determination of nucleic acid concentration

DNA and RNA amounts were determined using a spectrophotometer. The nucleic acid concentration was calculated as indicated below:

$$\text{DNA OD}_{260} \times 50 \mu\text{M/ml}$$

$$\text{RNA OD}_{260} \times 40 \mu\text{M/ml}$$

2.3.1.7 Amplification of DNA fragments

PCR is a method that relies on thermal cycling, consisting of denaturation by heat, annealing of oligonucleotide primers and extension of DNA sequence between the primers by a thermostable DNA polymerase. In further cycles the amplified DNA is used as a template itself for replication so that the DNA of interest is exponentially amplified (Mullis and Faloona, 1987).

PCRs were carried out to prepare DNA fragments for cloning (preparative PCR) or for genotyping (analytical PCR) using genomic DNA extracted from mouse tails as described in 2.3.2.2. Unless otherwise mentioned the following reaction setup and parameters were used for PCR:

Table 5

Reaction mix	Concentration	
	Preparative PCR	Analytical PCR
Template	~ 1 µg	2 µl (~ 10 ng-100 ng)
Forward primer	2.5 µl (0.5 µM)	0.5 µl (0.5 µM)
Reverse primer	2.5 µl (0.5 µM)	0.5 µl (0.5 µM)
Buffer / polymerase / dNTPs	25 µl Phusion® Mastermix	10 µl Phusion® Mastermix
DMSO	-	0.6 µl (3 %)
ddH ₂ O	to 50 µl	to 20 µl

Table 6

Step	Temperature	Time	Cycle
Initial denaturation	98°C	30 s	1x
Denaturation	98°C	10 s	
Annealing	T _m + 3°C	30 s	25x – 35x
Extension	72°C	20 s / 1 kb	
Final extension	72°C	10 min	1x
Hold	4°C	∞	1x

2.3.1.8 PCR product purification and analysis

PCR products were analysed with agarose gel electrophoresis and extracted using the “QIAquick Gel Extraction Kit” according to the manual provided. Clean up from enzymatic reactions was done with the “High Pure PCR Product Purification Kit”.

2.3.1.9 Total RNA preparation

The tissue was dissected as described in 2.3.3 and stored in Qiagen *RNAlater*[®] according to manual instructions. Total RNA preparation was done using Qiagen “*RNAeasy mini kit*” or “*RNAeasy midi kit*” depending on the amount of extracted tissue. RNA Isolation and cleaning was performed as described in the manual. Total RNA was dissolved in 30 – 50 µl RNase-free double-distilled H₂O, the concentration was determined spectrophotometrically and the RNA was stored at -80°C.

2.3.1.10 Reverse-transcription polymerase chain reaction (RT-PCR)

First strand cDNA synthesis was performed using avian myeloblastosis virus (AMV)- reverse transcriptase (Roche) according to the manufacturer’s instructions. Briefly, to 1 µg of total RNA 5x AMV buffer was added and everything was mixed with 1 µM oligo dTs and 1 mM of each dNTP. To ensure denaturation of RNA secondary structures the reaction mix was incubated for 2 min at 68°C. For cDNA synthesis 10 units of reverse transcriptase (RT) and 20 units of RNase inhibitor were added. For negative controls, the RT was replaced by RNase-free H₂O. To support the annealing of the oligo dTs the reaction mix was cooled down to 25°C for 10 min followed by an elongation period at 42°C for 40 min. For enzymatic degradation the mixture was incubated at 99°C for 5 min before the cDNA was cooled down to 4°C and stored at -20°C.

2.3.1.11 Quantitative real time PCR (qRT-PCR)

Quantitative real time PCR was performed utilizing the LightCycler 1.5 instrument (Roche). Specific primers were used to amplify and detect 220 – 460 bp of the different GIRK subunits in mouse and rat (table 2). Copy numbers were calculated by a standard concentration curve using serial dilutions of plasmid DNA (10^4 , 10^5 , 10^6 and 10^7 copies/µl) for each GIRK subunit. The copy number of each standard was estimated with the following formula:

$$\text{number of copies} = (\text{amount} * 6.022 \times 10^{23}) / (\text{length} * 1 \times 10^9 * 650)$$

Assays were performed using the Fast start DNA Master SYBR Green I assay (Roche) according to the manufacturer's instructions. All experiments were performed in duplicates or triplicates. To ensure detection of proper products all samples were analyzed by melting curves and sequenced once after amplification. Melting curves were automatically calculated by the LightCycler system and plotted as the ratio of changes of fluorescence to temperature changes [-ΔF1/ ΔT] over temperature. Data were analyzed using the LightCycler software 3.5 (Roche).

The following reaction setup and parameters were used for qRT-PCR:

Table 7

Component	Volume	Final concentration
Forward primer	1 µl	0.5 µM
Reverse primer	1 µl	0.5 µM
MgCl ₂	2.4 µl	4 mM
Fast start DNA Master mix (Fast start Taq DNA polymerase, SYBR green dye, dNTP mix and buffer)	2 µl	1x
Template (cDNA or standard)	2 µl	
ddH ₂ O	11.6 µl	
Final volume	20 µl	

According to the instructions of the manufacturer the temperature and time profiles were the following:

Table 8

Analysis mode	Cycles	Segment	Temperature	Time	Mode
none	1		95°C	10 min	None
Quantification	45	Denaturation	95°C	10 s	None
		Annealing	55°C -60°C primer dependent	8 s	None
		Extension	72°C single read at 84°C - 90°C dependent on the amplification product	18 s	Single
Melting curve	1	Denaturation	95°C	0 s	None
		Annealing	65°C	15 s	None
		Melting	95°C slope = 0.1°C / sec	0 s	Continuous
None	1	Cooling	40°C	30 s	None

2.3.2 Generation of BAC transgenic mice

The preparation of a transgenic mouse provides an experimental tool to analyse the effect of the overexpression of a gene *in vivo*. We generated transgenic animals by using a bacterial artificial chromosome (BAC) which is able to incorporate long DNA sequences (up to 300 kb). This gives the advantage to insert, beside the gene of interest, regulatory elements such as a promoter for direct, accurate and cell specific expression *in vivo*. Additionally, the protein of interest can be fused to an epitope tag (e.g. Flag-tag), for targeting of the recombinant protein in the transgenic animal. After the cloning of a BAC construct the DNA is injected into the nucleus of fertilized mouse oocytes following a transfer to pseudopregnant foster mothers. The arising pups have to be tested for the presence of the BAC transgene.

The BAC for Na_v1.8-GIRK2 mice was constructed by Dr. Jeanette Rientjes (EMBL Monterotondo, Italy). A mouse BAC clone (RP23-391G10) encompassing a 134 kb promoter region of *scn10a* (encodes Na_v1.8) and another complete gene *scn11a* (encodes Na_v1.9) was modified in several steps. First the kanamycin resistance marker was replaced by ampicillin. While doing so, the loxP site and 21 kb of the BAC insert were deleted. This led to a 113 kb *scn10a* promoter region and cut out the first 7 exons (12 kb) of *scn11a*. For selection into the BAC clone a flippase recognition target (FRT)-neomycin cassette was inserted downstream of the Flag-GIRK2-polyA construct. The start codon (ATG) of the Flag-GIRK2-polyA-FRT-neo-FRT construct was placed at the position of the start codon of the Na_v1.8. While doing so, the whole first Na_v1.8 coding exon and the splice donor of that exon were deleted. After the Flag-GIRK2-polyA construct was inserted into the BAC, the neo cassette was deleted leaving a FRT site behind downstream of the polyA sequence of the Flag-GIRK2-polyA construct. The described modifications led to a BAC encompassing the 113 kb promoter region of Na_v1.8 followed by the sequence of the Flag-GIRK2-polyA. The genes encoding Na_v1.8 and Na_v1.9 were trimmed in order to avoid functional expression of the two genes.

2.3.2.1 BAC DNA purification for transgenesis

All steps of BAC DNA isolation and purification were performed with the “*Large-construct kit*” (Qiagen) according to the manual provided. At the end the air-dried DNA pellet was dissolved in 100 µl 10 mM Tris-HCl pH 8.0 and incubated over night at room temperature. The next day another 100 µl of 10 mM Tris-HCl pH 8.0 were added. As a control the BAC DNA was digested with *SpeI* and *EcoRV*. Finally 1ng/µl linearized BAC DNA was used to inject fertilized oocytes of c57/Bl6-J mice.

2.3.2.2 Extraction of genomic DNA from mouse tails

For genotyping PCRs and southern blot, genomic DNA was extracted from mouse tails. The tissue was incubated over night at 55°C in 700 µl lysisbuffer and 35 µl proteinase K. The next day the samples were mixed by inverting the tubes. 250 µl of 5 M NaCl were added and samples were centrifuged at 5000 rpm for 15 min at 4°C. 800 µl of the supernatant were transferred into a new tube and mixed with 800 µl of isopropanol. The samples were mixed

by inverting the tubes and centrifuged for 15 min at 5000 rpm at 4°C. The supernatants were discarded and the pellets were washed with 1 ml of 70 % ethanol. The DNA was spun down at 5000 rpm for 5 min. The supernatants were neglected and the DNA was dried for 1-2 h at RT. To dissolve the DNA 50 µl of “*Elution Buffer*” (Qiagen Kit) were added to the genomic DNA and sat until the next day at RT. 2 µl of the genomic DNA were used as template in the genotyping PCRs.

2.3.2.3 Genotyping of transgenic mice

All genotyping PCRs were carried out with Phusion® polymerase. Beside the amplification of the Flag-GIRK2 construct, genomic GAPDH was amplified to ensure intact genomic DNA (primers listed in table 2).

The following table lists the reaction setup. The thermocycling parameters are listed in table 6.

Table 9

Reaction mix	Concentration
Template	2 µl
Forward primer (GAPDH upper)	0.5 µl (0.5 µM)
Forward primer (Na _v 1.8-GIRK2)	0.5 µl (0.5 µM)
Reverse primer (GAPDH lower)	0.5 µl (0.5 µM)
Reverse primer (Na _v 1.8-GIRK2)	0.5 µl (0.5 µM)
Buffer / Polymerase / dNTPs	10 µl Phusion® Mastermix
DMSO	0.6 µl (3 %)
ddH ₂ O	to 20 µl

2.3.2.4 Determination of transgenic copy number

It has been shown that an increased copy number of BACs, integrated into the genome of a founder, correlates with an increased expression of the protein encoded by the BAC. Therefore, it is important to determine the copy number of the founder to be used for the breeding of the transgenic mouse line. To detect the copy number of a transgene distinct standards are needed. For standardization genomic wildtype DNA was spiked with a certain amount of BAC DNA to obtain 2, 4, 8, 16 and 32 copy standards. The amount of BAC DNA added to the wildtype DNA was calculated using the following formula:

$$\text{number of copies} = (\text{amount} * 6.022 \times 10^{23}) / (\text{length} * 1 \times 10^9 * 650)$$

Based on the fact that the haploid mouse genome is 2716965481 bp long a 10 ng (qRT-PCR standard) solution of genomic DNA should contain 1705 copies. The BAC length (202465 bp) and concentration was used to calculate the amount of BAC DNA that was added to the genomic DNA to obtain the different standards. Southern blot standards were established with a 10 μ g solution of genomic DNA. For copy number detection qRT-PCR (see 2.3.1.11) and southern blot was used. The reaction setup as well as the temperature and time profile for qRT-PCR is described in table 7 and 8, primers are listed in table 2.

2.3.2.5 Southern blot

This method was used to determine the copy number of the transgenic founder and enables the detection of a gene sequence in a mix of DNA such as genomic DNA. DNA fragments are separated by electrophoresis and transferred to a nylon membrane. Finally, a fragment of the DNA can be verified through hybridization with a probe that recognizes the sequence of interest.

For membrane hybridization a 548 bp long probe was derived from BAC DNA using PCR with primers listed in table 2. The PCR product was isolated by gel electrophoresis and extracted with the “*MinElute Gel Extraction Kit*” (Qiagen).

To obtain short fragments for the electrophoresis, 8 μ g of genomic DNA from Na_v1.8-GIRK2 mice and wildtype c57/Bl6/J mice as well as 10 μ g of each standard (see 2.3.2.4) were digested with the restriction enzyme *Nco*I over night at 37°C. The digests were run on a 0.8 %

agarose gel for 13 h at 34 V. After analysis of the digestion the gel was washed twice with ddH₂O and equilibrated two times with alkaline solution for 20 min to denature the double-stranded DNA. This improves the binding of the negatively charged DNA to a positively charged membrane and destroys residual RNA. To transfer the DNA fragments onto the membrane the following construction was built. The agarose gel was set on 4 layers of 3M papers and the nylon membrane was placed on top of the gel followed by 3 layers of 3M papers. On top of the pile 2 boxes of paper towels and two bottles filled with 100 ml were used to ensure good and even contact between the gel and the membrane. The transfer of the DNA from the membrane to the gel was carried out by capillary action over night with a sufficient amount of fresh alkaline solution at the bottom of the blotting sandwich. The next day the blotting sandwich was removed and the membrane was equilibrated two times for 15 min in TRIS buffer before the membrane was dried at 37°C for 1 h. To permanently attach the transferred DNA to the membrane the nylon membrane was crosslinked for 2 h with UV light (Stratalinker). Before the DNA was exposed to the hybridization probe the membrane was prehybridized with 15 ml hybridization solution for 2 h at 65°C in a cylinder. In the meantime the probes were radioactively labelled with the “Random Primers DNA Labeling System” (Invitrogen) according to the manual. 25 ng of the cleaned PCR product was labelled with approximately 50 µCi [α -³²P]dGTP. The radioactive labelled probe was mixed with 15 ml fresh hybridization buffer and incubated with the membrane overnight.

The next day the hybridization reaction was discarded and the membrane was rinsed once with 15 ml wash buffer. Under gentle agitation the membrane was washed twice with wash buffer for 30 min at 65°C. Afterwards the radioactivity was measured. Finally the membrane was wrapped in plastic foil and exposed to an x-ray film in a cartridge for 24 h. The next day the film was developed in a phosphoimager.

2.3.3 Tissue preparation for immunohistochemistry and DRG culture

For DRG cultures mice or rats were sacrificed with isoflurane, the bones and the whole spinal cord were removed by laminectomy and the lumbar as well as a few thoracic DRGs were dissected. For immunohistochemistry animals were deeply anaesthetized with isoflurane and cleaned from blood by a transcardial wash with 1x PBS or 0.1 M PB. The tissue was fixed by transcardial perfusion with fixation buffer and dissected. The excised tissue was post-fixed for 2-4 h in fixation buffer and cryoprotected overnight in 30% sucrose. The DRGs and spinal

cord were frozen in 2-methylbutane on dry ice, embedded in frozen section medium and stored at -80°C. The cerebellum was directly embedded and stored at -80°C.

2.3.4 Cell culture methods

The analysis of the interaction between GIRK channels and opioid receptors was done in HEK293 cells and DRG neurons. As a control most of the experiments were performed primarily under simplified circumstances in transfected HEK293 in which the proteins of interest were overexpressed. Mammalian cells were grown at 37°C in 5 % CO₂ in a cell incubator and handled in a hood under sterile conditions. HEK293 cells were maintained in Dulbecco's Modified Eagle Medium (DMEM) supplemented with 10 % fetal bovine serum (FBS) and 1 % penicillin/streptomycin.

2.3.4.1 Transfection

Transfection is a process of inserting foreign DNA into cells to monitor and control protein expression. The transfection of HEK293 cells was done using FuGENE®HD, a multi-component nonliposomal transfection reagent which forms complexes with the exogenous DNA and enables its uptake into the cells. The reaction mix for a 35 mm cell culture plate contained 1.5 µg DNA (ratio 1:4 of plasmid DNA encoding GIRK or mu-opioid receptor respectively) and 6 µl FuGENE®HD in 100 µl OptiMEM medium. After 15 min incubation at room temperature the mix was dropwise added to the cells. A plasmid encoding yellow fluorescent protein (0.1 µg of pEYFP-C1) was used as a control to determine transfected cells. Cells used for electrophysiology were separated 12 h after transfection. Therefore, the culture medium was discarded, the cells were washed once with PBS and incubated with 500 µl trypsin for 3 min at 37°C. Dissociation was stopped by the addition of 1 ml culture medium. After centrifugation the cell pellet was resuspended in 1 ml fresh medium and 30 - 50 µl of the cell suspension were plated on poly-l-lysine (100 µg/ml) coated glass coverslips.

2.3.4.2 AAV infection of DRG neurons

Adeno-associated viruses (AAV) can infect dividing and non-dividing cells. This makes the virus a good candidate to infect neurons. There are different serotypes of AAVs known which show different preferences concerning the tissue type they infect. In our experiment the best studied serotype AAV-2 was used.

DRG neurons were infected with 1×10^9 virus particles plated on a 35 mm cell culture dish. The cells were incubated with the virus diluted in 700 μl mouse DRG medium for 45 min in the cell incubator. Afterwards 1.3 ml of DRG medium was added to the 700 μl and incubated for another 24 h. The next day the medium was changed and the DRG were left for 5 d in the incubator before patch clamp experiments were performed.

2.3.4.3 Primary mouse DRG culture

The tissue for the DRG cultures was dissected as described in 2.3.3 and collected in PBS. DRGs were incubated in 1 mg/ml collagenase IV followed by incubation in 0.05 % trypsin for 28 min respectively at 37°C. The DRGs were suspended in mouse DRG medium and dissociated by passing them through 18G, 22G and 25G needles. Separation of the cells from the debris was achieved by using a 40 μm cell strainer. After centrifugation the cell pellet was resuspended in 300 – 1000 μl mouse DRG medium. 60 – 100 μl of the cell suspension was seeded on poly-lysine (100 $\mu\text{g}/\text{ml}$) coated cell culture plates (35 mm) or glass coverslips and left to adhere for 30 min in the incubator before the plates were floated with 2 ml medium. On the next day the cells were used for AAV-infection, electrophysiology recordings, immunostainings or K⁺ imaging experiments.

2.3.4.4 Primary rat DRG culture

After dissection (2.3.3) rat DRGs were collected in 1 ml working medium (rat DRG medium without serum) and were incubated for 50 min with 3 mg/ml collagenase type II followed by a 10 min incubation with additional 1 mg/ml trypsin type I at 37°C, respectively. Trituration of the DRGs was achieved though the shearing forces of a 1 ml pipette by pipetting up and down for about 20 times. Debris and cells were separated with a 40 μm cell strainer and by a

centrifugation step with 5 % BSA (80 mg in 4 ml working medium). The supernatant was discarded and the pellet was resuspended in 5 ml working medium. After additional centrifugation the cells were solved in an appropriate amount of working medium (2 – 3 ml) and 200-300 µl of the cell suspension was seeded on poly-lysine (100 µg/ml) coated cell culture plates (35 mm) or glass coverslips and left to adhere for 30 min in the incubator before the plates were floated with 2 ml rat DRG medium (with serum). On the next day the cells were used for electrophysiology recordings or immunostainings.

2.3.5 Immunohistochemistry

Immunohistochemistry was used to determine the distribution and localization of GIRK channels in tissue sections. Visualization was achieved by two different approaches. Most of the stainings were visualized with immunofluorescence using first or secondary antibodies linked to different fluorophores. If the result with immunofluorescence was not convincing, antibodies conjugated to peroxidase were used. The peroxidase catalyzes a chemical reaction to produce a coloured product. Tissue was prepared as described in 2.3.3. DRGs and sciatic nerves were sectioned at 10 – 12 µm, spinal cord at 14 µm and the cerebellum was stained as floating sections with a thickness of 40 µm. The following table lists the steps of the protocol for both procedures. Anti-GIRK1 (Alomone) and anti-GIRK2 (Alomone) antibodies were used at 1:200. FITC-labeled IB4 (Vector Laboratories), a glycoprotein that binds to alpha-D-galactosyl residues on proteins or lipids, was also used in a dilution of 1:200. Anti-GIRK2 (Chemicon) and anti-FLAG (Sigma-Aldrich) antibodies were used in a dilution of 1:500 and NF200 (Sigma-Aldrich) in a dilution of 1:800. Dependent on the result of the staining, fluorescent secondary antibodies conjugated with FITC (goat anti-chicken, 1:200, Vector Laboratories) and Texas red (goat anti-rabbit, 1:200, Vector Laboratories) were used, or the sections were stained with diaminobenzidine (DAB) as a substrate, using biotinylated (goat anti-rabbit, VECTASTAIN Elite Kit; Vector Laboratories) secondary antibodies and a VECTASTAIN avidin-biotin peroxidase complex according to the manufacturer's instructions. All experiments were also performed without the first antibody to confirm their specificity.

Table 10

	Immunofluorescence	Immunoperoxidase
Blocking of endogenous peroxidase	-	45 min with 0.6% H ₂ O ₂ and 50% methanol in PBS ⁺
Washing	-	3 x with PBS for 1 h
Blocking to avoid background staining	for 1 h with PBS ⁺ and 5% normal serum from species the 2nd antibody is made in	for 1 h with PBS ⁺ and 5% normal serum from species the 2nd antibody is made in
Incubation with first antibody	overnight in 2% serum in PBS ⁺ , the first 30 min at RT then at 4°C	overnight in 2% serum in PBS ⁺ , the first 30 min at RT then at 4°C
Washing	3 x with PBS for 1 h	3 x with PBS for 1 h
Incubation with second antibody	for 1 h in 2% serum in PBS+	with “ABC Elite Kit” (Vector) according to the manual
Washing	3 x with PBS for 1 h	3 x with PBS for 1 h
Avidin-biotin peroxidase treatment	-	2 h at RT following instructions of “ABC Elite Kit” (Vector)
Washing		3 x with PBS for 1 h
DAB development	-	according to the manual of the “Peroxidase Substrate Kit, DAB” (Vector)
Dehydration		slices were incubated in 80%, 90%, 100% ethanol followed by incubation in 80%, 90%, 100% Xylol respectively
Mounting	slices were covered with Moviol	slices were covered with VectaMount (Vector)

2.3.6 Immunocytochemistry

To detect GIRQ channels in cultured DRG neurons immunocytochemistry was used. The cells were cultured as described in 2.3.4.3. The dissociated DRG neurons were washed twice with PBS followed by a fixation in 4% PFA and 4% sucrose in PBS for 15 min at RT. After fixation, the cells were washed 2 x for 5 min in PBS. For permeabilization the cells were incubated in 0.25% Triton X-100 in PBS for 5 min followed by two more washes with PBS for 5 min, respectively. To block all unspecific binding sites, the cells were treated with 10% BSA in PBS for 30 min at 37°C followed by incubation with the first antibodies in 3% BSA in PBS for 2 h at 37°C. Anti-GIRQ2 (Alomone), anti-FLAG M2 (Sigma-Aldrich), anti-CGRP (Biomol) and anti-mu-opioid receptor (MOR) (Abcam) antibodies were used 1:1000. FITC-labeled IB4 was used in a dilution of 1:500. After three washes with PBS for 5 min respectively, secondary antibodies conjugated with Texas red (goat anti-mouse, 1:1000, Vector Laboratories) and FITC (goat anti-rabbit, 1:1000, Vector Laboratories) were applied for 45 min at 37 °C in 3 % BSA in PBS. The cells were washed 3 x for 5 min in PBS and covered with Moviol. To confirm the specificity all stainings were also performed without the first antibody.

2.3.7 Western blot

To detect GIRQ channel protein in homogenates from spinal cord and DRG neurons, western blots were performed. By this method the proteins are separated by molecular weight using gel electrophoresis. Afterwards proteins are transferred to a nitrocellulose membrane and finally detection with antibodies helps to identify the protein of interest. All steps of the protein extraction were performed on ice to avoid protein denaturation and degradation. The dissected tissue was stored on dry ice until lysis buffer was added (500 µl to the spinal cord and 100 µl to the DRGs). The tissue was mechanically solubilized by using a homogenizer for the spinal cord and a pestle for the DRGs. Afterwards the tissue was incubated in lysis buffer for another 30 min. To remove the debris the samples were centrifuged for 20 min at 13000 rpm at 4°C and the supernatant was transferred to a new tube. The protein concentration was spectroscopically quantified using the Bradford protein assay (Bradford 1976).

Between 50 µg and 75 µg of protein was separated by SDS-PAGE (sodium dodecyl sulfate polyacrylamide gel electrophoresis), which allows separation by their molecular weight after

denaturation of the protein by the detergent SDS. The gels for the SDS page consisted out of 4% stacking gels and 12% separating gels. The loaded protein was separated for ~2 h in running buffer. In the beginning, separation took place at 60 V to ensure proper migration of the samples into the gel and later at 120 V. For estimation of protein size a pre-stained protein ladder was also loaded onto the gel.

For antibody detection the separated proteins were transferred from the gel onto a nitrocellulose membrane for 1 h at 350 mA in blotting buffer using the “*Mini Trans-Blot cell*” (Biorad).

To prevent unspecific binding of antibodies, the membrane was blocked by incubation with blocking solution for 30 min at RT or overnight at 4 °C

To detect GIRK channel protein the membrane was incubated in primary anti-GIRK1 or anti-GIRK2 (Sigma) antibodies diluted 1:200 in blocking solution. The first h of incubation was carried out at RT followed by incubation at 4°C overnight. The membrane was washed 4 times for 10 min in TBS-T followed by incubation with an anti-rabbit peroxidase conjugated secondary antibody diluted 1:3000 in TBS-T. Again, the membrane was washed 4 times in TBS-T for 10 min before the protein bands were detected by enhanced chemiluminescence (ECL). The ECL solution interacts with the secondary antibody-bound peroxidase, which results in the emission of light. This enables detection of the protein using a photographic film.

2.3.8 Electrophysiology

This technique allows the study of the transport of charged ions across the cell membrane and the characterization of the ion channels which are involved in that carriage. For patch clamp recordings a micropipette is brought very close to the cell membrane so that a tight seal between the micropipette and the membrane can be formed. The part of the membrane “patch” which is enclosed by the micropipette is very small and encircles only a few ion channels. The micropipette comprises a silver wire (electrode) that is surrounded by a solution which reflects the ionic composition of the cytoplasm of the cells. The electrode conducts the currents to an amplifier where the electric signal is intensified. Changes in current flow can be measured if the voltage of a cell is fixed so that the membrane potential is “clamped”. Alternatively changes in membrane voltage can be observed while keeping currents constant. The cells are then current clamped. The recordings can be done in whole-cell mode that

enables to measure currents through multiple ion channels at once, over the membrane of the entire cell.

Whole cell patch clamp recordings were made on DRG neurons or transfected HEK293 cells 12-24 h after plating at room temperature. Gigaseals were formed with glass electrodes that had a resistance between 3 and 5 M Ω and were filled with intracellular pipette solution. Membrane currents were recorded under voltage-clamp conditions using whole-cell patch-clamp configuration with an EPC-10 amplifier and analyzed using Pulse software. Data were sampled at 10-20 kHz and filtered at 2-5 kHz. Capacitance was continuously monitored and compensated using the auto function of pulse. Whole cell patch clamp recordings were performed as described elsewhere (Raveh et al., 2010). Briefly, gigaseals were formed in extracellular low K $^{+}$ bath solution. Afterwards the bath solution was changed to extracellular high K $^{+}$ solution. GIRK currents were recorded as inward currents at -80 mV. The mu-opioid agonist DAMGO (10 μ M) was used to elicit GIRK currents, Ba $^{2+}$ (3 mM) and the opioid receptor antagonist naloxone (20 μ M) were used to block the DAMGO-induced currents. To monitor inward currents in nociceptors and mechanoreceptors (as distinguished by the shape of the action potential) whole cell configuration was established in extracellular bath solution. The neurons were hyperpolarized using a voltage ramp from -40 to -120 mV. To induce action potentials the amplifier was switched to current-clamp mode and currents were injected from 80 to 500 pA for 80 ms.

2.3.9 FluxORTM potassium ion channel assay

This assay uses the ability of potassium channels to transport not only potassium ions but also thallium (Tl $^{+}$) ions, which have a similar size. After adding thallium to the cells, a stimulus opens the potassium channels and allows thallium ions to flow down its concentration gradient into the cells. Intracellularly, the thallium can bind to a fluorogenic dye loaded into the cells as a membrane-permeable Acetoxyethyl (AM) ester. The increase in cytosolic fluorescence can then be monitored over time to detect channel activity.

DRG neurons from wildtype or Na v 1.8-GIRK2 mice, or transfected HEK293 cells were plated on Poly-L-Lysin coated glass coverslips and used 12-24 h after plating. All experiments were performed at room temperature and data were analyzed using Tillvision software. For assay

establishment, experiments were first performed in HEK293 cells transfected with the mu-opioid receptor and GIRK2 channels.

The FluxOR™ Potassium Ion Channel Assay (Invitrogen) was carried out according to the manufacturer's instructions and fluorescence was measured at excitation wavelength of 495 nm for 5 min. Briefly, transfected HEK293 cells were washed once with PBS and loaded for 60 min in the dark with 1 ml of the loading buffer containing the thallium sensitive dye. Cells were washed 3 times with PBS and monitored in assay buffer. DAMGO (10 µM) was diluted in stimulus buffer containing the Tl₂SO₄ and was applied 20 s after the measurement started. DRG neurons were washed once with PBS and incubated for 90 min with 1 ml of the loading buffer in the dark. Neurons were washed three times with PBS following an incubation for 30 min with assay buffer containing Tetraethylammonium chloride (20 mM) and Glibenclamide (20 µM) to block voltage-gated and ATP-sensitive K⁺ channels. Twenty seconds after the recording started neurons were treated with DAMGO (10 µM) or the delta-opioid receptor agonist DPDPE (10 µM) diluted in stimulus buffer. As a control neurons were treated with stimulus buffer without opioids. For statistical analysis the area under the curve was calculated for each investigated cell. The DRG neurons were extracted from 3-4 animals.

2.3.10 Behavior

For behavioral tests mice were adapted to testing apparatuses for 7 d, 2-3 times a day before nociceptive tests were carried out. All experiments were performed in Na_v1.8-GIRK2 as well as in wildtype mice. In all experiments 6-8 animals per group were used. The experimenter was unaware of the type of treatments and the genotype of the animals.

2.3.10.1 Thermal nociception

Thermal hyperalgesia was analyzed using the Hargreaves test. Animals were trained to sit on a glass floor. Radiant heat was applied to the plantar surface of a hind paw with a high-intensity light beam, and paw withdrawal latency was measured with an electronic timer (ITC Inc/Life Science). The cut-off was 20 sec to avoid tissue damage. Measurements were done at least two times on each paw and the mean of the values were used for statistical analysis.

The effect of different DAMGO concentrations (volume 20 µl) injected into the right hind paw was measured 5, 15, 30, 45 and 60 min after injection.

2.3.10.2 Mechanical nociception

Mechanical withdrawal thresholds were measured by Dr. Dominika Labuz (Dep. of Anaesthesiology and Intensive Care Medicine, Charité, Campus Benjamin Franklin) using calibrated von Frey filaments applied to the plantar surface of the inflamed mouse hind paw (Stoelting, Wood Dale, IL). The measurements were started with a 3.9 mN hair (0.4 g). If the mouse withdrew the paw, a weaker hair was used for the next measurement. If there was no withdrawal of the hind paw a stronger hair was applied. The measurements were repeated 6-9 times and the strongest hair tested (cut-off) was 39.2 mN (4 g).

2.3.10.3 Induction of inflammation

20 µl of Complete Freund´s adjuvant (CFA) were injected into mouse right hind paws. The injection was performed under light isoflurane anesthesia. The animals showed an increased sensitivity to noxious stimuli (hyperalgesia) 48 h after induction of the inflammation, and the paw was swollen and hyperemic. No significant difference in feeding behavior, body temperature or body weight could be observed between animals with an inflammation and untreated control animals.

Two days after CFA injection mice were tested for responses to heat and mechanical stimuli as described in 2.3.10.1 and 2.3.10.2 and the antinociceptive effect of DAMGO injected into the right hind paw was determined as described above. The time point and concentration of maximum effect were used to test for opioid receptor specificity with the unselective opioid receptor antagonist naloxone-methiodide (5 µg) injected together with DAMGO into the paw. This antagonist is not able to cross the blood brain barrier, thus it acts only in the periphery.

2.3.11 Statistical data analysis

All data are presented as mean \pm s.e.m. For data analysis and plot drawing SigmaStat and SigmaPlot (Systat) software was used. Two-sample comparisons were made with the Student's t-test or, for non-parametric data, with the Mann-Whitney rank sum test.

For more than two experimental groups a one-way measurements analysis of variance (ANOVA) was used. A Kruskal-Wallis ANOVA on Ranks was used for non-parametric data followed by Dunn's method for all pairwise comparisons. If two different factors in more than two groups were verified a two-way ANOVA was used. Both were followed by a Holm-Sidak test for comparison versus a control group. For repeated measurements a one-way or two-way repeated ANOVA was used, followed by Bonferroni test for pairwise comparison or by Holm-Sidak test if the data were compared to a control group. For non-parametric data a one-way repeated measures ANOVA on Ranks was used.

3 Results

3.1 GIRK channel expression in peripheral sensory neurons

3.1.1 GIRK channel mRNA expression in DRG neurons of mice and rats

Using qRT-PCR I analyzed mRNA expression levels of all four GIRK subunits in different mouse tissues. Because it was shown that GIRK1, -2 and -3 are broadly expressed in the cerebellum (Aguado et al., 2008), this tissue was used as a positive control for mRNA expression of these subunits. The subunit GIRK4 is mainly expressed in atrial myocytes (Corey and Clapham, 1998; Kennedy et al., 1999; Krapivinsky et al., 1995). Therefore, cardiac muscle was used as a control for GIRK4. Gene expression of all four GIRK subunits was also determined in DRG neurons of healthy c57/Bl6 mice and in lumbar DRG neurons (L3 to L6) of mice with unilateral paw inflammation. The DRG neurons innervating the inflamed hind paw (ipsilateral) were compared to DRGs from the non-inflamed contralateral side (control).

As shown in figure 6 the mRNA levels of all four GIRK subunits were significantly lower in mouse DRG neurons compared to mouse cerebellum or heart. There was no mRNA up-regulation of any subunit due to hind paw inflammation.

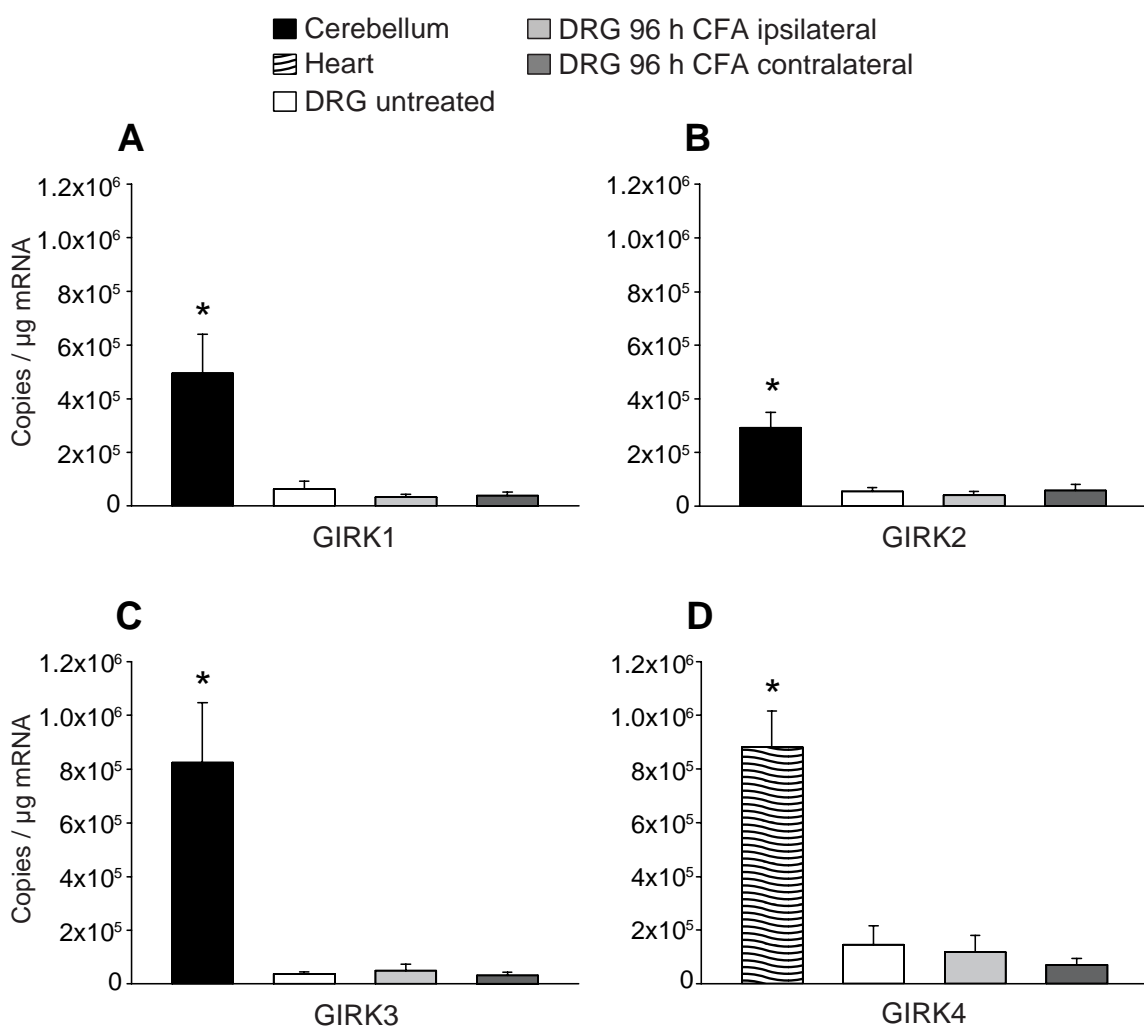


Figure 6 Quantification of Girk channel mRNA in mouse cerebellum, heart and DRG neurons. The mRNA of Girk1-4 (A, B, C and D) was examined in DRG neurons of untreated animals and in DRG neurons innervating the inflamed (ipsilateral) or the non-inflamed (contralateral) paw. As a positive control cerebellum (A-C) or heart (D) was used. Samples from at least 6 animals per group were measured. Data are expressed as mean \pm s.e.m. *P<0.05 indicates a significant difference compared to cerebellum or heart (Kruskal-Wallis ANOVA on Ranks, Dunn's method).

To determine Girk channel expression in peripheral sensory neurons of rats I examined mRNA levels of the subunits Girk1 and -2 in rat DRG neurons. These subunits are known to form heterotetramers in the spinal cord and contribute to mu-opioid receptor-mediated antinociception due to activation by $G_{\beta\gamma}$ subunits (Marker et al., 2005).

Expression levels were determined in cerebellum (positive control), in DRG neurons from healthy rats, and from rats with a 72 h paw inflammation. As shown in figure 7 Girk1 and Girk2 mRNA levels in rat DRG neurons were not significantly different from cerebellum.

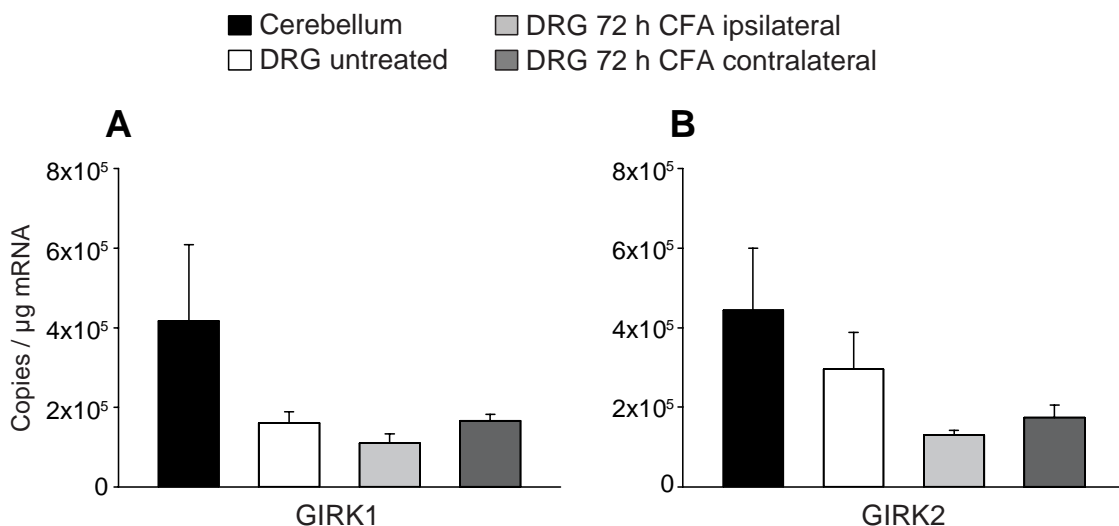


Figure 7 Quantification of GIRQ1- and -2-mRNA in rat cerebellum and DRG neurons. mRNA levels of GIRQ1 (A) and GIRQ2 (B) were examined in normal DRG neurons and in DRGs isolated 72 h after CFA injection into the right hind paw. Cerebellum was used as a positive control. Samples from at least 3 animals per group were measured in duplicates or triplicates. Data are expressed as mean \pm s.e.m. Statistical analysis showed no significant difference between cerebellum and DRG neurons (Kruskal-Wallis ANOVA on Ranks).

3.1.2 GIRQ channel protein expression in mouse and rat

To assess whether GIRQ protein is expressed in mouse and rat DRG neurons, I performed immunohistochemistry using antibodies against the subunits GIRQ1 and -2. The specificity of all antibodies was confirmed by omission of primary antibodies (Appendix, Fig. 33, 34, 35). Figure 8 illustrates staining of mouse cerebellum and DRGs from healthy animals. Mouse cerebellum was used as a positive control. In mice no GIRQ1 or GIRQ2 protein could be detected in DRG neurons whereas both antibodies produced immunoreactivity in the cerebellum.

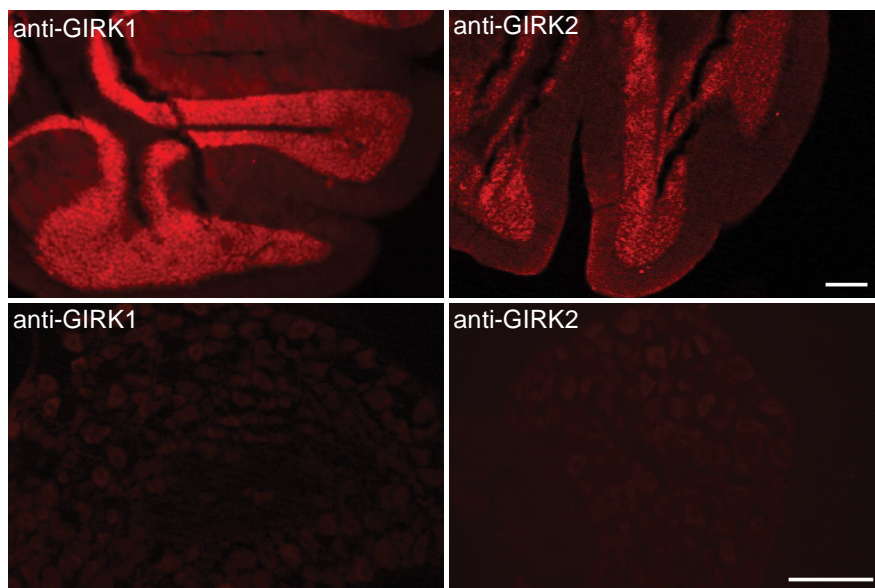


Figure 8 Immunoreactivity for GIRQ1 and GIRQ2 demonstrates the expression of GIRQ channel protein in mouse cerebellum (upper panel) but not in mouse DRG neurons (lower panel). Specificity of antibodies was confirmed by omission of the primary antibodies (Appendix, Fig. 33). The bars represent 50 μ m.

This was verified in western blot experiments. Figure 9 illustrates GIRQ channel protein in tissue lysates of mouse spinal cord stained with anti-GIRQ1 and anti-GIRQ2 antibodies. Spinal cord was used as a positive control since results using cerebellum as a positive control were not conclusive. Neither GIRQ1 nor GIRQ2 channel protein could be detected using the same antibodies on mouse DRG lysates. In the spinal cord GIRQ2 showed a higher molecular weight than expected from other studies (Chung et al., 2009; Jelacic et al., 2000; Liao et al., 1996).

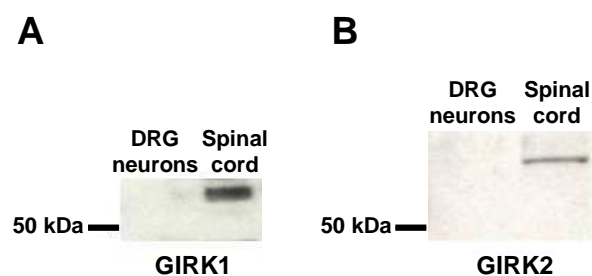


Figure 9 Western blot analysis of GIRQ channels in mouse DRG neurons and spinal cord. Tissue lysates were stained with anti-GIRQ1 (A) and anti-GIRQ2 (B) antibodies. 50 μ g of total protein was loaded per lane.

I also performed immunostainings on rat DRG sections with antibodies against GIRQ1 and -2. No positive control (e.g. cerebellum) was used since I obtained positive stainings for GIRQ1 and -2 in DRG neurons. To investigate the types of peripheral sensory neurons expressing GIRQ channels I performed co-staining with neuronal markers. Isolectin-B4 (IB4) was used to label nonpeptidergic C fibers and an antibody against neurofilament 200 (NF200) was used to designate myelinated A β and A δ fibers (Lawson and Waddell, 1991). Very few rat DRG neurons co-expressed GIRQ1 and NF200 whereas most of the GIRQ1 positive cells were also IB4 positive (yellow color in figure 10).

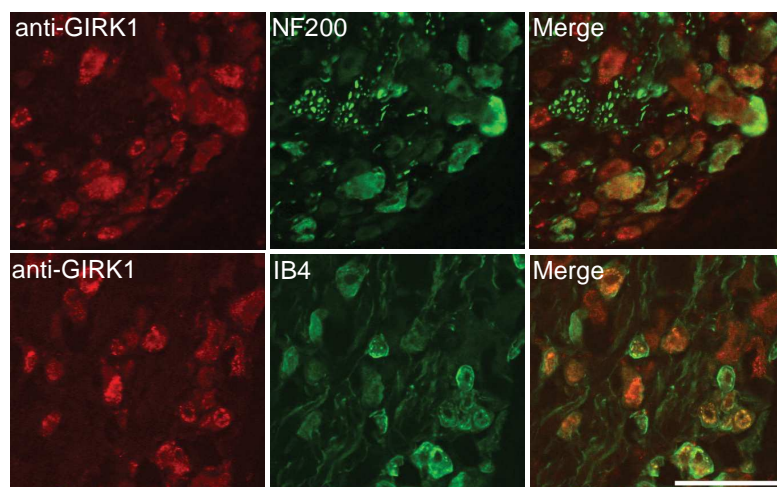


Figure 10 Immunoreactivity (yellow) for GIRQ1 channels in nonpeptidergic unmyelinated isolectin-B4 (IB4)-positive rat DRG neurons and to a lower extent in myelinated neurons expressing neurofilament 200 (NF200). Specificity of antibodies was confirmed by omission of primary antibodies (Appendix, Fig. 34). Scale bar represents 50 μ m.

Similarly, GIRQ2 channels were not expressed in myelinated NF200 positive rat neurons (figure 11, upper panel) but were mainly present in unmyelinated C-fibers indicated by the co-staining (yellow) of GIRQ2 and IB4 (figure 11, lower panel).

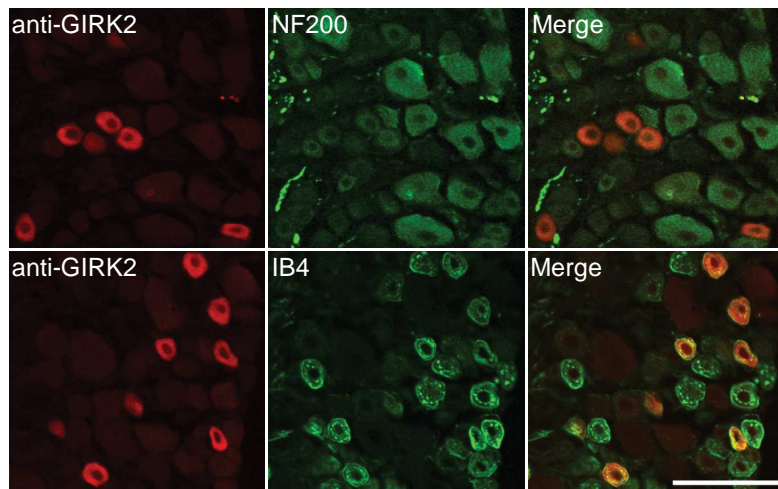


Figure 11 Immunoreactivity (yellow) for rat GIRQ2 in nonpeptidergic unmyelinated isolectin-B4 (IB4) positive DRG neurons but not in myelinated neurons expressing neurofilament 200 (NF200). Specificity of GIRQ2 antibodies was shown by immunoreactivity in DRGs from $\text{Na}_v1.8\text{-GIRQ2}$ mice. No immunoreactivity was detected in wildtype DRGs. In addition experiments were performed without primary antibodies to confirm their specificity (Appendix, Fig. 35). Scale bar, 50 μm .

Taken together, GIRQ1 and -2 channels are present in peripheral sensory neurons of rats and their expression is restricted to nonpeptidergic C-fibers.

3.2 Coupling of GIRQ channels and mu-opioid receptors in rat and mouse DRG neurons

To investigate functional coupling of GIRQ channels and opioid receptors in DRG neurons I used whole cell patch clamp recordings to measure GIRQ currents after opioid receptor activation.

3.2.1 Establishment of GIRQ channel whole cell patch-clamp recordings in DRG neurons

The protocol was first tested in HEK293 cells transfected with plasmid DNA encoding GIRQ subunits 1 and 2 and the mu-opioid receptor. Recordings were done in whole cell mode and

voltage ramps from -40 down to -120 mV from a holding potential of -50 mV were applied. I measured inward currents after activation of mu-opioid receptors with 10 μ M DAMGO. To ensure that the recorded inward currents were evoked by GIRQ channels I used the GIRQ blocker tertiapin-Q (100 nM). The basic inward currents were -165.4 pA. DAMGO application increased peak inward currents to -742.2 pA and tertiapin-Q reduced the currents to -30.9 pA. Figure 12 shows averaged inward currents of 7 cells. The currents were normalized to basic currents elicited by hyperpolarizing voltage steps (control). Since some of the cells died during tertiapin-Q treatment the currents of only 4 cells were used for analysis after application of the antagonist.

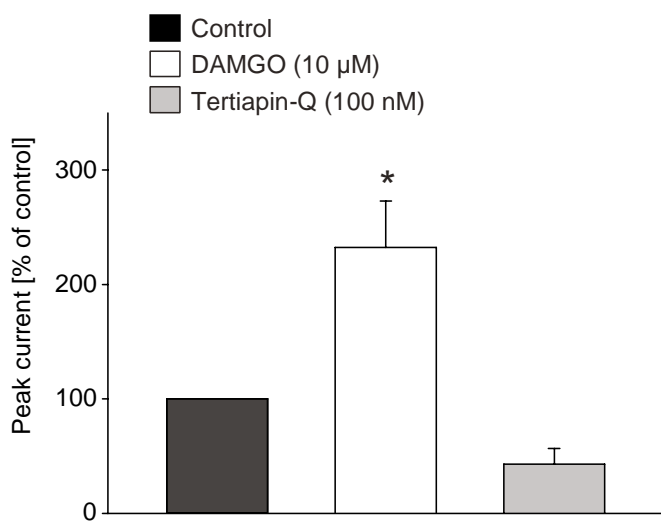


Figure 12 Peak inward currents in HEK293 cells transfected with GIRQ1, GIRQ2 and the mu-opioid receptor. A voltage ramp from -40 to -120 mV was applied, whole cell currents were induced by DAMGO ($n = 7$) and inhibited with tertiapin-Q ($n= 4$). Data are expressed as mean \pm s.e.m. * $P<0.05$ indicates a significant difference against control and tertiapin-Q group (one way repeated measures ANOVA on Ranks on raw values).

Next I investigated GIRQ-specific inward currents evoked by a voltage ramp from -40 to -120 mV in normal mouse DRG neurons and in mouse DRG neurons infected with an adeno-associated virus (AAV) that led to the expression of GIRQ2. This was confirmed by immunostaining (not shown). Figure 13 shows voltage-ramp-induced currents of normal and infected mouse DRG neurons. The averaged currents of AAV-GIRQ2 infected neurons differed in their inward rectifying behavior compared to control currents since the expression

of GIRK channels alone without any activation by G_{i/o}-coupled (e.g. opioid) receptors already produced larger inward currents compared to those recorded from control cells.

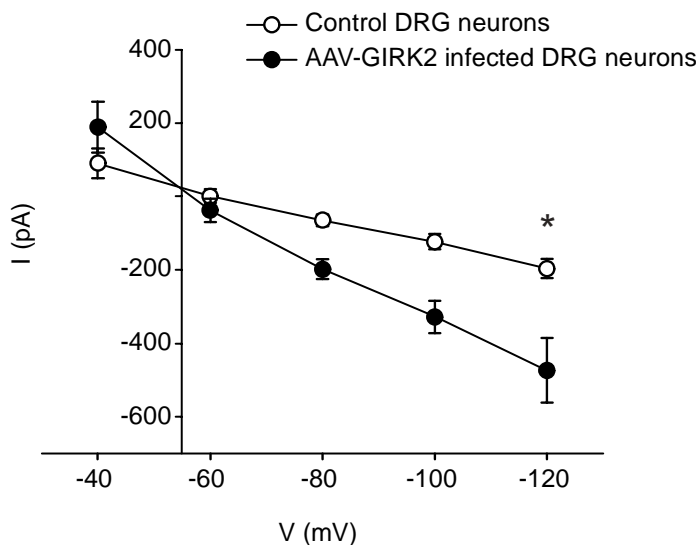


Figure 13 Inward currents evoked by voltage-ramps from -40 to -120 mV from a holding potential of -60 mV in normal mouse DRG neurons (control n = 6) and in mouse DRG neurons infected with AAV-GIRK2 (n = 4). Data are expressed as mean ± s.e.m. *P<0.05 indicates a significant difference compared to control cells at -120 mV (two way repeated measures ANOVA followed by Bonferroni t-test).

3.2.2 No functional coupling of GIRK channels and mu-opioid receptors in normal mouse DRG neurons

The same protocol as described in 3.2.1 was used. Normal mouse DRG neurons were stimulated with a voltage ramp from -40 down to -120 mV and treated with the mu-opioid receptor agonist DAMGO (10 µM) or with the antagonist tertiapin-Q (100 nM). As shown in figure 14 the application of DAMGO did not induce GIRK currents and the inward currents did not decrease after application of tertiapin-Q. The inward currents presented in figure 13 and 14 are not comparable since the DRG neurons infected with the AAV-GIRK2 virus as well as the control cells were 6 days old whereas the currents shown in figure 14 were recorded from 1 day old DRG neurons.

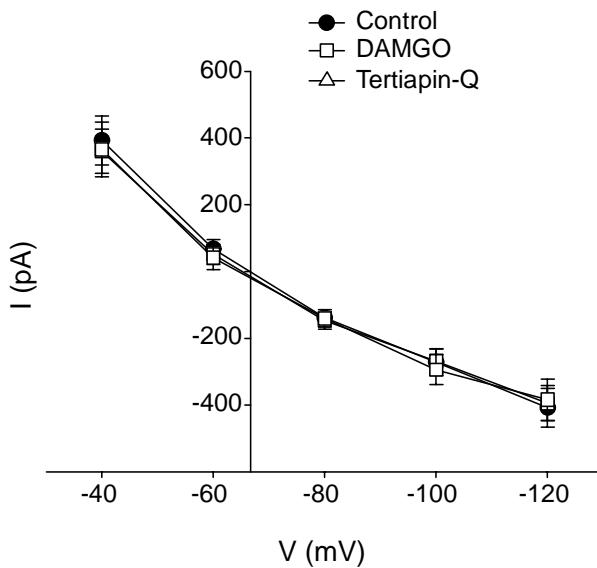


Figure 14 Inwardly rectifying currents in normal mouse DRG neurons. Cells ($n=55$) were stimulated with a voltage ramp from -40 to -120 mV and treated with $10 \mu\text{M}$ DAMGO ($n=47$) or with the GIRK channel blocker tertiapin-Q ($n=10$). Data are expressed as mean \pm s.e.m. Statistical analysis showed no significant differences (two way repeated measures ANOVA).

Nociceptors typically have small soma diameters ($< 25 \mu\text{m}$) and broad action potentials with a characteristic inflection in their falling phase (figure 15A). In contrast, mechanoreceptors are big diameter neurons ($> 25 \mu\text{m}$) with strait action potentials (figure 15A).

The patch clamp recordings illustrated in figure 14 represent an average of the inward currents from both mechanoreceptors and nociceptors. To examine DAMGO induced inward currents from nociceptors exclusively, I differentiated the cells based on their soma size and action potential shape. Mouse DRG neurons were stimulated by a voltage ramp from -40 to -120 mV and treated with $10 \mu\text{M}$ DAMGO. Peak currents at -120 mV from nociceptors were compared to the peak currents from mechanoreceptors. As seen in figure 15B there was no difference between these subtypes of mouse DRG neurons.

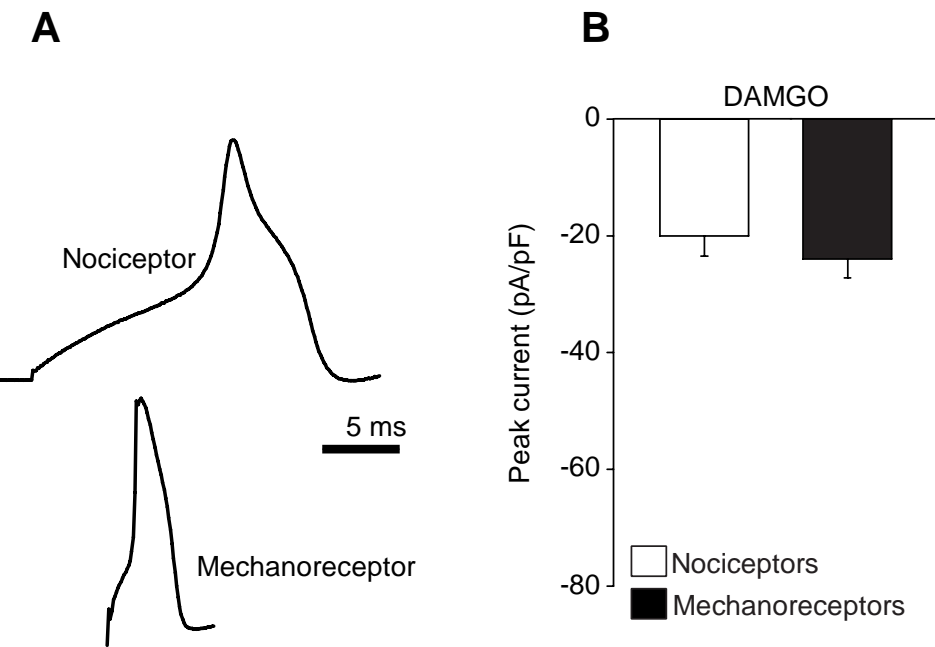


Figure 15 No difference between inward currents in mouse nociceptors and mechanoreceptors after DAMGO (10 μ M) application. (A) Representative action potential shapes of nociceptors (upper panel) and mechanoreceptors (lower panel) used to distinguish between DRG neuron subtypes. (B) No differences between average peak currents in mouse nociceptors and mechanoreceptors evoked by a hyperpolarizing step of -120 mV, n = 19-28 cells per group. Data are expressed as mean \pm s.e.m. Statistical analysis showed no significant difference (Mann-Whitney Rank Sum test).

To exclude the possibility that the voltage ramp used desensitized GIRK channels and thereby prevented GIRK current recording I performed patch clamp recordings on neurons held at -80 mV. In these and subsequent experiments I used barium chloride (Ba^{2+}) instead of tertiapin-Q as a blocker to assure inhibition of all possible GIRK channel combinations including homotetramers of GIRK2. This was based on our finding that inward currents in HEK293 cells transfected with GIRK2 alone were insensitive to tertiapin-Q (data not shown) whereas currents from cells transfected with both GIRK1 and -2 could be blocked with tertiapin-Q (figure 12).

Gigaseals were formed in low K^+ bath solution which was changed afterwards to high K^+ content. Inward currents were recorded at -80 mV and 10 μ M DAMGO was applied. The cells were treated with the GIRK channel blocker Ba^{2+} (3 mM) or with the non-selective opioid receptor antagonist naloxone (20 μ M). As shown in figure 16 no GIRK currents could

be measured after application of DAMGO and no changes occurred with antagonist treatments.

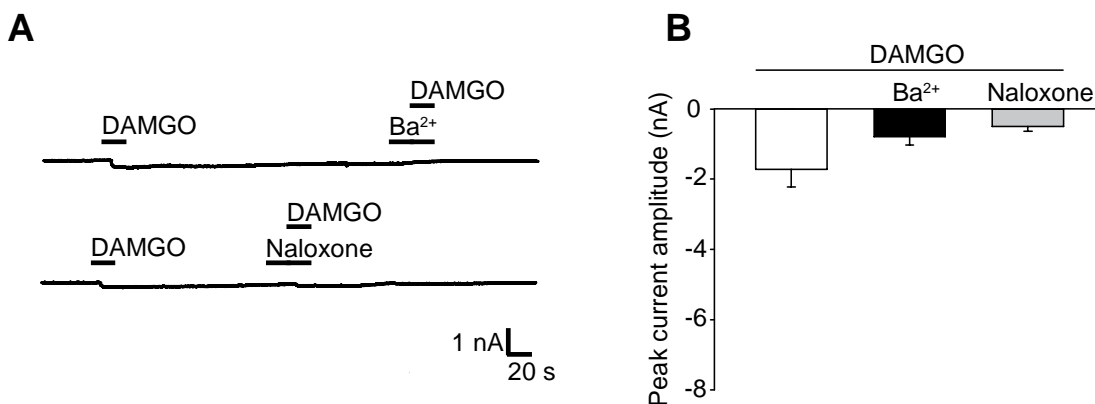


Figure 16 No presence of GIRK currents after DAMGO application in mouse DRG neurons voltage-clamped at -80 mV. (A) Representative inward currents measured after application of 10 µM DAMGO, 3 mM Ba²⁺ or 20 µM naloxone. (B) Average peak currents after agonist and antagonist application, n = 8 cells per group. Data are expressed as mean ± s.e.m. Statistical analysis showed no significant difference (one way repeated measures ANOVA).

Taken together, I found no evidence for inwardly rectifying currents in mouse DRG neurons in response to hyperpolarizing voltage steps, in voltage-clamped cells or to DAMGO treatment. Furthermore, mouse DRG neurons exhibited no basal activity of GIRK channels because application of tertiapin-Q or barium did not significantly change inward currents.

3.2.3 GIRK channels are coupled to mu-opioid receptors in rat DRG neurons

To record GIRK currents from rat DRG neurons I used the same protocol as described above. The application of DAMGO induced large inward currents which could be blocked by co-application of Ba²⁺ or naloxone. Representative current traces are shown in figure 17A. Statistical analyses of all DAMGO-induced currents and their blockage are shown in figure 17B.

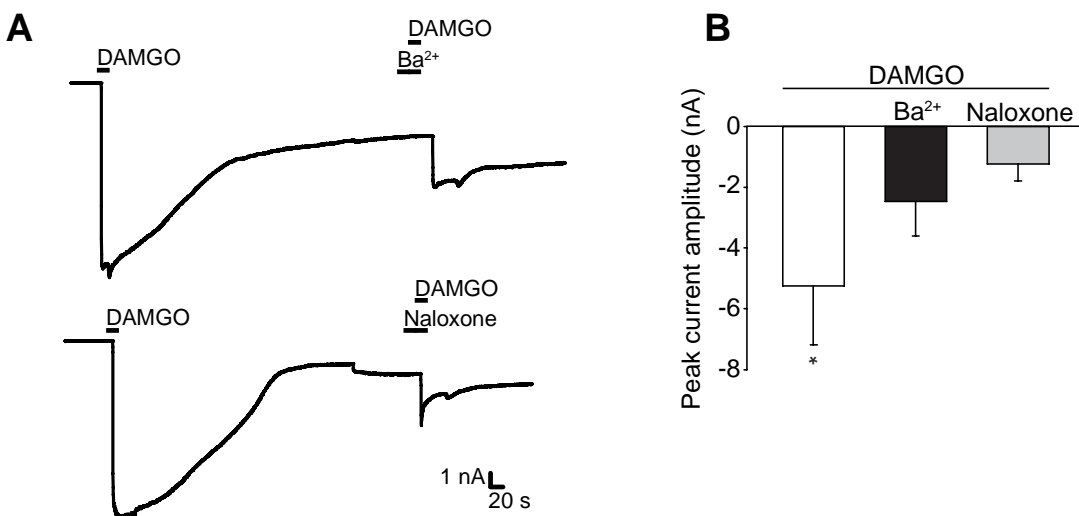


Figure 17 Functional coupling of GIRQ channels and mu-opioid-receptors in rat DRG neurons. (A) Typical GIRQ current traces induced by the application of DAMGO and inhibited by Ba^{2+} and naloxone. (B) Average peak currents after agonist and antagonist application. * $P < 0.05$ (one way repeated measures ANOVA, Holm-Sidak method), $n = 7$ cells per group. Data are expressed as mean \pm s.e.m.

3.3 Generation of BAC transgenic GIRQ2 mice

To examine our hypothesis that GIRQ channels are required for a significant response to opioids we generated a transgenic mouse line expressing GIRQ channels in DRG neurons. To this end we used the promoter of the tetrodotoxin (TTX)-resistant sodium channel $\text{Na}_v1.8$ to restrict this expression to DRG neurons. For the transgene we only used GIRQ2 because this subunit can form functional channels on its own (Inanobe et al., 1999). For easier detection of the exogenous GIRQ2 we attached a Flag-tag to the N-terminus of the subunit. Figure 18 shows a schematic diagram of the BAC (constructed by Dr. Jeanette Rientjes, EMBL Monterotondo) encompassing the $\text{Na}_v1.8$ flanking region, the Flag-tag and the coding sequence of GIRQ2.

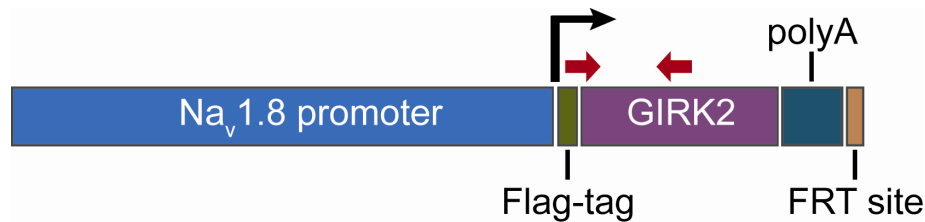


Figure 18 Schematic diagram of the BAC containing the $\text{Na}_v1.8$ promoter region, a Flag-tag upstream of the GIRK2 sequence and a polyA tail downstream. The FRT site was used for integration of the GIRK2 sequence into the BAC by homologous recombination. The red arrows indicate the primer binding sites for genotyping.

We obtained 6 possible transgenic founders which were analyzed by genotyping PCR. The binding sites of the primers are indicated in figure 18. This analysis detected one positive founder carrying the transgene (figure 19, number 4 indicated by the red arrow). The expected product was about 500 bp long.

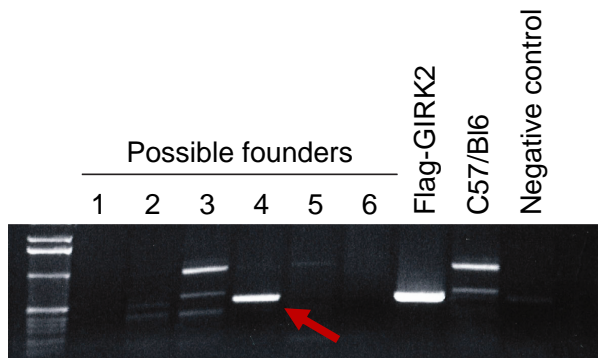


Figure 19 Genotype analysis of 6 possible transgenic founders. Number 4 (red arrow) was tested as positive whereas the others are negative. Flag-GIRK2 plasmid DNA was used as a positive control, genomic DNA isolated from c57/Bl6 mice as a negative control.

The positive founder was further analyzed by southern blot. Beside the analysis of the genotype the southern blot was used to determine the copy number of the BACs which integrated into the genome of the positive founder. Copy number standards were established with genomic wildtype DNA spiked with 1, 2, 4, 8 and 16 BAC copies (figure 20). By comparing the band intensity (number of pixels) of the positive founder with the bands of the standards we estimated that 9 copies of the BAC integrated into the genome of the positive founder.

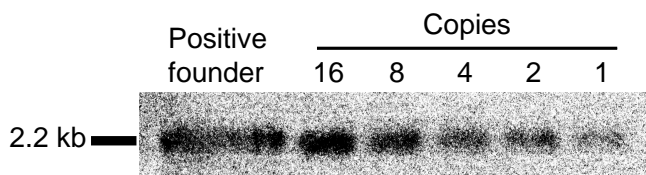


Figure 20 Genotyping of the positive founder and determination of BAC copy number by southern blot. Genomic DNA was digested with *Nco*I and an exon 3/4 spanning probe was used to detect exogenous GIRK2. The pixel intensity of the positive founder was compared to distinct standards with the result that about 9 copies of the BAC integrated into the genome of the founder.

Several studies demonstrated a correlation between the number of BACs integrated into the genome and the level of protein expression in transgenic mice (Chandler et al., 2007; Schedl et al., 1993). For further copy number analysis in our transgenic mouse line (designated as $\text{Na}_v1.8\text{-GIRK2}$) I performed qRT-PCR experiments. Exogenous GIRK2 was amplified using the genotyping primers and distinct standards were used to determine the copy number of the integrated BAC. The qRT-PCR (figure 21) experiments indicated that 9 BAC copies integrated into the genome of $\text{Na}_v1.8\text{-GIRK2}$ mice.

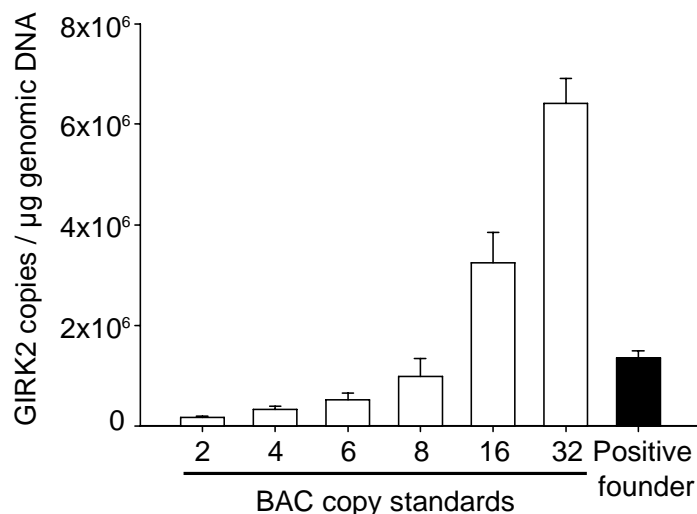


Figure 21 Integration of 9 BAC copies into the genome of $\text{Na}_v1.8\text{-GIRK2}$ mice. Genotyping primers were used for qRT-PCR analysis to amplify exogenous GIRK2 in distinct standards and in genomic DNA isolated from $\text{Na}_v1.8\text{-GIRK2}$ mice. Samples from 3 animals per group were measured in triplicates. Data are expressed as mean \pm s.e.m.

3.3.1 Expression of GIRK2 in $\text{Na}_v1.8$ -GIRK2 mice

To confirm that transgenesis using the $\text{Na}_v1.8$ promoter correctly targeted the expression of GIRK2 to DRG neurons, I used qRT-PCR and immunostaining. qRT-PCR was performed on mRNA isolated from different tissues of $\text{Na}_v1.8$ -GIRK2 mice and wildtype littermates. As illustrated in figure 22 wildtype littermates and $\text{Na}_v1.8$ -GIRK2 mice showed comparable GIRK2 mRNA expression levels in cerebellum and spinal cord. However, I found highly increased expression of GIRK2 mRNA in DRG neurons of $\text{Na}_v1.8$ -GIRK2 mice.

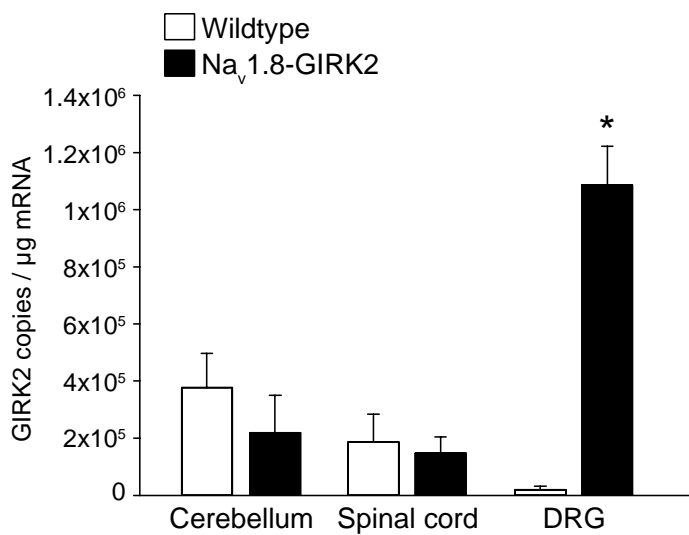


Figure 22 qRT-PCR analysis of GIRK2 mRNA expression in cerebellum, spinal cord and DRG neurons of $\text{Na}_v1.8$ -GIRK2 and wildtype mice. * $P<0.05$ (Kruskal-Wallis ANOVA on Ranks, Dunn's method), $n = 3$ animals per group, each sample was measured in triplicates. Data are expressed as mean \pm s.e.m.

To assess GIRK2 protein expression I performed immunostaining with anti-GIRK2 and anti-Flag antibodies. The specificity of all antibodies was confirmed by omission of primary antibodies (Appendix, Fig. 36) and, in case of GIRK2 and Flag antibodies, by a loss of immunoreactivity in tissue from wildtype animals. Figure 23 demonstrates immunoreactivity for GIRK2 and for the Flag-tag in DRG sections from $\text{Na}_v1.8$ -GIRK2 mice but not in sections from wildtype littermates.

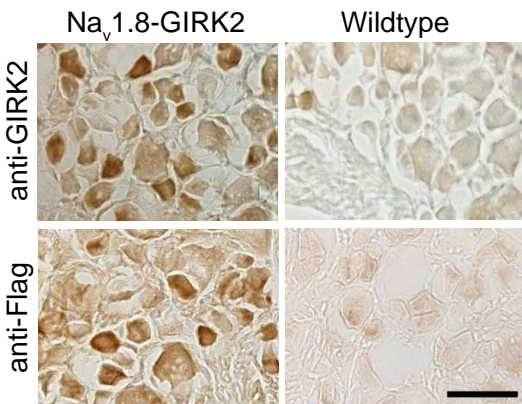


Figure 23 GIRK2 protein in DRG neurons of $\text{Na}_v1.8$ -GIRK2 mice. DRG sections stained with anti-GIRK2 and anti-Flag antibodies demonstrate Flag-GIRK2 only in $\text{Na}_v1.8$ -GIRK2 mice and not in wildtype littermates. The scale bar represents 50 μm .

The somata of peripheral sensory neurons are located in the DRG and innervate the skin and the dorsal horn of the spinal cord. To examine if GIRK2 protein is transported from the DRG along the fibers to the terminals we stained sections of the sciatic nerve with an anti-Flag antibody. As shown in figure 24A Flag-GIRK2 protein is located in the sciatic nerve of $\text{Na}_v1.8$ -GIRK2 mice but absent in wildtype sciatic nerve.

I observed expression of endogenous GIRK2 in the dorsal horn of the spinal cord in both wildtype and transgenic mice using anti-GIRK2 antibodies (figure 24B, upper panel), whereas staining for Flag-GIRK2 revealed no immunoreactivity in the spinal cord of either $\text{Na}_v1.8$ -GIRK2 or wildtype animals (figure 24B, lower panel). These findings suggest a transportation of transgenic GIRK2 along the axons to peripheral but not to the central terminals of sensory neurons.

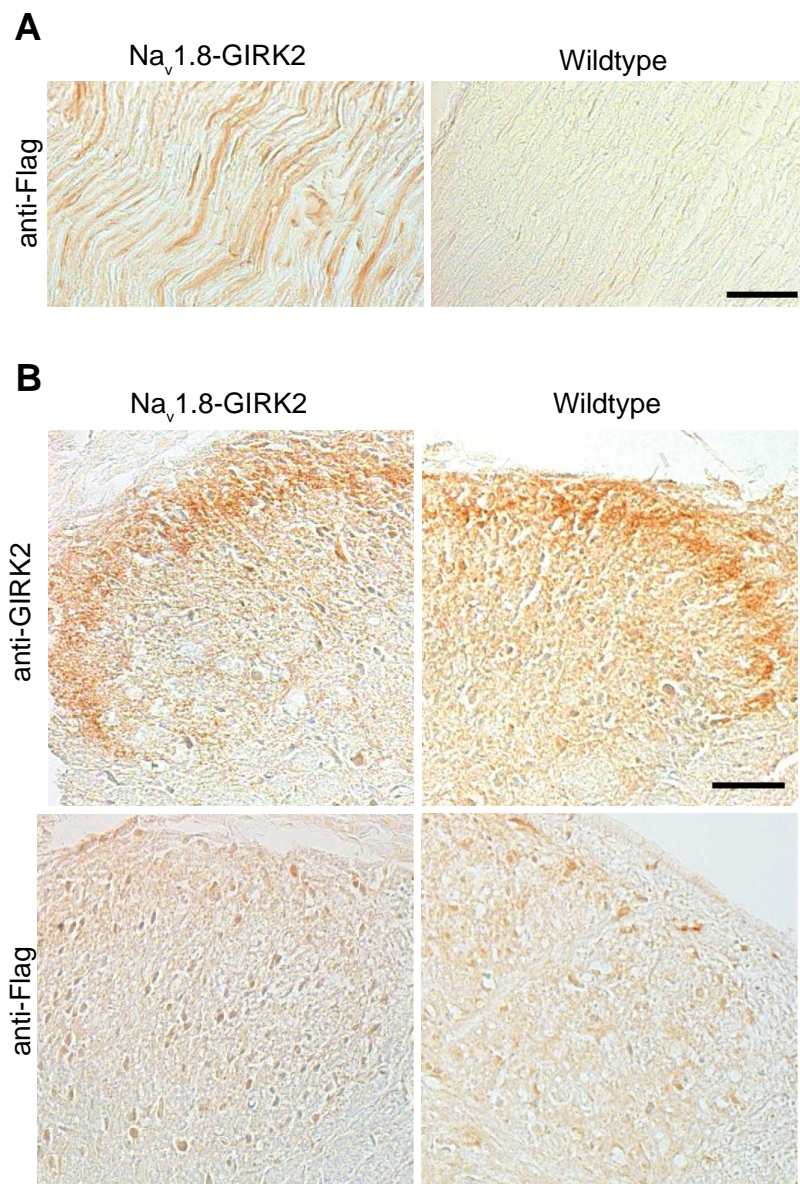


Figure 24 GIRK2 protein is transported towards the peripheral terminals of DRG neurons in Na_v1.8-GIRK2 mice. Sections of the sciatic nerve (A) stained with anti-Flag antibody. Staining of the spinal cord (B) with anti-GIRK2 and anti-Flag antibodies demonstrates expression of endogenous GIRK2 in the dorsal horn of the spinal cord of both wildtype and Na_v1.8-GIRK2 mice but no expression of the Flag-GIRK2. Specificity of GIRK2 and Flag antibodies was shown by immunoreactivity in DRGs and sciatic nerve from Na_v1.8-GIRK2 mice. No immunoreactivity was detected in tissue from wildtype animals. The scale bars represent 50 μ m.

To gain further insights into transgenic GIRK2 expression in DRG subpopulations, co-staining of dissociated DRG cultures with cellular markers were performed. Since the Na_v1.8

promoter targets the expression to nociceptors, markers for peptidergic and non-peptidergic nociceptors were used. Figure 25 shows total co-expression of both GIRK2 and the Flag-tag (upper panel) in cells from $\text{Na}_v1.8$ -GIRK2 mice. Co-staining using an anti-Flag antibody and an antibody against calcitonin gene related peptide (CGRP) contained in the subpopulation of peptidergic nociceptors showed only a few co-expressing cells (middle panel). However, cells stained with IB4 and anti-Flag showed prominent co-expression (lower panel). Taken together, transgenic GIRK2 is apparently expressed mostly in nonpeptidergic unmyelinated C-fibers.

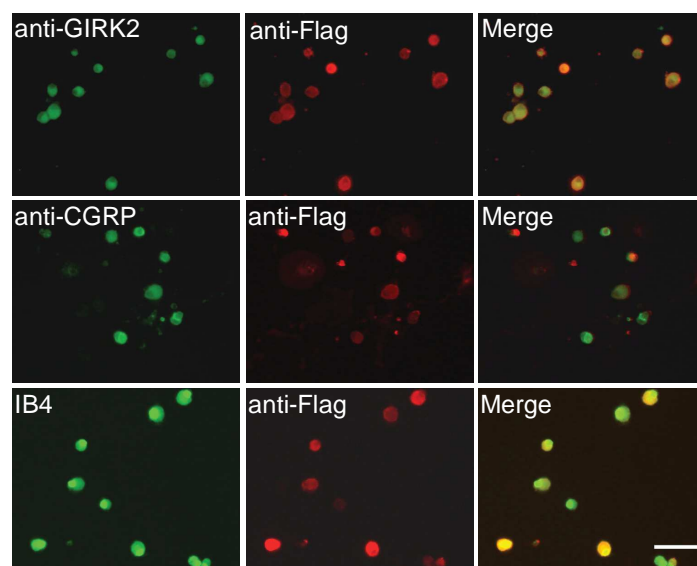


Figure 25 Immunocytochemistry of dissociated DRG cultures from $\text{Na}_v1.8$ -GIRK2 mice. All cells show immunoreactivity for anti-Flag and anti-GIRK2 (upper panel). Nonpeptidergic nociceptors positive for IB4 also express exogenous GIRK2 (lower panel, yellow) whereas only few peptidergic nociceptors expressing CGRP are also positive for exogenous GIRK2 (middle). Omission of primary antibodies and incubation with secondary antibodies only confirmed their specificity (Appendix, Fig. 36). The bar indicates 50 μm .

To examine whether exogenous GIRK2 and mu-opioid receptors are expressed in the same cells, dissociated DRG cultures from wildtype and $\text{Na}_v1.8$ -GIRK2 mice were co-stained with antibodies against both proteins. I found an overlap of Flag-GIRK2 and mu-opioid receptors (figure 26, upper panel, yellow color). Neither staining for anti-Flag nor co-staining for Flag-

GIRK2 and mu-opioid receptors could be observed in DRG neurons from wildtype mice (figure 26, lower panel).

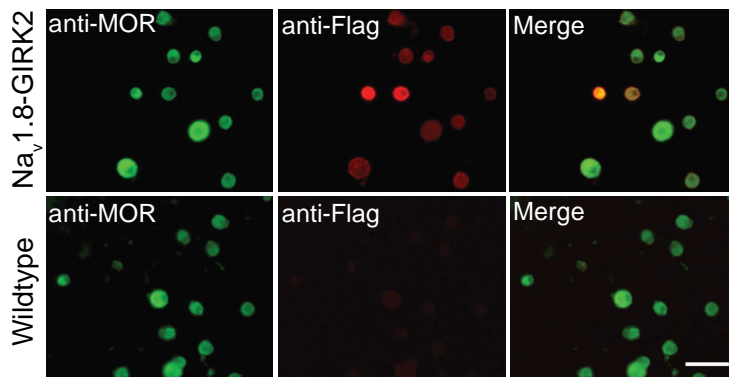


Figure 26 Immunocytochemistry of dissociated DRG neurons from $\text{Na}_v1.8$ -GIRK2 and wildtype mice stained with antibodies against mu-opioid receptors and the Flag-tag. Co-expression of both proteins can be observed in cells of $\text{Na}_v1.8$ -GIRK2 mice (upper panel, yellow) whereas wildtype DRG neurons lack the expression of exogenous GIRK2 (lower panel). Specificity of primary antibodies was confirmed by omission of the first antibody (Appendix, Fig. 36) or, in case of the anti-Flag antibody, by a loss of immunoreactivity in wildtype DRG neurons. Scale bar represents 50 μm .

3.3.2 Functional characterization of $\text{Na}_v1.8$ -GIRK2 mice

To test the hypothesis that the expression of Flag-GIRK2 promotes peripheral opioid antinociception in mice, it was necessary to examine whether the exogenous GIRK2 is functionally expressed and coupled to opioid receptors in DRG neurons of $\text{Na}_v1.8$ -GIRK2 mice.

3.3.2.1 Analysis of opioid receptor and GIRK channel coupling in $\text{Na}_v1.8$ -GIRK2 mice

Whole cell patch clamp recording was performed on dissociated DRG neurons from $\text{Na}_v1.8$ -GIRK2 and wildtype mice using the same protocol as described above (3.2.3). Recordings were done in high K^+ bath solution at -80 mV. GIRK currents were induced by DAMGO (10 μM) and inhibited by co-application of Ba^{2+} (3 mM) or naloxone (20 μM). As shown in figure

27 (B, C and D) DAMGO induced large inward currents in DRG neurons from $\text{Na}_v1.8$ -GIRK2 mice (B) but not in DRGs from wildtype littermates (A and C). The application of either Ba^{2+} or naloxone blocked these currents in $\text{Na}_v1.8$ -GIRK2 DRG neurons (figure 27 D).

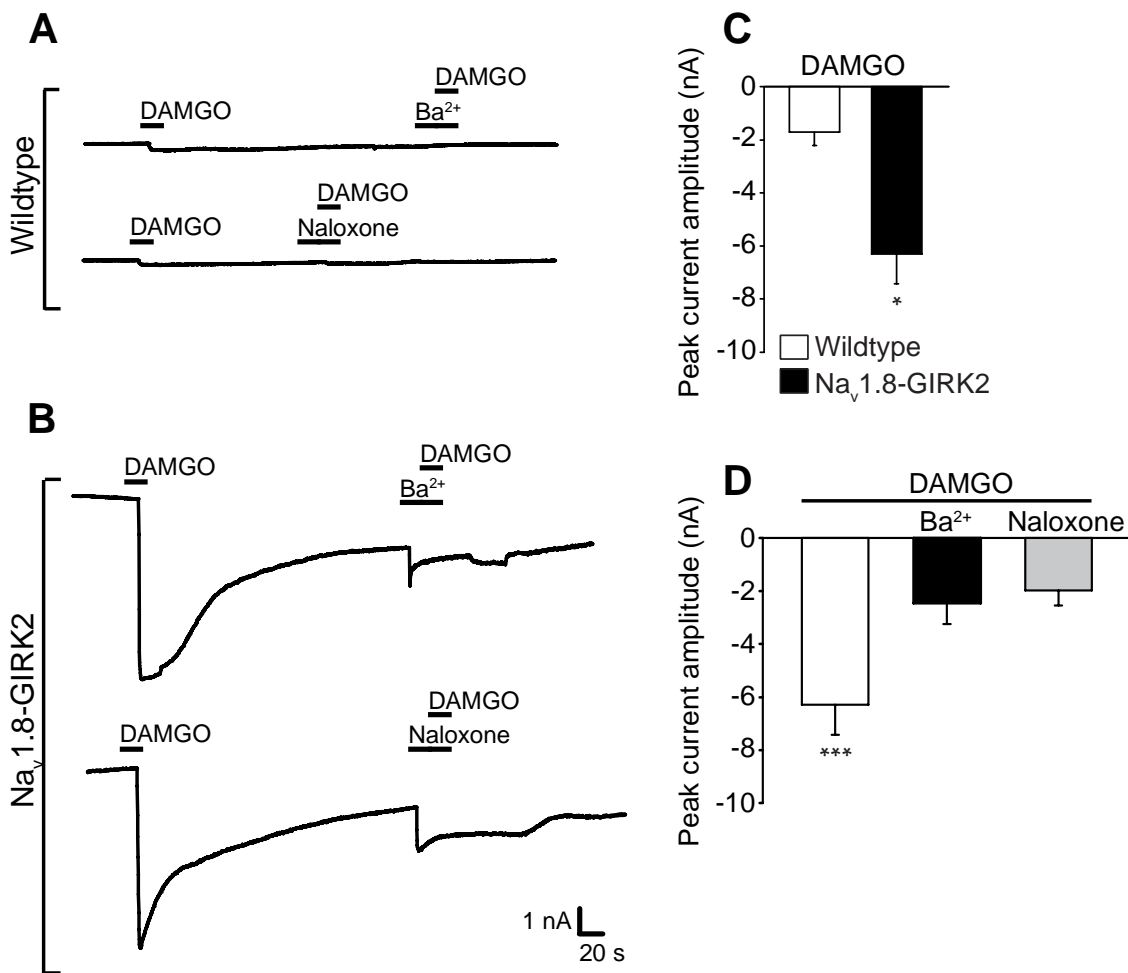


Figure 27 DAMGO-evoked function of GIRK channels in DRG neurons isolated from $\text{Na}_v1.8$ -GIRK2 mice. (A, B) Representative current traces of wildtype and $\text{Na}_v1.8$ -GIRK2 DRG neurons induced by DAMGO (10 μM) and inhibited by Ba^{2+} (3 mM) or naloxone (20 μM). (C) Average peak DAMGO-induced currents in wildtype and $\text{Na}_v1.8$ -GIRK2 DRGs. *P < 0.05 (student's t-test), n = 8-12 cells per group. (D) Average peak GIRK currents in $\text{Na}_v1.8$ -GIRK2 DRG neurons after application of agonist and antagonists. ***P < 0.001 (one way repeated measures ANOVA, Holm-Sidak method), n = 9-12 cells per group. Data are expressed as mean \pm s.e.m.

The functional coupling of GIRK2 and opioid receptors was confirmed by potassium (K^+) imaging experiments. This technique was used as an indicator for GIRK channel activity by measuring the up-take of thallium (Tl^+) ions after influx through potassium channels (figure 28).

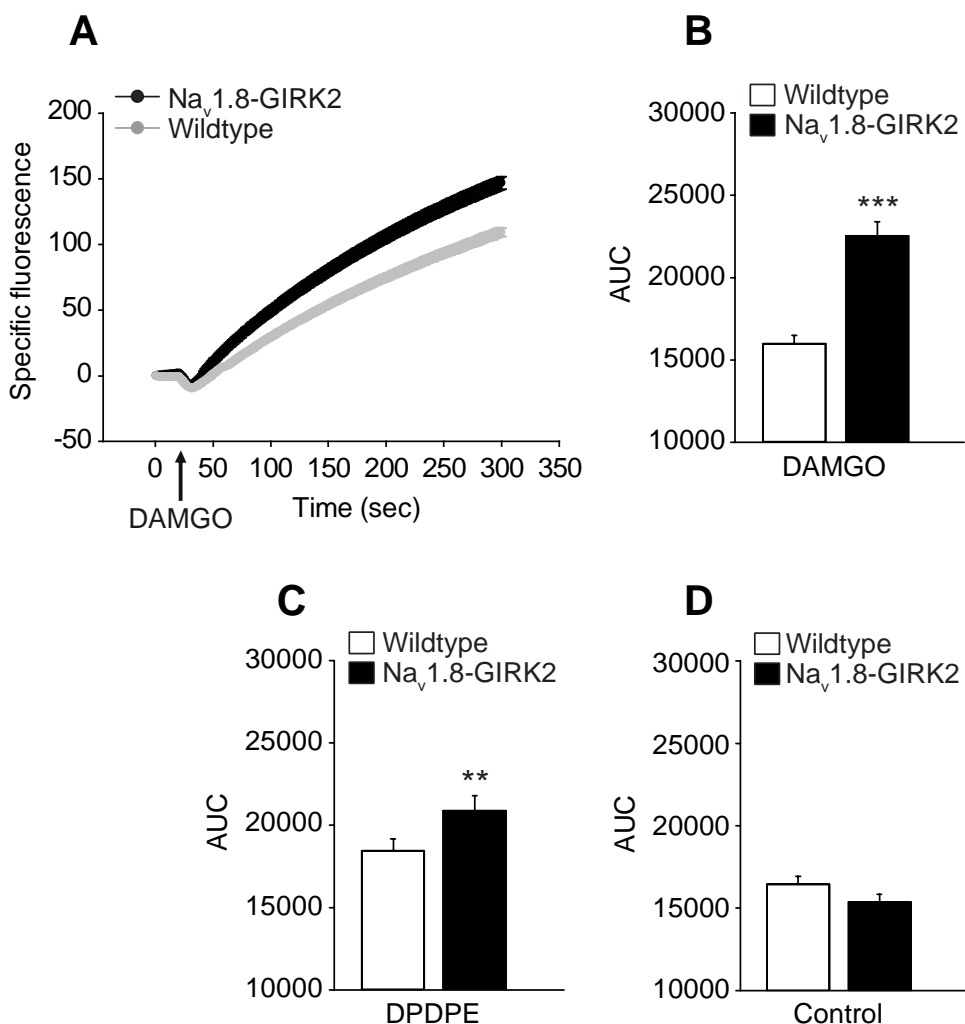


Figure 24 Opioid agonists induce thallium (Tl^+) influx and uptake in DRG neurons from $Na_v1.8$ -GIRK2 or wildtype mice loaded with the thallium-sensitive dye FluxOR. (A) Time course of fluorescence at 488 nm, normalized to baseline. (B, C, D) Average area under the curve of the fluorescence measured in wildtype and $Na_v1.8$ -GIRK2 DRG neurons treated with 10 μ M DAMGO (B) or 10 μ M DPDPE (C). Control displays the fluorescent increase in DRG neurons without stimulation with opioid receptor agonists (D). ***P < 0.001, **P < 0.01 (Mann-Whitney Rank Sum test), n = 200 - 300 cells per group isolated from 4 animals. Data are expressed as mean \pm s.e.m.

DRG neurons loaded with the thallium-sensitive dye FluxOR revealed a higher uptake of thallium ions (indicating a higher influx through potassium channels) upon application of mu-(DAMGO) or delta-agonists (DPDPE), if isolated from $\text{Na}_v1.8\text{-GIRK2}$ mice compared to wildtype littermates (figure 28A, B and C). No difference of thallium uptake was detected in $\text{Na}_v1.8\text{-GIRK2}$ or wildtype mice if no opioids were applied (figure 28 D).

3.3.3 Behavioral analysis of $\text{Na}_v1.8\text{-GIRK2}$ mice

Next we investigated how transgenic expression of GIRK2 affects opioid antinociception in mice by measuring hindpaw withdrawal responses to heat (Hargreaves et al., 1988) or mechanical stimuli (Chaplan et al., 1994). I started with healthy $\text{Na}_v1.8\text{-GIRK2}$ mice and wildtype littermates to examine whether the presence of an “artificial” ion channel which controls the excitability of neurons can lead to different nociception in general and can promote peripheral opioid antinociception even without inflammatory tissue injury.

Responses to thermal stimuli were determined by the Hargreaves test. Paw withdrawal latencies were measured before, and 5, 15, 30, 45 and 60 min after intraplantar (i.pl.) injection of DAMGO or NaCl (control) into the right hindpaw. Figure 29A (right paw) and figure 29B (left paw) summarize the results. Pre-injection thresholds in $\text{Na}_v1.8\text{-GIRK2}$ mice were indistinguishable from wildtypes. Different DAMGO concentrations administered to healthy $\text{Na}_v1.8\text{-GIRK2}$ or wildtype mice did not increase paw withdrawal latency to a noxious thermal stimulus (figure 29A, B).

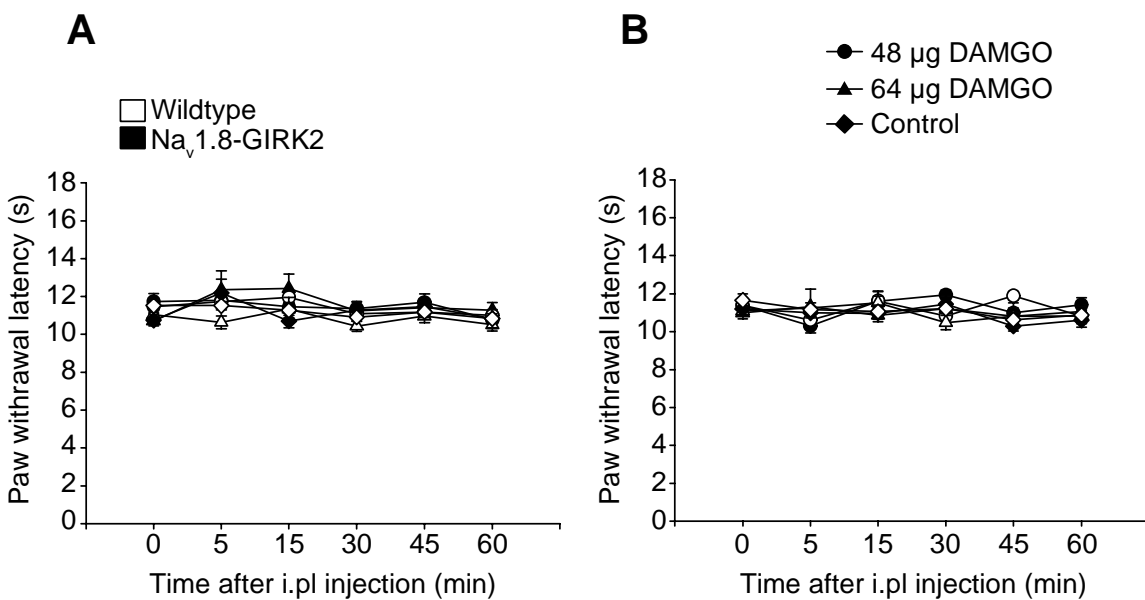


Figure 29 Thermal nociceptive thresholds of $\text{Na}_v1.8$ -GIRK2 and wildtype mice. Paw withdrawal latency in the right (A) and left (B) paw was measured after injection of DAMGO or NaCl into the right hindpaw (i.pl). No differences were detected at baseline or after the injection of DAMGO. n= 8. Data are expressed as mean \pm s.e.m.

Since it is known that opioids reverse hyperalgesia in rats if applied locally to injured tissue (Antonijevic et al., 1995; Obara et al., 2009), we examined effects in $\text{Na}_v1.8$ -GIRK2 mice with inflamed paws using two different behavioral tests. First the response to heat (Hargreaves test) was tested in mice with (48h) CFA inflammation of the right hindpaw. Different doses of DAMGO (32 μ g, 48 μ g, 56 μ g and 64 μ g) were used. As shown in figure 30A, baseline sensitivity to a noxious thermal stimulus was similar in $\text{Na}_v1.8$ -GIRK2 mice and wildtype littermates. Both developed ipsilateral thermal hyperalgesia two days after induction of paw inflammation. Intraplantar DAMGO dose-dependently elevated thermal nociceptive thresholds in inflamed paws of $\text{Na}_v1.8$ -GIRK2 mice but not of wildtype littermates (figure 30B). Heat hyperalgesia was fully reversed to baseline at a dose of 48 μ g. No differences in paw withdrawal latencies were detected in contralateral noninflamed paws (not shown). The peak effect of DAMGO in $\text{Na}_v1.8$ -GIRK2 mice was blocked by i.pl. co-administration of naloxone methiodide (NLXM), a non-selective opioid receptor antagonist which does not cross the blood-brain barrier and blocks only peripheral opioid receptors.

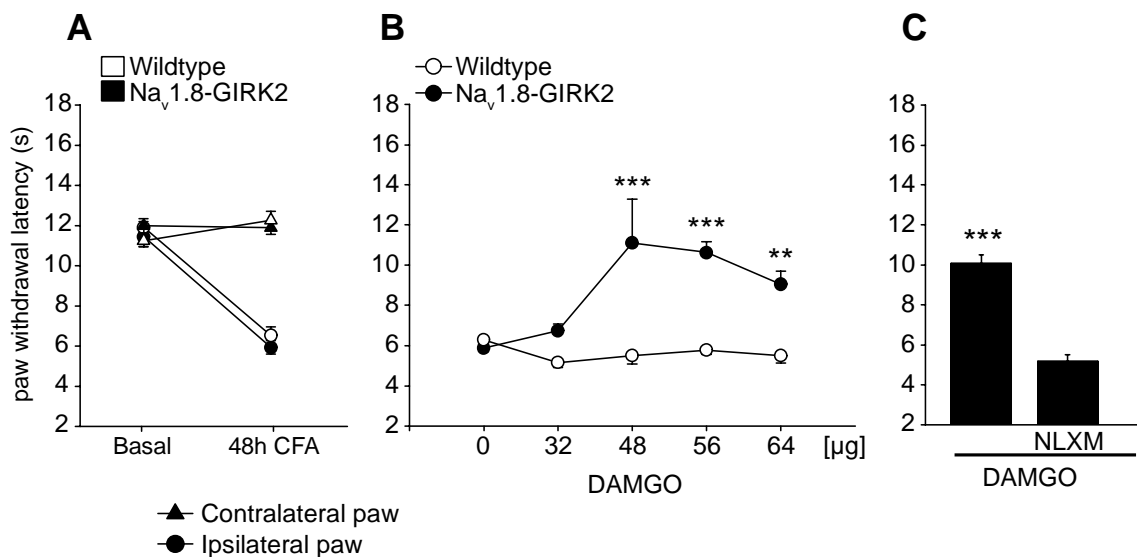


Figure 30 DAMGO reverses inflammatory hyperalgesia to normal baseline levels in $\text{Na}_v1.8\text{-GIRK2}$ but not in wildtype mice. (A) Changes in paw withdrawal latency in response to radiant heat upon induction of inflammation (ipsilateral) compared to noninflamed (contralateral) side in $\text{Na}_v1.8\text{-GIRK2}$ and wildtype mice. (B) Elevation of inflamed paw withdrawal latency 5 min after i.pl. injection of DAMGO or NaCl (0 µg). ***P < 0.001, **P < 0.01 (two way ANOVA, Holm-Sidak method), n = 7-8 animals per group. No significant changes were observed in contralateral paws (not shown). (C) DAMGO-induced antinociception (48 µg) is reversed by co-injection of naloxone methiodide (NLXM, 5 µg) into the inflamed paw. ***P < 0.001 (student's unpaired t-test), n= 7-8 animals per group. Data are expressed as mean ± s.e.m.

To assess responses to noxious mechanical stimuli paw withdrawal thresholds were measured using calibrated von Frey filaments applied to the plantar surface of the paw (experiments were performed by Dr. Dominika Labuz). After induction of unilateral inflammation both $\text{Na}_v1.8\text{-GIRK2}$ and wildtype mice developed allodynia with much lower mechanical thresholds in ipsilateral compared to contralateral healthy paws (figure 31A). Intraplantar injection of different doses of DAMGO (1µg, 2µg and 4µg) were tested. At 2 µg DAMGO reduced mechanical allodynia in $\text{Na}_v1.8\text{-GIRK}$ but not in wildtype mice (figure 31B). No differences in mechanical thresholds were detected in the noninflamed paw (not shown). As shown in figure 31C, the antinociceptive effect of 2 µg DAMGO in $\text{Na}_v1.8\text{-GIRK2}$ mice was blocked by i.pl. co-administration of NLXM.

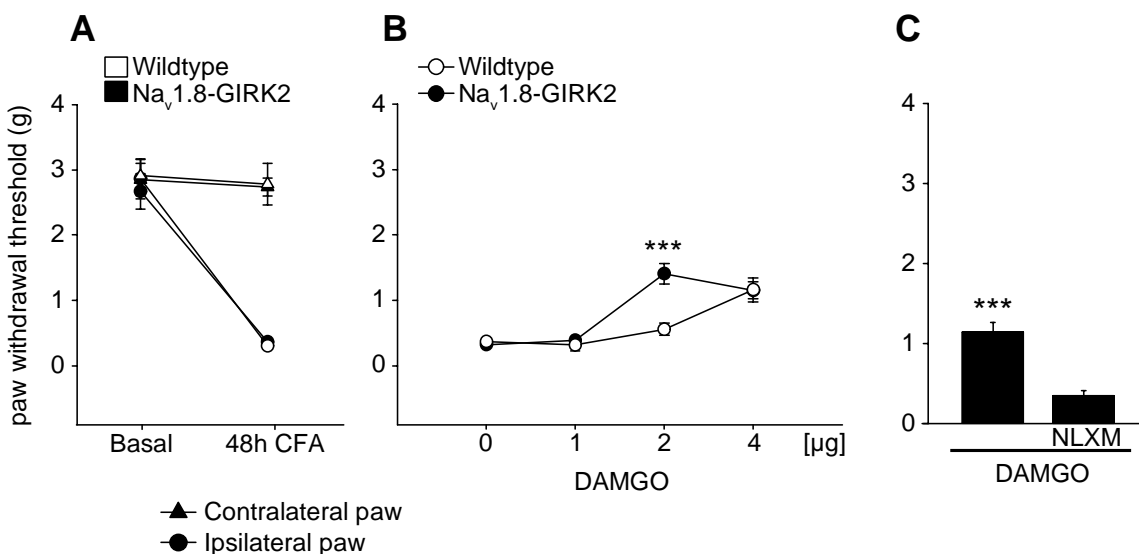


Figure 31 DAMGO (2 μ g) reduces mechanical allodynia in Na_v1.8-GIRK2 mice but not in wildtype littermates. (A) Changes in paw withdrawal threshold in response to mechanical stimuli upon induction of inflammation in (ipsilateral) compared to noninflamed (contralateral) side in Na_v1.8-GIRK2 and wildtype mice. (B) Paw withdrawal threshold was elevated 5 min after i.pl. injection of 2 μ g DAMGO in the inflamed paw of Na_v1.8-GIRK2 but not of wildtype mice. ***P < 0.001 (two way ANOVA, Holm-Sidak method), n = 8 animals per group. No significant changes were observed in contralateral paws (not shown). (C) DAMGO (2 μ g)-induced antinociception is reversed by co-injection of naloxone methiodide (NLXM, 5 μ g) into the inflamed paw. ***P < 0.001 (student's unpaired t-test), n= 8 animals per group. Data are expressed as mean \pm s.e.m.

As mRNA expression of Na_v1.8 can be enhanced by paw inflammation (Yu et al., 2011) I examined whether the mRNA expression of GIRK2 in Na_v1.8-GIRK2 mice is influenced by CFA inflammation of the paw using qRT-PCR. The mRNA was isolated from DRG neurons innervating the inflamed (ipsilateral) and the contralateral paws. As shown in figure 32, CFA inflammation did not induce any changes of GIRK2 mRNA expression on either side.

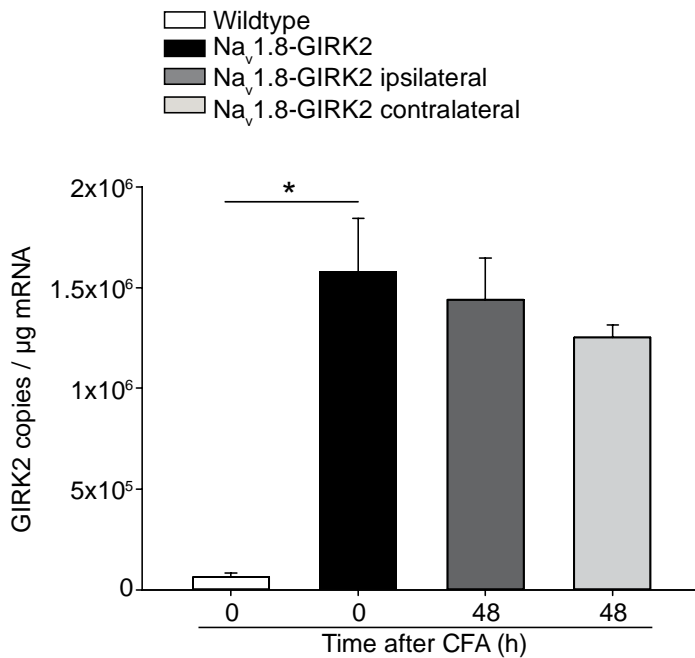


Figure 32 Quantification of GIRQ2 mRNA in DRG neurons from $\text{Na}_v1.8\text{-GIRK2}$ mice 48 h after unilateral CFA-induced hindpaw inflammation. GIRQ2 mRNA levels in DRG neurons innervating the inflamed paw (ipsilateral) or the noninflamed paw (contralateral), and from healthy $\text{Na}_v1.8\text{-GIRK2}$ animals and wildtype littermates were analyzed. Samples from at least 3 animals per group were measured in triplicates. Data are expressed as mean \pm s.e.m. *P < 0.05 (Kruskal-Wallis one way ANOVA on Ranks).

Taken together, peripherally administered DAMGO induced significant antinociception in transgenic mice expressing GIRQ2 in nociceptive sensory neurons but not in wildtype mice lacking GIRQ channels in DRG neurons.

4 Discussion

The major finding of this thesis is the direct demonstration that GIRQ channels in DRG neurons play a major and species-specific role in opioid-induced peripheral antinociception in rodents. In the present study I examined two main hypotheses:

Hypothesis 1: A lack of GIRQ channel expression in peripheral sensory neurons of mice underlies the observed weak peripheral opioid antinociception. Rats express GIRQ channels in their peripheral sensory neurons and they are functionally coupled to opioid receptors. This contributes to the observed potent peripheral opioid antinociception in rats.

I demonstrated that GIRQ1 and 2 are functionally expressed in peripheral sensory neurons of rats and that these channels are coupled to the mu-opioid receptor. Consistent with my results, numerous studies demonstrated that opioids induce peripheral antinociception in rats (Antonijevic et al., 1995; Obara et al., 2009; Stein and Machelska, 2011). I did not observe significant expression of any of the 4 GIRQ subunits in mouse DRG neurons and I found no indication for a functional coupling of GIRQ channels and mu-opioid receptors in peripheral sensory neurons of mice.

Hypothesis 2: Expression of GIRQ channels in peripheral sensory neurons of transgenic mice leads to coupling of the channels to opioid receptors and to an increased functional response to peripherally applied opioids.

After generation of a transgenic mouse line ($\text{Na}_v1.8\text{-GIRQ2}$) expressing a Flag-GIRQ2 construct in nociceptive sensory neurons, I recorded DAMGO-evoked GIRQ currents from DRG neurons. No GIRQ currents were observed in cultured DRG neurons isolated from wildtype littermates. This indicates a functional coupling of mu-opioid receptors and GIRQ channels in $\text{Na}_v1.8\text{-GIRQ2}$ mice. We also observed significant DAMGO-induced antinociception in these transgenic mice but not in their wildtype littermates.

These data suggest that GIRQ channels are crucially involved in peripheral opioid antinociception. These findings could lead to promising novel strategies for pain treatment

without centrally mediated side effects. A more detailed understanding of molecular mechanisms underlying nociceptive processes will help us to develop novel analgesics. As demonstrated in this thesis, the choice of species for preclinical studies is crucial because it might have an impact on the design and outcome of subsequent clinical trials (Le Bars et al., 2001; Whiteside et al., 2008; Wilson and Mogil, 2001).

4.1 Functional GIRK channel expression in peripheral sensory neurons of rats indicates a role of GIRQ channels in peripheral opioid antinociception in rats but not in mice

It is well known that activation of mu-opioid receptors in the CNS activates GIRQ channels and inhibits voltage-dependent Ca^{2+} channels as well as adenylyl cyclases (North et al., 1987; Pepper and Henderson, 1980; Tokimasa et al., 1981; Werz and Macdonald, 1983b; Williams et al., 1982; Yoshimura and North, 1983). However it is still under debate whether GIRQ channel activation is involved in signaling mechanisms underlying opioid-induced peripheral antinociception. GIRQ channel expression in the peripheral nervous system has been studied only by few research groups. Their results are quite diverse and species differences were not considered (Gao et al., 2007; Kanjhan et al., 2005; Khodorova et al., 2003; Mitrovic et al., 2003).

In this study we could show that the presence of GIRQ channels in peripheral sensory neurons and their functional coupling to mu-opioid receptors, contributes to peripheral opioid-induced antinociception. If GIRQ channels are not expressed in peripheral sensory neurons, as shown in mice, and therefore do not contribute to opioid receptor signaling, peripheral opioid induced antinociception is much less pronounced, if not lacking.

A possible role of GIRQ channels in peripheral opioid-induced antinociception was suggested previously by Khodorova and colleagues. They described a peripheral opioid-dependent analgesic pathway where activation of endothelin-B (ET_B) receptors on keratinocytes triggered the release of the endogenous opioid peptide β -endorphin. Thereafter, β -endorphin activated mu-opioid receptors on nociceptors. Indirect evidence suggested an activation of GIRQ channels (Khodorova et al., 2003). Expression of GIRQ2 on sensory nerve endings in the epidermis of rat hind paws and in small and medium-sized DRG neurons was shown by immunohistochemistry using anti-GIRQ2 antibodies. Furthermore, they illustrated co-expression of GIRQ2 with mu-opioid receptors or with CGRP on peripheral nerve terminals

in rats. In behavioral experiments endothelin-1 (ET-1) injection into rat hindpaws induced nociceptive responses due to activation of ET_A receptors but also antinociception via ET_B activation. The antinociceptive effect was enhanced by an ET_B receptor agonist and was reversed by co-injection of the GIRK channel blocker tertiapin-Q or by opioid receptor antagonists. These experiments point to a role of GIRK channels in peripheral opioid antinociception in rats. However, the *in vivo* injection of the GIRK channel blocker into the animals' paws does not permit any conclusions as to the anatomical location of functional GIRK channels involved in these effects. In fact, such channels could be located on any cell type found in injured tissue (e.g. immune cells, fibroblasts, muscles, neurons etc.). Notwithstanding, this study confirms our results about the expression of GIRK channels in rat primary sensory afferents.

Surprisingly, this study also showed that injection of ET-1 into the hind paw of general GIRK2 knockout mice produced a longer duration of nociceptive behaviors compared to wildtype mice, suggesting a role of GIRK2 in the generation of ET-1-mediated antinociception in mice (Khodorova et al., 2003). Again, the ubiquitous knock-out of GIRK2 does not permit conclusions as to the anatomical location of the channels. It is extremely unlikely that peripheral GIRK channels were involved in this process because I could clearly show that GIRK channels are neither expressed nor functionally coupled to mu-opioid receptors in peripheral sensory neurons of mice. Several other mechanisms might underlie the observed differences of ET-1 mediated antinociception in GIRK2 knockout mice. It has been known for many years that noxious peripheral stimulation leads to a release of the neurotransmitter substance P from nociceptive primary afferent fibers in the spinal cord dorsal horn (De Koninck and Henry, 1991). Already in 1983 Tang and colleagues showed that substance P triggers the release of endogenous opioid peptides in the spinal cord. This effect is Ca²⁺ dependent and intracellular calcium increases after noxious stimulation of peripheral nerve fibers (Tang et al., 1983). Spinal cord lamina II neurons express GIRK channels and opioid receptors, which can be activated by the endogenous opioids and produce antinociception (Marker et al., 2006; Marker et al., 2005). Furthermore it was suggested that endogenous substance P contributes to descending antinociceptive pathways originating in the periaqueductal gray (Prochaska et al., 2004) and that stimulation of brain regions produces antinociception through the release of endogenous serotonin (5-HT) in the spinal cord (Basbaum and Fields, 1984; Furst, 1999; Taylor and Basbaum, 1995). 5-HT receptors are known to activate GIRK channels in the CNS (Douznik et al., 1997; Luscher et al., 1997). Such mechanisms might provide an additional explanation for the contribution of GIRK

channels to the antinociceptive effect of ET-1 in mice described by Khodorova and colleagues. Thus, one would predict that by altering the activity of GIRK2-expressing dorsal horn neurons through a general deletion of the subunit GIRK2, the transmission of painful stimuli as well as endogenous antinociceptive mechanisms are influenced.

Consistent with our *in vivo* results that GIRK channels do not play a functional role in peripheral opioid antinociception in mice, we were unable to record inwardly rectifying currents elicited by hyperpolarizing voltage steps in mouse DRG neurons. Neither of the GIRK channel inhibitors, Ba²⁺ or tertiapin-Q, had an effect on currents evoked by hyperpolarization (Kanjhan et al., 2005). Other studies also reported a lack of GIRK2 immunoreactivity in mouse DRG neurons (Mitrovic et al., 2003), and no increase of K⁺ conductance at resting membrane potentials in mouse and chicken DRG neurons upon opioid treatment (Werz and MacDonald, 1983a). These studies confirm our results and strongly suggest that GIRK channels do not play a role in the modulation of the excitability of mouse DRG neurons.

In contrast, in rat DRG neurons a potassium current which was receptor coupled and sensitive to blockade by Ba²⁺ was first described in 1994 by Scroggs and colleagues (Scroggs et al., 1994). Three years later mRNA expression of the subunits GIRK1, 2 and 3 was shown in embryonic rat DRGs (Karschin and Karschin, 1997). In 2007 the first evidence for a functional expression of GIRK channels in peripheral sensory neurons of rats was reported. It was shown that GIRK channels are functionally coupled to GABA_B receptors in adult rat DRG neurons (Gao et al., 2007). Similar to opioid receptors, GABA_B receptors are G_{i/o}-protein coupled receptors (Padgett and Slesinger, 2010). Extending these findings and the indirect evidence by Khodorova et al. (Khodorova et al., 2003) we now report for the first time that GIRK channels are functionally expressed and coupled to opioid receptors in peripheral sensory neurons of rats.

Furthermore, our results indicate that functional expression and coupling of GIRK channels to opioid receptors in primary sensory afferents has an impact on peripheral opioid antinociception. We and other research groups observed a marked difference in peripheral opioid antinociception between mice and rats. For example, pronounced antinociception elicited by peripherally acting opioids was observed in rats (Cunha et al., 2010; Joris et al., 1987; Stein et al., 1988a; Stein et al., 1989; Stein et al., 1988b) but only weak antinociception in a model of neuropathic pain if injected into the hind paw of mice (Labuz, 2012). Moreover in a mouse model of inflammatory pain much higher doses of opioids were needed to obtain an analgesic effect at all and a peripheral effect was not confirmed by using opioid receptor

antagonists that are restricted to the periphery (Cunha et al., 2010). Our results strongly suggest that the observed species differences are due to the presence or absence of GIRK channels in DRG neurons because we provide evidence for a contribution of GIRK channels to peripheral opioid antinociception if GIRK channels are expressed and functionally coupled to opioid receptors in such neurons.

4.2 A genetic approach to target the nociceptive pathway by using BAC transgenesis

To further strengthen our findings, we used a genetic approach. We sought to generate Bacterial Artificial Chromosome (BAC)-mediated transgenic mice as the conventional transgenic approach using a plasmid has several limitations. Thus, for conventional transgenesis a construct (plasmid) < 20 kb encompassing the artificial gene is generated. However, several problems can hamper the expression of the gene of interest. For example, the chromatin structures at the site of integration can prevent the expression of the gene. Furthermore, the plasmids are often too small to integrate the whole region of a promoter, thus lacking some regulatory elements up- or down-stream of the promoter. This can lead to complete absence or unspecific expression of the artificial gene. An additional problem is the development of concatemers during integration of short DNA fragments. This can lead to methylation of the sequence and may prevent expression of the gene (Gong et al., 2002; Sparwasser and Eberl, 2007; Yang and Gong, 2005). To avoid these problems, BACs can be used. They can carry inserts up to 200-300 kb and show high clonal stability rates. In addition to the promoter elements upstream of the gene, BACs are able to carry also *cis*- and *trans*-regulatory elements such as enhancers and silencers. These elements contribute to a specific expression of the artificial gene independent of the place of integration within the genome. Additionally, it is possible to tag the artificial gene to be recognized by highly specific antibodies. This facilitates localization studies of the transgene (Gong et al., 2002; Heintz, 2001; Yang and Gong, 2005).

We generated BAC transgenic mice with a GIRK2 construct that contains the “Flag” epitope fused to the N-terminus of GIRK2 in order distinguish between the artificial GIRK2 and the endogenous one. Not many studies are published using a Flag-tag fused to artificial genes in transgenic animals (Lu et al., 2009; Oster-Granite et al., 1996). By performing double immunofluorescent staining of DRG neurons with antibodies against GIRK2 and the Flag-tag, we confirmed the expression of the artificial gene. Flag-GIRK2 positive DRG neurons were

only present in transgenic mice but not in wildtype littermates. Furthermore, our patch clamp recordings demonstrated that the N-terminal tagged GIRK2 was efficiently processed and formed functional homotetramers, as we were able to record typical GIRK currents from DRG neurons isolated from transgenic animals. Since we also demonstrated functional coupling of mu-opioid receptors and Flag-GIRK2, we can assume that activation of exogenous GIRK channels by G_{βγ} subunits is not influenced by fusion of the hydrophilic Flag sequence to the N-terminus of GIRK2.

Numerous previous studies have shown that nociceptors express mu-opioid receptors (Scherrer et al., 2009). To target the expression of GIRK2 to peripheral sensory neurons we controlled the expression of Flag-GIRK2 by using the promoter of the voltage gated sodium channel Na_v1.8. The expression pattern of Na_v1.8 has been thoroughly studied by different groups (Akopian et al., 1996; Djouhri et al., 2003; Stirling et al., 2005). Although there are some exceptions under pathological conditions (Arroyo et al., 2002; Damarjian et al., 2004; Ulzheimer et al., 2004), it is generally accepted that it is restricted to DRG neurons in normal animals. For example, Agarwal et al. demonstrated lacZ (encodes β-galactosidase) staining in 93 % of small diameter sensory neurons isolated from a mouse line where the expression of the β-galactosidase gene was under control of the Na_v1.8 promoter. Half of the sensory neurons were also positive for substance P (peptidergic) and the other half for IB4 (nonpeptidergic). No lacZ staining was observed in spinal cord or brain (Agarwal et al., 2004). Using a BAC with the same promoter region enables us to express Flag-GIRK2 in nociceptive neurons co-expressing the mu-opioid receptor (Li et al., 1998; Wang et al., 2010). Additionally, other mouse lines have been described expressing artificial genes in sensory neurons (Hasegawa et al., 2007; Zhou et al., 2002; Zurborg et al., 2011). By using regulatory elements of the *Peripherin* gene the expression of the transgene was directed to peripheral sensory neurons but also to sympathetic neurons. Thus the *Peripherin* locus is not the optimal choice to target expression of an artificial gene to nociceptors (Zhou et al., 2002). *Advillin* is another gene locus which is known to be selectively expressed in peripheral sensory neurons of dorsal root and trigeminal ganglia. Unfortunately, ectopic expression was found also in the brainstem and midbrain (Zurborg et al., 2011). Agarwal and colleagues showed that nearly all peptidergic and non-peptidergic small-diameter (and few large-sized) DRG neurons were positive for transgene expression by using regulatory elements of the Na_v1.8 promoter (Agarwal et al., 2004). In addition, a lack of Cre expression in the CNS was demonstrated in Na_v1.8-Cre mice (Agarwal et al., 2004; Stirling et al., 2005). Thus, we can assume that Flag-GIRK2 expression remains restricted to DRG neurons by driving its expression under the

control of $\text{Na}_v1.8$ regulatory elements. Indeed, by double immunohistochemistry we confirmed that we specifically targeted expression of Flag-GIRK2 to nociceptors.

Usually BACs integrate randomly into the genome via tandem repeats and are mostly present in just one locus of the genome (Chandler et al., 2007; Heaney and Bronson, 2006; Yang and Gong, 2005). Since there is a strong correlation between the number of BAC copies integrated into the genome and an increased BAC transgene (Chandler et al., 2007), we determined the BAC copy number of our $\text{Na}_v1.8$ -GIRK2 mouse line. Using southern blot and quantitative real-time PCR we could show that $\text{Na}_v1.8$ -GIRK2 mice contain nine copies of the transgene in their genome. Although BAC transgenic mice usually do not carry more than five copies, higher copy numbers have also been reported (Antoch et al., 1997; Chandler et al., 2007; Schedl et al., 1993). As it had been shown that the copy number remains unchanged in the following generations (Chandler et al., 2007) and in order to keep the expression of the exogenous GIRK2 at a physiological level, we did not breed homozygous mice which would have carried 18 copies of the transgene. This provided the additional advantage to use the wildtype littermates as controls.

4.2.1 Inflammation enhanced DAMGO induced antinociception in $\text{Na}_v1.8$ -GIRK2 mice

We next examined whether the transgenic expression of GIRK channels in peripheral sensory neurons and the functional coupling to mu-opioid receptors has differential *in vivo* effects on peripheral opioid antinociception under normal versus pathological conditions. We observed significant DAMGO-induced antinociception in transgenic $\text{Na}_v1.8$ -GIRK2 mice with an inflamed hind paw. This effect was reversible by the peripherally restricted opioid-receptor antagonist naloxone-methiodide and it was much less pronounced in wildtype animals. Intraplantar injection of DAMGO did not produce antinociception in healthy $\text{Na}_v1.8$ -GIRK2 mice or wildtype littermates.

It is well known that peripherally active opioids are often ineffective if applied to healthy tissue, whereas in injured or inflamed tissue activation of mu- (and other) opioid receptors elicits pronounced antinociception (Joris et al., 1987; Stein et al., 2003; Stein and Zollner, 2009). It was shown that mu-opioid receptor mRNA is up-regulated in corresponding DRGs of rats with hind paw inflammation. Furthermore, the protein content of mu-opioid receptors in rat DRG neurons and the number of mu-opioid receptor expressing sensory nerve terminals

was increased (Hassan et al., 1993; Puehler et al., 2004), suggesting that inflammation enhances axonal transport of mu-opioid receptors. In addition, enhanced G-protein coupling of opioid receptors was reported and the access of opioid ligands to their receptors is facilitated due to a disruption of the perineurial barrier caused by inflammation (Antonijevic et al., 1995; Zollner et al., 2003). Importantly, all studies mentioned above determined the regulation of mu-opioid receptors during inflammation in rats. In mice much less is known about the influence of inflammation on opioid receptor expression. One study showed that inflammation in the gut of mice induced an up-regulation of mu-opioid receptor mRNA and its protein on sensory nerve endings innervating the gut as well as an increase in the number of neurons expressing the mu-opioid receptor (Pol et al., 2001). Recently, Yamamoto and colleagues demonstrated increased levels of mu-opioid receptor protein in mouse DRG neurons after CFA inflammation of the hind paw (Yamamoto et al., 2008). In contrast, an enhancement of morphine-induced spinal antinociception in mice with hind paw inflammation was not associated with an up-regulation of spinal mu-opioid receptors (Gonzalez-Rodriguez et al., 2010).

Many studies demonstrated that paw inflammation enhances mRNA expression of different transcripts in DRG neurons innervating the inflamed paw. This was shown for TRPA1 channels, mu-opioid receptors and the TTX-resistant sodium channel $\text{Na}_v1.8$ (Obata et al., 2005; Puehler et al., 2004; Waxman et al., 1999; Yu et al., 2011). Therefore, we also examined GIRK2 mRNA but did not observe significant changes after induction of hind paw inflammation in DRGs of mice or rats.

Besides, there is evidence for increased GIRK channel activity during inflammation. González-Rodríguez and colleagues proposed that enhanced intrathecal morphine antinociception during inflammation is generated through enhanced activity of GIRK channels in the spinal cord. They showed that a lower concentration of the GIRK channel antagonist tertiapin was needed to inhibit morphine induced antinociception in mice with an inflamed hind paw compared to healthy mice (Gonzalez-Rodriguez et al., 2010), indicating that less GIRK channels are needed to induce maximal antinociception in this situation. Another study demonstrating enhanced presence of GIRK channels at the cell surface upon activation of NMDA receptors contributed to the idea of increased GIRK channel activity upon inflammation. This study showed that activation of NMDA receptors in hippocampal neurons enhanced surface expression of GIRK1 and GIRK2 following dephosphorylation of Ser-9 which subsequently increased the delivery of GIRK channels from recycling endosomes (Chung et al., 2009). Spinal NMDA receptor activation can also be induced by peripheral

inflammation (Svendsen et al., 1999). A main characteristic of painful inflammation is the acidification of the affected tissue (Häbler, 1929; Steen et al., 1996). Interestingly, several members of the K_{ir} family (including GIRK channels) seem to be pH sensitive (Coulter et al., 1995; Mao et al., 2002; Xu et al., 2001). Extracellular acidification enhanced GIRK channel activity due to direct binding of protons to a histidine residue in the extracellular domain (Mao et al., 2002). Thus, it is possible that the binding of protons changes GIRK gating properties or the frequency of opening of GIRK channels. In addition, GIRK channels are positively modulated by ATP which is known to increase intracellularly during inflammation (Hamilton et al., 1999). The presence of ATP enhanced $G_{\beta\gamma}$ activated GIRK currents and was associated with long-lasting channel openings (Han et al., 2003).

Although we did not detect an up-regulation of GIRK channel mRNA expression during inflammation, an increased presence of GIRK channel protein at the cell membrane may still occur due to enhanced delivery of GIRK channels from endosomes. This may underly the enhanced opioid-induced antinociception during inflammation. Indeed, the mechanisms described above point to a role of GIRK channels in the potentiation of opioid antinociception in the context of inflammation. We assume that GIRK channels substantially participate in this potentiation as it was particularly prominent in $Na_v1.8$ -GIRK2 mice.

4.2.2 Unidirectional protein transport of Flag-GIRK2 in peripheral sensory neurons of $Na_v1.8$ -GIRK2 mice

It is well known that proteins produced in the cell body of peripheral sensory neurons are transported along the axons to both peripheral and central terminals (Besse et al., 1990; Guo et al., 1999; Hassan et al., 1993; Li et al., 1998; Truong et al., 2003; Vulchanova et al., 1998). To see whether Flag-GIRK2 of $Na_v1.8$ -GIRK2 mice is transported in the same manner, I performed immunohistochemistry with anti-Flag antibodies. As shown before (Marker et al., 2006), I observed expression of endogenous GIRK2 in the dorsal horn of the spinal cord using anti-GIRK2 antibodies. Surprisingly, I found immunoreactivity for Flag-GIRK2 in the sciatic nerve but not in the spinal cord. These results suggest a transportation of Flag-GIRK2 to peripheral but not to the central terminals in the dorsal horn of the spinal cord. Unidirectional protein transport within peripheral sensory neurons is quite uncommon. So far it has been demonstrated for just one other sensory ion channel, the DEG/ENaC ion channel BNaC1 α (Garcia-Anoveros et al., 2001).

Interestingly, two other studies using the $\text{Na}_v1.8$ promoter to drive the expression of Cre reported a lack of protein in the spinal cord after crossing $\text{Na}_v1.8$ -Cre mice with *lacZ* reporter mice (Agarwal et al., 2004; Stirling et al., 2005). In these mice, Cre recombinase excises a floxed STOP-cassette which inhibits synthesis of β -galactosidase (encoded by *lacZ*), so that functional Cre expression can be visualized by X-gal staining (Soriano, 1999). Although these two $\text{Na}_v1.8$ reporter mice were generated by different strategies, both studies found no X-gal staining in the dorsal horn of the spinal cord. However, neither investigated β -galactosidase expression in the peripheral terminals, e.g. in the sciatic nerve. Importantly, after synthesis of the $\text{Na}_v1.8$ channel itself in the DRG, it is bidirectionally transported (Amaya et al., 2000; Novakovic et al., 1998). As transportation along the peripheral terminals was not investigated, it is possible that β -galactosidase is not transported at all and stays in the DRG cell bodies. So far, no mechanism that controls or sorts unilateral protein transport is known in peripheral sensory neurons and further studies need to examine possible regulatory mechanisms.

4.3 Do GIRK channels play a role in human peripheral opioid analgesia?

Since initial studies had shown that low doses of intraarticularly injected morphine reduces pain after knee surgery and injection of naloxone reversed this pain reduction, it was assumed that the observed pain relieving effect was achieved by activating peripheral opioid receptors (Stein et al., 1991). In addition, another clinical study demonstrated interaction of endogenous opioid peptides released from immune cells in patients undergoing knee surgery. In this study intraarticular administration of naloxone increased postoperative pain compared to controls receiving intravenous naloxone at the same dose (Stein et al., 1993). Many subsequent studies demonstrated similar actions of low doses of opioids if applied intraarticularly (Allen et al., 1993; Dalsgaard et al., 1994; Khouri et al., 1992).

In contrast, diverse results were produced if opioids were applied to other peripheral tissues. For example, intraperitoneal or intrapleural administration of morphine to patients undergoing laparoscopic surgery failed to produce analgesia in these patients (Schulte-Steinberg et al., 1995). Furthermore, intrapleural application of morphine to patients after thoracotomy did not produce enhanced analgesia compared to the effect of morphine administered systemically and did not improve pulmonary function (Welte et al., 1992). On the other hand, administration of morphine to the axillary nerve improved postoperative analgesia in patients undergoing elective upper extremity surgery (Bourke and Furman, 1993). Some of these

studies may have revealed no peripheral effect of opioids due to insufficient doses. However, it is difficult to draw general conclusions, because the degree of local inflammation influences opioid actions (as discussed under 4.2.1). Moreover, the physical characteristics, cellular barriers (e.g. nerve sheaths) and extracellular composition of different tissues might have an impact on the access of opioids to their receptors. With regard to GIRK channels, all four subunits can be found in humans. Their expression has been reported in the central nervous system and in cardiac tissue. Since nothing is known about GIRK channel expression in human peripheral sensory neurons (Gaborit et al., 2007; Schoots et al., 1999; Spaanschus et al., 1996), further studies are needed to examine whether GIRK channels play a role in peripheral analgesia in humans.

4.4 The choice of species for preclinical studies

This study provided novel insights into different molecular mechanisms of antinociception in mice versus rats, two species used in practically all preclinical studies in this field (Mogil, 2009). Recent prominent reviews have repeatedly pointed at the prevalent lack of successful translation of preclinical findings into novel clinical applications (Macleod, 2011; Rice et al., 2008; Woolf, 2010). As seen in the present study, to investigate the pain relieving effect of novel compounds it would be important to perform preclinical studies in animals that present the same molecular components as humans. To date it is not known whether humans express GIRK channels in their peripheral sensory neurons. However, novel analgesic drug candidates, initially declared as safe and effective based on studies performed in animal models, often fail in human trials due to adverse side effects and a lack of efficacy (Mogil, 2009). As demonstrated here, species differences apparently play a major role for the predictivity of animal models.

Mice and rats are the two species typically used to identify novel targets for analgesics and to test the efficacy of new therapeutic drugs (Berge, 2011). Most new potential analgesics that have been shown to be effective in animal models failed in clinical trials (Kola and Landis, 2004; Rice et al., 2008). One example, although a non-opioid therapeutic agent, is the failure of NK₁ (substance P) receptor antagonist in clinical trials. Animal studies provided strong evidence for substance P antagonists acting as effective analgesics. For example, it was shown that substance P plays a role in nociception and hypersensitivity and is a neurotransmitter mainly present in primary sensory neurons. Studies with NK₁ receptor

knockout mice or antagonists revealed a reduced response to chronic pain states such as inflammation or nerve injury whereas the response to acute nociception was fairly unchanged (Hill, 2000). Surprisingly, in clinical trials no analgesic effect was observed in patients testing NK₁ receptor antagonists. One obvious explanation for the failure of NK₁ receptor antagonists in humans are species differences in the physiology of substance P and the distribution of NK₁ receptors (Dionne, 1999).

Other studies demonstrated enhanced opioid antinociception and reduced tolerance in animals treated with NMDA receptor antagonists combined with opioids. Again, in clinical trials the combination of NMDA receptor antagonists and morphine neither showed a reduction in opioid tolerance nor enhanced antinociception (Galer et al., 2005).

We cannot draw any conclusions about non-opioid analgesics from our results, but at least for opioid-induced pain inhibition we discovered marked species differences in molecular mechanisms of opioid action in the peripheral nervous system. This is important for the choice of species in preclinical studies and, if taken into account in the future, might increase the success rate of the outcome of clinical trials.

4.5 GIRK channels as a possible therapeutic target

To consider GIRK channel-specific agonists or the channel itself (e.g. by gene therapy) as novel analgesic strategies one has to make sure that DRG neurons are targeted specifically. Changes in GIRK channel activity in the CNS have been implicated in many disorders such as Parkinson's disease, epilepsy, addiction or Down's syndrome (Luscher and Slesinger, 2010). One possibility to improve the action of opioids in the PNS is the enhanced expression of GIRK channels and their functional coupling to opioid receptors. This was illustrated with our transgenic Na_v1.8-GIRK2 mouse line that showed enhanced DAMGO induced antinociception due to the presence of GIRK channels.

If GIRK channel expression could be verified in human DRG neurons, it might be reasonable to develop specific GIRK channel agonists selectively acting on peripheral GIRK channels. To our knowledge no specific GIRK channel agonist exists, except the G_{βγ} subunits of G_{i/o}-proteins which activate not only GIRK channels but affect a lot of other receptors and channels (Clapham and Neer, 1997). If future studies show that humans lack GIRK channels in their primary sensory afferents, one might envision to induce GIRK channel expression in

DRG neurons by gene-therapeutic approaches such as virus based vectors (Fink et al., 2011; Raja, 2011; Zhang et al., 2008).

For example, several animal studies performed transgene expression in nociceptive neurons with adeno-associated viral vectors. In fact, injection of an AAV-based vector encoding the mu-opioid receptor into DRGs of rats led to enhanced expression of the receptor for at least six months and increased the effect of subcutaneously injected morphine (Xu et al., 2003). Zhang and colleagues used a herpes simplex virus (HSV)-based vector encoding the mu-opioid receptor to enhance peripheral antinociception in mice. HSV naturally targets primary afferent neurons. Following infection with this vector by subcutaneous injection, enhanced mu-opioid receptor expression was found in the skin, in the cell bodies of primary afferent neurons as well as in their central and peripheral terminals. Behavioral experiments demonstrated enhanced antinociception after subcutaneous injection of loperamide, a mu-opioid receptor agonist that does not cross the blood-brain barrier (Zhang et al., 2008).

Interestingly, Fink and colleagues performed a clinical study using replication-defective herpes simplex virus-based vectors encoding for preproenkephalin (PENK). Proteolytic cleavage of PENK within the nucleus leads to the production of two opioid peptides, leu-enkephalin and met-enkephalin (Busch-Dienstfertig and Stein, 2010). Repeated intradermal injections of the HSV-based vector produced dose-dependent antinociception in patients suffering from cancer pain (Fink et al., 2011).

Since the infection of mouse DRG neurons with an AAV-GIRK2 led to functional expression of GIRK channels and our transgenic mouse line $\text{Na}_v1.8$ -GIRK2 provided further promising results, it would be interesting to see whether GIRK channel expression in DRGs driven by virus-based vectors would enhance peripheral opioid antinociception in future studies.

4.6 Conclusion and outlook

Taken together, our results demonstrate that GIRK channels in DRG neurons are crucially involved in peripheral opioid antinociception. Mice, normally lacking GIRK channels in their primary sensory neurons, show much lesser responses to peripherally applied opioids compared to rats that normally express such GIRK channels. Importantly, the mu-opioid agonist DAMGO induced significant peripheral antinociceptive effects in transgenic $\text{Na}_v1.8$ -GIRK2 mice expressing functional GIRK channels in their DRG neurons. Of course, one of the major questions is whether GIRK channels are expressed in human primary sensory

afferents. Since it is difficult to get access to human tissue, it would be a good start to use mRNA isolated from cadaver DRGs to investigate GIRK channel expression on the transcriptional level. Our finding that, in healthy paw tissue, DAMGO did not evoke effects in $\text{Na}_v1.8$ -GIRK2 or wildtype mice suggests that the access of opioids to neurons is hampered by the perineural barrier and/or that opioid receptors or GIRK channels require enhanced expression and activity driven by pathological conditions such as inflammation. Fentanyl, a mu-opioid receptor agonist which easily crosses the perineural barrier due to its lipophilic properties, might be used in future experiments to examine the first hypothesis. Another interesting problem may be neuropathic pain. A recent study reported that the $\text{Na}_v1.8$ positive population of peripheral sensory neurons is critical for initiating neuropathic pain (Emery et al., 2011). Since we evoked expression of GIRK2 selectively in $\text{Na}_v1.8$ positive neurons, it would be interesting to see whether peripherally applied opioids can abolish neuropathic pain in $\text{Na}_v1.8$ -GIRK2 mice. Thus, our findings provide new insights into molecular mechanisms underlying pain inhibition in different species and they provoke interesting questions for future basic and clinical research.

5 Summary

The use of opioids for pain management is complicated by associated adverse side effects. Nevertheless, opioids are the gold standard for the treatment of pain. A better understanding of the mechanisms underlying opioid analgesia, particularly in the peripheral nervous system (PNS), would help to develop opioids acting specifically at sites of peripheral tissue injury to inhibit pain without centrally mediated unwanted effects. Activation of opioid receptors typically inhibits neuronal voltage-gated calcium (Ca^{2+})-channels and activates G protein-coupled inwardly rectifying potassium (GIRK) channels through the binding of G-protein $\text{G}_{\beta\gamma}$ subunits in the central nervous system (CNS). Both events reduce membrane excitability. However, studies on GIRK channel expression and function in the PNS are scarce and have produced conflicting results. Here we report for the first time that GIRK channels in peripheral sensory (dorsal root ganglion; DRG) neurons are crucially involved in the generation of opioid antinociception.

We found strong mRNA expression of different GIRK subunits in the cerebellum of mice and rats, whereas GIRK mRNA was expressed only at very low levels in DRG of naïve mice. However, expression of GIRK1 and -2 mRNA was prominent in DRG neurons of naïve rats. We detected GIRK1 and -2 protein in mouse cerebellum but not in DRG, whereas both proteins were present in rat DRG. By using the whole cell patch-clamp technique we recorded GIRK currents after mu-opioid receptor activation in rat but not in mouse DRG neurons.

We generated transgenic mice expressing a Flag-GIRK2 construct selectively in DRG neurons. The mu-opioid agonist DAMGO evoked GIRK currents in DRG neurons isolated from these $\text{Na}_v1.8$ -GIRK2 mice but not from wildtype littermates. This indicates a functional coupling of mu-opioid receptors and GIRK channels in $\text{Na}_v1.8$ -GIRK2 mice. We assessed how expression of GIRK2 affects nociceptive behavior by measuring hindpaw withdrawal in response to noxious heat or mechanical stimuli using a model of inflammatory pain. $\text{Na}_v1.8$ -GIRK2 mice exhibited normal baseline sensitivities as well as normal thermal and mechanical hyperalgesia after induction of paw inflammation. Local injection of DAMGO abolished the thermal and mechanical hypersensitivity in $\text{Na}_v1.8$ -GIRK2 mice but not in wildtype littermates with inflamed paws.

In summary, these data show that expression of GIRK channels in peripheral sensory neurons is crucial for the generation of peripheral opioid antinociception and that there are important species-specific differences in rodents. Potent DAMGO-induced antinociception was

redeemed in transgenic mice expressing sensory neuron-specific GIRK2. Our findings provide new insights into molecular mechanisms underlying pain inhibition in different species and they provoke interesting questions for future basic and clinical research.

Zusammenfassung

Opiode werden sehr häufig in der Schmerztherapie verwendet obwohl sie starke Nebenwirkungen hervorrufen. Trotzdem sind Opiode bis heute die wirksamsten Analgetika um starke Schmerzen zu lindern. Ein besseres Verständnis der Mechanismen welche der Opioid-Analgesie insbesondere im peripheren Nervensystem (PNS) zugrunde liegen, würde helfen um neue Opiode zu entwickeln, die direkt in verletztem Gewebe wirken und somit den Schmerz dort inhibieren wo er entsteht, ohne zentrale Nebenwirkungen hervorzurufen. Aktivierung der G-Protein gekoppelten Opioidrezeptoren führt zur Inhibition von spannungs-kontrollierten Kalziumkanälen und, im zentralen Nervensystem (ZNS), zur Aktivierung von bestimmten Kaliumkanälen, den „G protein-coupled inwardly rectifying potassium“ (GIRK) Kanälen. Beides geschieht durch Bindung der $G_{\beta\gamma}$ Untereinheit des Opioidrezeptors an die Ionenkanäle und führt zur geringeren Erregbarkeit der Nervenzelle. Studien über die Expression der GIRK Ionenkanäle im PNS zeigen widersprüchliche Ergebnisse. In dieser Dissertation konnte zum ersten Mal gezeigt werden, dass GIRK Ionenkanäle eine entscheidende Rolle in der peripheren Opioidanalgesie spielen.

Starke mRNA Expression verschiedener GIRK Untereinheiten konnte im Kleinhirn, nicht aber in den Hinterwurzelganglien (DRGs) der peripheren sensorischen Neurone von Mäusen nachgewiesen werden. Im Gegensatz dazu wurde eine deutliche mRNA Expression der Untereinheiten GIRK1 und -2 in den Hinterwurzelganglien der Ratte gezeigt. Mit Hilfe von Patch clamp Experimenten konnten GIRK Ströme nach Aktivierung des mu-Opioidrezeptors in DRG Neuronen der Ratte nicht aber der Maus gemessen werden.

Es wurde eine transgene Mauslinie generiert, welche ein Flag-GIRK2 Konstrukt selektiv in peripheren sensorischen Neuronen exprimiert. Wir konnten DAMGO-induzierte GIRK Ströme in peripheren sensorischen Neuronen der transgenen Mäuse, nicht aber der wildtyp Geschwister messen. Dies deutet auf eine funktionelle Kopplung von mu-Opioidrezeptoren und Flag-GIRK2 Ionenkanälen in den transgenen Mäusen hin. Wir untersuchten, wie die Expression von Flag-GIRK2 das Schmerzverhalten und die Opioidanalgesie in

Verhaltensexperimenten beeinflusst. Die basale Sensitivität für schmerzhafte Hitzestimuli und Mechanische Reize war bei transgenen Mäusen unverändert gegenüber wildtyp Geschwistern. Zwei Tage nach Induktion einer Pfotenentzündung entwickelten auch beide eine thermale und mechanische Hyperalgesie. Injektion des mu-Opioidagonisten DAMGO in die entzündete Pfote reduzierte jedoch Hitzeschmerz sowie mechanische Hyperalgesie nur in den transgenen Mäusen.

Zusammenfassend konnte gezeigt werden, dass GIRK Ionenkanäle in peripheren sensorischen Neuronen äußerst wichtig sind für die Manifestation von peripherer Opioidanalgesie in Nagern. Wir konnten DAMGO-induzierte Analgesie in transgenen Mäusen messen, welche den GIRK2 Ionenkanal in peripheren sensorischen Neuronen exprimieren, nicht aber in wildtyp Mäusen die keine GIRK Ionenkäne im PNS aufweisen. Übereinstimmend mit unseren Ergebnissen, haben viele andere Studien periphere Opioidanalgesie in Ratten nachgewiesen, welche GIRK Ionenkanäle normalerweise in ihren peripheren sensorischen Neuronen exprimieren.

6 References

- Agarwal, N., Offermanns, S., and Kuner, R.** (2004). Conditional gene deletion in primary nociceptive neurons of trigeminal ganglia and dorsal root ganglia. *Genesis* 38, 122-129.
- Aguado, C., Colon, J., Ciruela, F., Schlaudraff, F., Cabanero, M.J., Perry, C., Watanabe, M., Liss, B., Wickman, K., and Lujan, R.** (2008). Cell type-specific subunit composition of G protein-gated potassium channels in the cerebellum. *Journal of neurochemistry* 105, 497-511.
- Akil, H., Owens, C., Gutstein, H., Taylor, L., Curran, E., and Watson, S.** (1998). Endogenous opioids: overview and current issues. *Drug and alcohol dependence* 51, 127-140.
- Akins, P.T., and McCleskey, E.W.** (1993). Characterization of potassium currents in adult rat sensory neurons and modulation by opioids and cyclic AMP. *Neuroscience* 56, 759-769.
- Akopian, A.N., Sivilotti, L., and Wood, J.N.** (1996). A tetrodotoxin-resistant voltage-gated sodium channel expressed by sensory neurons. *Nature* 379, 257-262.
- Akopian, A.N., Souslova, V., England, S., Okuse, K., Ogata, N., Ure, J., Smith, A., Kerr, B.J., McMahon, S.B., Boyce, S., et al.** (1999). The tetrodotoxin-resistant sodium channel SNS has a specialized function in pain pathways. *Nature neuroscience* 2, 541-548.
- Allen, G.C., St Amand, M.A., Lui, A.C., Johnson, D.H., and Lindsay, M.P.** (1993). Postarthroscopy analgesia with intraarticular bupivacaine/morphine. A randomized clinical trial. *Anesthesiology* 79, 475-480.
- Amaya, F., Decosterd, I., Samad, T.A., Plumpton, C., Tate, S., Mannion, R.J., Costigan, M., and Woolf, C.J.** (2000). Diversity of expression of the sensory neuron-specific TTX-resistant voltage-gated sodium ion channels SNS and SNS2. *Molecular and cellular neurosciences* 15, 331-342.
- Antoch, M.P., Song, E.J., Chang, A.M., Vitaterna, M.H., Zhao, Y., Wilsbacher, L.D., Sangoram, A.M., King, D.P., Pinto, L.H., and Takahashi, J.S.** (1997). Functional identification of the mouse circadian Clock gene by transgenic BAC rescue. *Cell* 89, 655-667.
- Antonijevic, I., Mousa, S.A., Schafer, M., and Stein, C.** (1995). Perineurial defect and peripheral opioid analgesia in inflammation. *The Journal of neuroscience : the official journal of the Society for Neuroscience* 15, 165-172.
- Arroyo, E.J., Xu, T., Grinspan, J., Lambert, S., Levinson, S.R., Brophy, P.J., Peles, E., and Scherer, S.S.** (2002). Genetic dysmyelination alters the molecular architecture of the nodal region. *The Journal of neuroscience : the official journal of the Society for Neuroscience* 22, 1726-1737.
- Basbaum, A.I., Bautista, D.M., Scherrer, G., and Julius, D.** (2009). Cellular and molecular mechanisms of pain. *Cell* 139, 267-284.
- Basbaum, A.I., and Fields, H.L.** (1984). Endogenous pain control systems: brainstem spinal pathways and endorphin circuitry. *Annual review of neuroscience* 7, 309-338.
- Berge, O.G.** (2011). Predictive validity of behavioural animal models for chronic pain. *British journal of pharmacology* 164, 1195-1206.
- Besse, D., Lombard, M.C., Zajac, J.M., Roques, B.P., and Besson, J.M.** (1990). Pre- and postsynaptic distribution of mu, delta and kappa opioid receptors in the superficial layers of the cervical dorsal horn of the rat spinal cord. *Brain research* 521, 15-22.

- Bichet, D., Haass, F.A., and Jan, L.Y.** (2003). Merging functional studies with structures of inward-rectifier K(+) channels. *Nature reviews Neuroscience* 4, 957-967.
- Bourke, D.L., and Furman, W.R.** (1993). Improved postoperative analgesia with morphine added to axillary block solution. *Journal of clinical anesthesia* 5, 114-117.
- Busch-Dienstfertig, M., and Stein, C.** (2010). Opioid receptors and opioid peptide-producing leukocytes in inflammatory pain--basic and therapeutic aspects. *Brain, behavior, and immunity* 24, 683-694.
- Chandler, K.J., Chandler, R.L., Broeckelmann, E.M., Hou, Y., Southard-Smith, E.M., and Mortlock, D.P.** (2007). Relevance of BAC transgene copy number in mice: transgene copy number variation across multiple transgenic lines and correlations with transgene integrity and expression. *Mammalian genome : official journal of the International Mammalian Genome Society* 18, 693-708.
- Chaplan, S.R., Bach, F.W., Pogrel, J.W., Chung, J.M., and Yaksh, T.L.** (1994). Quantitative assessment of tactile allodynia in the rat paw. *Journal of neuroscience methods* 53, 55-63.
- Chen, Y., Mestek, A., Liu, J., Hurley, J.A., and Yu, L.** (1993). Molecular cloning and functional expression of a mu-opioid receptor from rat brain. *Molecular pharmacology* 44, 8-12.
- Chung, H.J., Qian, X., Ehlers, M., Jan, Y.N., and Jan, L.Y.** (2009). Neuronal activity regulates phosphorylation-dependent surface delivery of G protein-activated inwardly rectifying potassium channels. *Proceedings of the National Academy of Sciences of the United States of America* 106, 629-634.
- Clancy, S.M., Fowler, C.E., Finley, M., Suen, K.F., Arrabit, C., Berton, F., Kosaza, T., Casey, P.J., and Slesinger, P.A.** (2005). Pertussis-toxin-sensitive Galphai subunits selectively bind to C-terminal domain of neuronal GIRK channels: evidence for a heterotrimeric G-protein-channel complex. *Molecular and cellular neurosciences* 28, 375-389.
- Clapham, D.E., and Neer, E.J.** (1997). G protein beta gamma subunits. *Annual review of pharmacology and toxicology* 37, 167-203.
- Corey, S., and Clapham, D.E.** (1998). Identification of native atrial G-protein-regulated inwardly rectifying K⁺ (GIRK4) channel homomultimers. *The Journal of biological chemistry* 273, 27499-27504.
- Corey, S., and Clapham, D.E.** (2001). The stoichiometry of Gbeta gamma binding to G-protein-regulated inwardly rectifying K⁺ channels (GIRKs). *The Journal of biological chemistry* 276, 11409-11413.
- Coulter, K.L., Perier, F., Radeke, C.M., and Vandenberg, C.A.** (1995). Identification and molecular localization of a pH-sensing domain for the inward rectifier potassium channel HIR. *Neuron* 15, 1157-1168.
- Cox, J.J., Reimann, F., Nicholas, A.K., Thornton, G., Roberts, E., Springell, K., Karbani, G., Jafri, H., Mannan, J., Raashid, Y., et al.** (2006). An SCN9A channelopathy causes congenital inability to experience pain. *Nature* 444, 894-898.
- Cruz, H.G., Berton, F., Sollini, M., Blanchet, C., Pravettoni, M., Wickman, K., and Luscher, C.** (2008). Absence and rescue of morphine withdrawal in GIRK/Kir3 knock-out mice. *The Journal of neuroscience : the official journal of the Society for Neuroscience* 28, 4069-4077.
- Cunha, T.M., Roman-Campos, D., Lotufo, C.M., Duarte, H.L., Souza, G.R., Verri, W.A., Jr., Funez, M.I., Dias, Q.M., Schivo, I.R., Domingues, A.C., et al.** (2010). Morphine peripheral analgesia depends on activation of the PI3Kgamma/AKT/nNOS/NO/KATP signaling pathway. *Proceedings of the National Academy of Sciences of the United States of America* 107, 4442-4447.
- Dalsgaard, J., Felsby, S., Juulsgaard, P., and Froekjaer, J.** (1994). Low-dose intra-articular morphine analgesia in day case knee arthroscopy: a randomized double-blinded prospective study. *Pain* 56, 151-154.

- Damarjian, T.G., Craner, M.J., Black, J.A., and Waxman, S.G.** (2004). Upregulation and colocalization of p75 and Nav1.8 in Purkinje neurons in experimental autoimmune encephalomyelitis. *Neuroscience letters* 369, 186-190.
- De Koninck, Y., and Henry, J.L.** (1991). Substance P-mediated slow excitatory postsynaptic potential elicited in dorsal horn neurons in vivo by noxious stimulation. *Proceedings of the National Academy of Sciences of the United States of America* 88, 11344-11348.
- Dib-Hajj, S.D., Yang, Y., and Waxman, S.G.** (2008). Genetics and molecular pathophysiology of Na(v)1.7-related pain syndromes. *Advances in genetics* 63, 85-110.
- Dionne, R.A.** (1999). Clinical analgesic trials of NK₁ antagonists. *Current Opinion in Investigational Drugs* 1, 82-85.
- Djouhri, L., Fang, X., Okuse, K., Wood, J.N., Berry, C.M., and Lawson, S.N.** (2003). The TTX-resistant sodium channel Nav1.8 (SNS/PN3): expression and correlation with membrane properties in rat nociceptive primary afferent neurons. *The Journal of physiology* 550, 739-752.
- Doupmik, C.A., Davidson, N., Lester, H.A., and Kofuji, P.** (1997). RGS proteins reconstitute the rapid gating kinetics of gbetagamma-activated inwardly rectifying K⁺ channels. *Proceedings of the National Academy of Sciences of the United States of America* 94, 10461-10466.
- Dubin, A.E., and Patapoutian, A.** (2010). Nociceptors: the sensors of the pain pathway. *The Journal of clinical investigation* 120, 3760-3772.
- Emery, E.C., Young, G.T., Berrocoso, E.M., Chen, L., and McNaughton, P.A.** (2011). HCN2 ion channels play a central role in inflammatory and neuropathic pain. *Science* 333, 1462-1466.
- Evans, C.J., Keith, D.E., Jr., Morrison, H., Magendzo, K., and Edwards, R.H.** (1992). Cloning of a delta opioid receptor by functional expression. *Science* 258, 1952-1955.
- Fields, H.** (2004). State-dependent opioid control of pain. *Nature reviews Neuroscience* 5, 565-575.
- Fink, D.J., Wechuck, J., Mata, M., Glorioso, J.C., Goss, J., Krisky, D., and Wolfe, D.** (2011). Gene therapy for pain: results of a phase I clinical trial. *Annals of neurology* 70, 207-212.
- Furst, S.** (1999). Transmitters involved in antinociception in the spinal cord. *Brain research bulletin* 48, 129-141.
- Gaborit, N., Le Bouter, S., Szuts, V., Varro, A., Escande, D., Nattel, S., and Demolombe, S.** (2007). Regional and tissue specific transcript signatures of ion channel genes in the non-diseased human heart. *The Journal of physiology* 582, 675-693.
- Galer, B.S., Lee, D., Ma, T., Nagle, B., and Schlagheck, T.G.** (2005). MorphiDex (morphine sulfate/dextromethorphan hydrobromide combination) in the treatment of chronic pain: three multicenter, randomized, double-blind, controlled clinical trials fail to demonstrate enhanced opioid analgesia or reduction in tolerance. *Pain* 115, 284-295.
- Gao, X.F., Zhang, H.L., You, Z.D., Lu, C.L., and He, C.** (2007). G protein-coupled inwardly rectifying potassium channels in dorsal root ganglion neurons. *Acta pharmacologica Sinica* 28, 185-190.
- Garcia-Anoveros, J., Samad, T.A., Zuvela-Jelaska, L., Woolf, C.J., and Corey, D.P.** (2001). Transport and localization of the DEG/ENaC ion channel BNaC1alpha to peripheral mechanosensory terminals of dorsal root ganglia neurons. *The Journal of neuroscience : the official journal of the Society for Neuroscience* 21, 2678-2686.
- Gold, M.S., Dastmalchi, S., and Levine, J.D.** (1996). Co-expression of nociceptor properties in dorsal root ganglion neurons from the adult rat in vitro. *Neuroscience* 71, 265-275.

- Gold, M.S., and Gebhart, G.F.** (2010). Nociceptor sensitization in pain pathogenesis. *Nature medicine* *16*, 1248-1257.
- Gong, S., Yang, X.W., Li, C., and Heintz, N.** (2002). Highly efficient modification of bacterial artificial chromosomes (BACs) using novel shuttle vectors containing the R6Kgamma origin of replication. *Genome research* *12*, 1992-1998.
- Gonzalez-Rodriguez, S., Hidalgo, A., Baamonde, A., and Menendez, L.** (2010). Involvement of Gi/o proteins and GIRK channels in the potentiation of morphine-induced spinal analgesia in acutely inflamed mice. *Naunyn-Schmiedeberg's archives of pharmacology* *381*, 59-71.
- Grosse, G., Eulitz, D., Thiele, T., Pahner, I., Schroter, S., Takamori, S., Grosse, J., Wickman, K., Tapp, R., Veh, R.W., et al.** (2003). Axonal sorting of Kir3.3 defines a GABA-containing neuron in the CA3 region of rodent hippocampus. *Molecular and cellular neurosciences* *24*, 709-724.
- Guo, A., Vulchanova, L., Wang, J., Li, X., and Elde, R.** (1999). Immunocytochemical localization of the vanilloid receptor 1 (VR1): relationship to neuropeptides, the P2X3 purinoceptor and IB4 binding sites. *The European journal of neuroscience* *11*, 946-958.
- Gutman, G.A., Chandy, K.G., Adelman, J.P., Aiyar, J., Bayliss, D.A., Clapham, D.E., Covarrubias, M., Desir, G.V., Furuichi, K., Ganetzky, B., et al.** (2003). International Union of Pharmacology. XLI. Compendium of voltage-gated ion channels: potassium channels. *Pharmacological reviews* *55*, 583-586.
- Häbler, C.** (1929). Über den Ka+ - und Ca++ -Gehalt von Eiter und Exsudaten und seine Beziehungen zum Entzündungsschmerz. *Klin Wochenschr* *8*, 1569-1572.
- Hamilton, S.G., Wade, A., and McMahon, S.B.** (1999). The effects of inflammation and inflammatory mediators on nociceptive behaviour induced by ATP analogues in the rat. *British journal of pharmacology* *126*, 326-332.
- Han, J., Kang, D., and Kim, D.** (2003). Properties and modulation of the G protein-coupled K+ channel in rat cerebellar granule neurons: ATP versus phosphatidylinositol 4,5-bisphosphate. *The Journal of physiology* *550*, 693-706.
- Hargreaves, K., Dubner, R., Brown, F., Flores, C., and Joris, J.** (1988). A new and sensitive method for measuring thermal nociception in cutaneous hyperalgesia. *Pain* *32*, 77-88.
- Harper, A.A., and Lawson, S.N.** (1985). Conduction velocity is related to morphological cell type in rat dorsal root ganglion neurones. *The Journal of physiology* *359*, 31-46.
- Hasegawa, H., Abbott, S., Han, B.X., Qi, Y., and Wang, F.** (2007). Analyzing somatosensory axon projections with the sensory neuron-specific Advillin gene. *The Journal of neuroscience : the official journal of the Society for Neuroscience* *27*, 14404-14414.
- Hassan, A.H., Ableitner, A., Stein, C., and Herz, A.** (1993). Inflammation of the rat paw enhances axonal transport of opioid receptors in the sciatic nerve and increases their density in the inflamed tissue. *Neuroscience* *55*, 185-195.
- Heaney, J.D., and Bronson, S.K.** (2006). Artificial chromosome-based transgenes in the study of genome function. *Mammalian genome : official journal of the International Mammalian Genome Society* *17*, 791-807.
- Heginbotham, L., Lu, Z., Abramson, T., and MacKinnon, R.** (1994). Mutations in the K+ channel signature sequence. *Biophysical journal* *66*, 1061-1067.
- Heinke, B., Gingl, E., and Sandkuhler, J.** (2011). Multiple targets of mu-opioid receptor-mediated presynaptic inhibition at primary afferent Adelta- and C-fibers. *The Journal of neuroscience : the official journal of the Society for Neuroscience* *31*, 1313-1322.

- Heintz, N.** (2001). BAC to the future: the use of bac transgenic mice for neuroscience research. *Nature reviews Neuroscience* 2, 861-870.
- Hescheler, J., Rosenthal, W., Trautwein, W., and Schultz, G.** (1987). The GTP-binding protein, Go, regulates neuronal calcium channels. *Nature* 325, 445-447.
- Hibino, H., Inanobe, A., Furutani, K., Murakami, S., Findlay, I., and Kurachi, Y.** (2010). Inwardly rectifying potassium channels: their structure, function, and physiological roles. *Physiological reviews* 90, 291-366.
- Hill, R.** (2000). NK1 (substance P) receptor antagonists--why are they not analgesic in humans? *Trends in pharmacological sciences* 21, 244-246.
- Hollmann, M.W., Strumper, D., Herroeder, S., and Durieux, M.E.** (2005). Receptors, G proteins, and their interactions. *Anesthesiology* 103, 1066-1078.
- Huang, C.L., Slesinger, P.A., Casey, P.J., Jan, Y.N., and Jan, L.Y.** (1995). Evidence that direct binding of G beta gamma to the GIRK1 G protein-gated inwardly rectifying K⁺ channel is important for channel activation. *Neuron* 15, 1133-1143.
- Hughes, J., Smith, T.W., Kosterlitz, H.W., Fothergill, L.A., Morgan, B.A., and Morris, H.R.** (1975). Identification of two related pentapeptides from the brain with potent opiate agonist activity. *Nature* 258, 577-580.
- Hunt, S.P., and Mantyh, P.W.** (2001). The molecular dynamics of pain control. *Nature reviews Neuroscience* 2, 83-91.
- Ikeda, K., Kobayashi, T., Kumanishi, T., Niki, H., and Yano, R.** (2000). Involvement of G-protein-activated inwardly rectifying K (GIRK) channels in opioid-induced analgesia. *Neuroscience research* 38, 113-116.
- Inanobe, A., Yoshimoto, Y., Horio, Y., Morishige, K.I., Hibino, H., Matsumoto, S., Tokunaga, Y., Maeda, T., Hata, Y., Takai, Y., et al.** (1999). Characterization of G-protein-gated K⁺ channels composed of Kir3.2 subunits in dopaminergic neurons of the substantia nigra. *The Journal of neuroscience : the official journal of the Society for Neuroscience* 19, 1006-1017.
- Jelacic, T.M., Kennedy, M.E., Wickman, K., and Clapham, D.E.** (2000). Functional and biochemical evidence for G-protein-gated inwardly rectifying K⁺ (GIRK) channels composed of GIRK2 and GIRK3. *The Journal of biological chemistry* 275, 36211-36216.
- Joris, J.L., Dubner, R., and Hargreaves, K.M.** (1987). Opioid analgesia at peripheral sites: a target for opioids released during stress and inflammation? *Anesthesia and analgesia* 66, 1277-1281.
- Julius, D., and Basbaum, A.I.** (2001). Molecular mechanisms of nociception. *Nature* 413, 203-210.
- Kanjhan, R., Coulson, E.J., Adams, D.J., and Bellingham, M.C.** (2005). Tertiapin-Q blocks recombinant and native large conductance K⁺ channels in a use-dependent manner. *The Journal of pharmacology and experimental therapeutics* 314, 1353-1361.
- Karschin, C., and Karschin, A.** (1997). Ontogeny of gene expression of Kir channel subunits in the rat. *Molecular and cellular neurosciences* 10, 131-148.
- Kennedy, M.E., Nemec, J., Corey, S., Wickman, K., and Clapham, D.E.** (1999). GIRK4 confers appropriate processing and cell surface localization to G-protein-gated potassium channels. *The Journal of biological chemistry* 274, 2571-2582.
- Khodorova, A., Navarro, B., Jouaville, L.S., Murphy, J.E., Rice, F.L., Mazurkiewicz, J.E., Long-Woodward, D., Stoffel, M., Strichartz, G.R., Yukhananov, R., et al.** (2003). Endothelin-B receptor activation triggers an endogenous analgesic cascade at sites of peripheral injury. *Nature medicine* 9, 1055-1061.

- Khoury, G.F., Chen, A.C., Garland, D.E., and Stein, C.** (1992). Intraarticular morphine, bupivacaine, and morphine/bupivacaine for pain control after knee videoarthroscopy. *Anesthesiology* 77, 263-266.
- Kieffer, B.L., Befort, K., Gaveriaux-Ruff, C., and Hirth, C.G.** (1992). The delta-opioid receptor: isolation of a cDNA by expression cloning and pharmacological characterization. *Proceedings of the National Academy of Sciences of the United States of America* 89, 12048-12052.
- Kieffer, B.L., and Evans, C.J.** (2009). Opioid receptors: from binding sites to visible molecules in vivo. *Neuropharmacology* 56 Suppl 1, 205-212.
- Kola, I., and Landis, J.** (2004). Can the pharmaceutical industry reduce attrition rates? *Nature reviews Drug discovery* 3, 711-715.
- Koltzenburg, M., Stucky, C.L., and Lewin, G.R.** (1997). Receptive properties of mouse sensory neurons innervating hairy skin. *Journal of neurophysiology* 78, 1841-1850.
- Koyrakh, L., Lujan, R., Colon, J., Karschin, C., Kurachi, Y., Karschin, A., and Wickman, K.** (2005). Molecular and cellular diversity of neuronal G-protein-gated potassium channels. *The Journal of neuroscience : the official journal of the Society for Neuroscience* 25, 11468-11478.
- Krapivinsky, G., Gordon, E.A., Wickman, K., Velimirovic, B., Krapivinsky, L., and Clapham, D.E.** (1995). The G-protein-gated atrial K⁺ channel IKACH is a heteromultimer of two inwardly rectifying K(+) -channel proteins. *Nature* 374, 135-141.
- Kunkel, M.T., and Peralta, E.G.** (1995). Identification of domains conferring G protein regulation on inward rectifier potassium channels. *Cell* 83, 443-449.
- Labuz, D.S., Y. and Machelska, H.** (2012). Opioid receptors at the injured nerve trunk govern efficient analgesia in neuropathic pain. Submitted.
- Law, P.Y., Wong, Y.H., and Loh, H.H.** (2000). Molecular mechanisms and regulation of opioid receptor signaling. *Annual review of pharmacology and toxicology* 40, 389-430.
- Lawson, S.N., and Waddell, P.J.** (1991). Soma neurofilament immunoreactivity is related to cell size and fibre conduction velocity in rat primary sensory neurons. *The Journal of physiology* 435, 41-63.
- Le Bars, D., Gozariu, M., and Cadden, S.W.** (2001). Animal models of nociception. *Pharmacological reviews* 53, 597-652.
- Lee, Y., Lee, C.H., and Oh, U.** (2005). Painful channels in sensory neurons. *Molecules and cells* 20, 315-324.
- Li, J.L., Ding, Y.Q., Li, Y.Q., Li, J.S., Nomura, S., Kaneko, T., and Mizuno, N.** (1998). Immunocytochemical localization of mu-opioid receptor in primary afferent neurons containing substance P or calcitonin gene-related peptide. A light and electron microscope study in the rat. *Brain research* 794, 347-352.
- Liao, Y.J., Jan, Y.N., and Jan, L.Y.** (1996). Heteromultimerization of G-protein-gated inwardly rectifying K⁺ channel proteins GIRK1 and GIRK2 and their altered expression in weaver brain. *The Journal of neuroscience : the official journal of the Society for Neuroscience* 16, 7137-7150.
- Loeser, J.D., and Treede, R.D.** (2008). The Kyoto protocol of IASP Basic Pain Terminology. *Pain* 137, 473-477.
- Lu, X.H., Fleming, S.M., Meurers, B., Ackerson, L.C., Mortazavi, F., Lo, V., Hernandez, D., Sulzer, D., Jackson, G.R., Maidment, N.T., et al.** (2009). Bacterial artificial chromosome transgenic mice expressing a truncated mutant parkin exhibit age-dependent hypokinetic motor deficits, dopaminergic neuron degeneration, and accumulation of proteinase K-resistant alpha-synuclein. *The Journal of neuroscience : the official journal of the Society for Neuroscience* 29, 1962-1976.

- Lumpkin, E.A., and Caterina, M.J.** (2007). Mechanisms of sensory transduction in the skin. *Nature* *445*, 858-865.
- Luscher, C., Jan, L.Y., Stoffel, M., Malenka, R.C., and Nicoll, R.A.** (1997). G protein-coupled inwardly rectifying K⁺ channels (GIRKs) mediate postsynaptic but not presynaptic transmitter actions in hippocampal neurons. *Neuron* *19*, 687-695.
- Luscher, C., and Slesinger, P.A.** (2010). Emerging roles for G protein-gated inwardly rectifying potassium (GIRK) channels in health and disease. *Nature reviews Neuroscience* *11*, 301-315.
- Ma, D., Zerangue, N., Raab-Graham, K., Fried, S.R., Jan, Y.N., and Jan, L.Y.** (2002). Diverse trafficking patterns due to multiple traffic motifs in G protein-activated inwardly rectifying potassium channels from brain and heart. *Neuron* *33*, 715-729.
- Macleod, M.** (2011). Why animal research needs to improve. *Nature* *477*, 511.
- Mao, J., Li, L., McManus, M., Wu, J., Cui, N., and Jiang, C.** (2002). Molecular determinants for activation of G-protein-coupled inward rectifier K⁺ (GIRK) channels by extracellular acidosis. *The Journal of biological chemistry* *277*, 46166-46171.
- Marker, C.L., Lujan, R., Colon, J., and Wickman, K.** (2006). Distinct populations of spinal cord lamina II interneurons expressing G-protein-gated potassium channels. *The Journal of neuroscience : the official journal of the Society for Neuroscience* *26*, 12251-12259.
- Marker, C.L., Lujan, R., Loh, H.H., and Wickman, K.** (2005). Spinal G-protein-gated potassium channels contribute in a dose-dependent manner to the analgesic effect of mu- and delta- but not kappa-opioids. *The Journal of neuroscience : the official journal of the Society for Neuroscience* *25*, 3551-3559.
- Marker, C.L., Stoffel, M., and Wickman, K.** (2004). Spinal G-protein-gated K⁺ channels formed by GIRK1 and GIRK2 subunits modulate thermal nociception and contribute to morphine analgesia. *The Journal of neuroscience : the official journal of the Society for Neuroscience* *24*, 2806-2812.
- Martin, W.R., Eades, C.G., Thompson, J.A., Huppler, R.E., and Gilbert, P.E.** (1976). The effects of morphine- and nalorphine-like drugs in the nondependent and morphine-dependent chronic spinal dog. *The Journal of pharmacology and experimental therapeutics* *197*, 517-532.
- Millan, M.J.** (1999). The induction of pain: an integrative review. *Progress in neurobiology* *57*, 1-164.
- Mitrovic, I., Margeta-Mitrovic, M., Bader, S., Stoffel, M., Jan, L.Y., and Basbaum, A.I.** (2003). Contribution of GIRK2-mediated postsynaptic signaling to opiate and alpha 2-adrenergic analgesia and analgesic sex differences. *Proceedings of the National Academy of Sciences of the United States of America* *100*, 271-276.
- Mogil, J.S.** (2009). Animal models of pain: progress and challenges. *Nature reviews Neuroscience* *10*, 283-294.
- Moises, H.C., Rusin, K.I., and Macdonald, R.L.** (1994). mu-Opioid receptor-mediated reduction of neuronal calcium current occurs via a G(o)-type GTP-binding protein. *The Journal of neuroscience : the official journal of the Society for Neuroscience* *14*, 3842-3851.
- Mousa, S.A., Cheppudira, B.P., Shaqura, M., Fischer, O., Hofmann, J., Hellweg, R., and Schafer, M.** (2007). Nerve growth factor governs the enhanced ability of opioids to suppress inflammatory pain. *Brain : a journal of neurology* *130*, 502-513.
- Mullis, K.B., and Faloona, F.A.** (1987). Specific synthesis of DNA in vitro via a polymerase-catalyzed chain reaction. *Methods in enzymology* *155*, 335-350.
- Navarro, B., Kennedy, M.E., Velimirovic, B., Bhat, D., Peterson, A.S., and Clapham, D.E.** (1996). Nonselective and G betagamma-insensitive weaver K⁺ channels. *Science* *272*, 1950-1953.

- North, R.A., Williams, J.T., Surprenant, A., and Christie, M.J.** (1987). Mu and delta receptors belong to a family of receptors that are coupled to potassium channels. *Proceedings of the National Academy of Sciences of the United States of America* *84*, 5487-5491.
- Novakovic, S.D., Tzoumaka, E., McGivern, J.G., Haraguchi, M., Sangameswaran, L., Gogas, K.R., Eglen, R.M., and Hunter, J.C.** (1998). Distribution of the tetrodotoxin-resistant sodium channel PN3 in rat sensory neurons in normal and neuropathic conditions. *The Journal of neuroscience : the official journal of the Society for Neuroscience* *18*, 2174-2187.
- Obara, I., Parkitna, J.R., Korostynski, M., Makuch, W., Kaminska, D., Przewlocka, B., and Przewlocki, R.** (2009). Local peripheral opioid effects and expression of opioid genes in the spinal cord and dorsal root ganglia in neuropathic and inflammatory pain. *Pain* *141*, 283-291.
- Obata, K., Katsura, H., Mizushima, T., Yamanaka, H., Kobayashi, K., Dai, Y., Fukuoka, T., Tokunaga, A., Tominaga, M., and Noguchi, K.** (2005). TRPA1 induced in sensory neurons contributes to cold hyperalgesia after inflammation and nerve injury. *The Journal of clinical investigation* *115*, 2393-2401.
- Ocana, M., Cendan, C.M., Cobos, E.J., Entrena, J.M., and Baeyens, J.M.** (2004). Potassium channels and pain: present realities and future opportunities. *European journal of pharmacology* *500*, 203-219.
- Oster-Granite, M.L., McPhie, D.L., Greenan, J., and Neve, R.L.** (1996). Age-dependent neuronal and synaptic degeneration in mice transgenic for the C terminus of the amyloid precursor protein. *The Journal of neuroscience : the official journal of the Society for Neuroscience* *16*, 6732-6741.
- Padgett, C.L., and Slesinger, P.A.** (2010). GABAB receptor coupling to G-proteins and ion channels. *Adv Pharmacol* *58*, 123-147.
- Patil, N., Cox, D.R., Bhat, D., Faham, M., Myers, R.M., and Peterson, A.S.** (1995). A potassium channel mutation in weaver mice implicates membrane excitability in granule cell differentiation. *Nature genetics* *11*, 126-129.
- Peleg, S., Varon, D., Ivanina, T., Dessauer, C.W., and Dascal, N.** (2002). G(alpha)(i) controls the gating of the G protein-activated K(+) channel, GIRK. *Neuron* *33*, 87-99.
- Pepper, C.M., and Henderson, G.** (1980). Opiates and opioid peptides hyperpolarize locus coeruleus neurons in vitro. *Science* *209*, 394-395.
- Pert, C.B., and Snyder, S.H.** (1973). Opiate receptor: demonstration in nervous tissue. *Science* *179*, 1011-1014.
- Pol, O., Alameda, F., and Puig, M.M.** (2001). Inflammation enhances mu-opioid receptor transcription and expression in mice intestine. *Molecular pharmacology* *60*, 894-899.
- Ponce, A., Bueno, E., Kentros, C., Vega-Saenz de Miera, E., Chow, A., Hillman, D., Chen, S., Zhu, L., Wu, M.B., Wu, X., et al.** (1996). G-protein-gated inward rectifier K⁺ channel proteins (GIRK1) are present in the soma and dendrites as well as in nerve terminals of specific neurons in the brain. *The Journal of neuroscience : the official journal of the Society for Neuroscience* *16*, 1990-2001.
- Prochaska, J.J., Rossi, J.S., Redding, C.A., Rosen, A.B., Tsoh, J.Y., Humfleet, G.L., Eisendrath, S.J., Meisner, M.R., and Hall, S.M.** (2004). Depressed smokers and stage of change: implications for treatment interventions. *Drug and alcohol dependence* *76*, 143-151.
- Puehler, W., Zollner, C., Brack, A., Shaqura, M.A., Krause, H., Schafer, M., and Stein, C.** (2004). Rapid upregulation of mu opioid receptor mRNA in dorsal root ganglia in response to peripheral inflammation depends on neuronal conduction. *Neuroscience* *129*, 473-479.
- Raja, S.N.** (2011). Modulating Pain in the Periphery: Gene-Based Therapies to Enhance Peripheral Opioid Analgesia: Bonica Lecture, ASRA 2010. *Regional anesthesia and pain medicine*.

- Raveh, A., Cooper, A., Guy-David, L., and Reuveny, E.** (2010). Nonenzymatic rapid control of GIRK channel function by a G protein-coupled receptor kinase. *Cell* 143, 750-760.
- Rhim, H., and Miller, R.J.** (1994). Opioid receptors modulate diverse types of calcium channels in the nucleus tractus solitarius of the rat. *The Journal of neuroscience : the official journal of the Society for Neuroscience* 14, 7608-7615.
- Rice, A.S., Cimino-Brown, D., Eisenach, J.C., Kontinen, V.K., Lacroix-Fralish, M.L., Machin, I., Mogil, J.S., and Stohr, T.** (2008). Animal models and the prediction of efficacy in clinical trials of analgesic drugs: a critical appraisal and call for uniform reporting standards. *Pain* 139, 243-247.
- Riven, I., Iwanir, S., and Reuveny, E.** (2006). GIRK channel activation involves a local rearrangement of a preformed G protein channel complex. *Neuron* 51, 561-573.
- Roychowdhury, S.M., and Fields, H.L.** (1996). Endogenous opioids acting at a medullary mu-opioid receptor contribute to the behavioral antinociception produced by GABA antagonism in the midbrain periaqueductal gray. *Neuroscience* 74, 863-872.
- Sadja, R., Alagem, N., and Reuveny, E.** (2002). Graded contribution of the G β gamma binding domains to GIRK channel activation. *Proceedings of the National Academy of Sciences of the United States of America* 99, 10783-10788.
- Sambrook, J.a.R., D.** (2001). Molecular Cloning: A Laboratory Manual. Cold Spring Harbor: Laboratory Press.
- Schedl, A., Montoliu, L., Kelsey, G., and Schutz, G.** (1993). A yeast artificial chromosome covering the tyrosinase gene confers copy number-dependent expression in transgenic mice. *Nature* 362, 258-261.
- Scherrer, G., Imamachi, N., Cao, Y.Q., Contet, C., Mennicken, F., O'Donnell, D., Kieffer, B.L., and Basbaum, A.I.** (2009). Dissociation of the opioid receptor mechanisms that control mechanical and heat pain. *Cell* 137, 1148-1159.
- Schmidt, M.J., Sawyer, B.D., Perry, K.W., Fuller, R.W., Foreman, M.M., and Ghetti, B.** (1982). Dopamine deficiency in the weaver mutant mouse. *The Journal of neuroscience : the official journal of the Society for Neuroscience* 2, 376-380.
- Scholz, J., and Woolf, C.J.** (2002). Can we conquer pain? *Nature neuroscience* 5 Suppl, 1062-1067.
- Schoots, O., Wilson, J.M., Ethier, N., Bigras, E., Hebert, T.E., and Van Tol, H.H.** (1999). Co-expression of human Kir3 subunits can yield channels with different functional properties. *Cellular signalling* 11, 871-883.
- Schroeder, J.E., Fischbach, P.S., Zheng, D., and McCleskey, E.W.** (1991). Activation of mu opioid receptors inhibits transient high- and low-threshold Ca $^{2+}$ currents, but spares a sustained current. *Neuron* 6, 13-20.
- Schulte-Steinberg, H., Weninger, E., Jokisch, D., Hofstetter, B., Misera, A., Lange, V., and Stein, C.** (1995). Intraperitoneal versus interpleural morphine or bupivacaine for pain after laparoscopic cholecystectomy. *Anesthesiology* 82, 634-640.
- Scroggs, R.S., Todorovic, S.M., Anderson, E.G., and Fox, A.P.** (1994). Variation in IH, IIR, and ILEAK between acutely isolated adult rat dorsal root ganglion neurons of different size. *Journal of neurophysiology* 71, 271-279.
- Sharma, S.K., Klee, W.A., and Nirenberg, M.** (1977). Opiate-dependent modulation of adenylate cyclase. *Proceedings of the National Academy of Sciences of the United States of America* 74, 3365-3369.
- Simon, E.J., Hiller, J.M., and Edelman, I.** (1973). Stereospecific binding of the potent narcotic analgesic (3H) Etorphine to rat-brain homogenate. *Proceedings of the National Academy of Sciences of the United States of America* 70, 1947-1949.

- Soriano, P.** (1999). Generalized lacZ expression with the ROSA26 Cre reporter strain. *Nature genetics* 21, 70-71.
- Sparwasser, T., and Eberl, G.** (2007). BAC to immunology--bacterial artificial chromosome-mediated transgenesis for targeting of immune cells. *Immunology* 121, 308-313.
- Spauschus, A., Lentes, K.U., Wischmeyer, E., Dissmann, E., Karschin, C., and Karschin, A.** (1996). A G-protein-activated inwardly rectifying K⁺ channel (GIRK4) from human hippocampus associates with other GIRK channels. *The Journal of neuroscience : the official journal of the Society for Neuroscience* 16, 930-938.
- Steen, K.H., Steen, A.E., Kreysel, H.W., and Reeh, P.W.** (1996). Inflammatory mediators potentiate pain induced by experimental tissue acidosis. *Pain* 66, 163-170.
- Stein, C., Comisel, K., Haimerl, E., Yassouridis, A., Lehrberger, K., Herz, A., and Peter, K.** (1991). Analgesic effect of intraarticular morphine after arthroscopic knee surgery. *The New England journal of medicine* 325, 1123-1126.
- Stein, C., Hassan, A.H., Lehrberger, K., Giefing, J., and Yassouridis, A.** (1993). Local analgesic effect of endogenous opioid peptides. *Lancet* 342, 321-324.
- Stein, C., and Machelska, H.** (2011). Modulation of peripheral sensory neurons by the immune system: implications for pain therapy. *Pharmacological reviews* 63, 860-881.
- Stein, C., Machelska, H., and Schafer, M.** (2001). Peripheral analgesic and antiinflammatory effects of opioids. *Zeitschrift fur Rheumatologie* 60, 416-424.
- Stein, C., Millan, M.J., Shippenberg, T.S., and Herz, A.** (1988a). Peripheral effect of fentanyl upon nociception in inflamed tissue of the rat. *Neuroscience letters* 84, 225-228.
- Stein, C., Millan, M.J., Shippenberg, T.S., Peter, K., and Herz, A.** (1989). Peripheral opioid receptors mediating antinociception in inflammation. Evidence for involvement of mu, delta and kappa receptors. *The Journal of pharmacology and experimental therapeutics* 248, 1269-1275.
- Stein, C., Millan, M.J., Yassouridis, A., and Herz, A.** (1988b). Antinociceptive effects of mu- and kappa-agonists in inflammation are enhanced by a peripheral opioid receptor-specific mechanism. *European journal of pharmacology* 155, 255-264.
- Stein, C., Schafer, M., and Machelska, H.** (2003). Attacking pain at its source: new perspectives on opioids. *Nature medicine* 9, 1003-1008.
- Stein, C., and Zollner, C.** (2009). Opioids and sensory nerves. *Handbook of experimental pharmacology*, 495-518.
- Stirling, L.C., Forlani, G., Baker, M.D., Wood, J.N., Matthews, E.A., Dickenson, A.H., and Nassar, M.A.** (2005). Nociceptor-specific gene deletion using heterozygous NaV1.8-Cre recombinase mice. *Pain* 113, 27-36.
- Stucky, C.L., and Lewin, G.R.** (1999). Isolectin B(4)-positive and -negative nociceptors are functionally distinct. *The Journal of neuroscience : the official journal of the Society for Neuroscience* 19, 6497-6505.
- Svendsen, F., Rygh, L.J., Hole, K., and Tjolsen, A.** (1999). Dorsal horn NMDA receptor function is changed after peripheral inflammation. *Pain* 83, 517-523.
- Takeda, M., Tsuboi, Y., Kitagawa, J., Nakagawa, K., Iwata, K., and Matsumoto, S.** (2011). Potassium channels as a potential therapeutic target for trigeminal neuropathic and inflammatory pain. *Molecular pain* 7, 5.
- Tang, J., Chou, J., Yang, H.Y., and Costa, E.** (1983). Substance P stimulates the release of Met5-enkephalin-Arg6-Phe7 and Met5-enkephalin from rat spinal cord. *Neuropharmacology* 22, 1147-1150.

- Taylor, B.K., and Basbaum, A.I.** (1995). Neurochemical characterization of extracellular serotonin in the rostral ventromedial medulla and its modulation by noxious stimuli. *Journal of neurochemistry* 65, 578-589.
- Thompson, R.C., Mansour, A., Akil, H., and Watson, S.J.** (1993). Cloning and pharmacological characterization of a rat mu opioid receptor. *Neuron* 11, 903-913.
- Tokimasa, T., Morita, K., and North, A.** (1981). Opiates and clonidine prolong calcium-dependent after-hyperpolarizations. *Nature* 294, 162-163.
- Truong, W., Cheng, C., Xu, Q.G., Li, X.Q., and Zochodne, D.W.** (2003). Mu opioid receptors and analgesia at the site of a peripheral nerve injury. *Annals of neurology* 53, 366-375.
- Ulzheimer, J.C., Peles, E., Levinson, S.R., and Martini, R.** (2004). Altered expression of ion channel isoforms at the node of Ranvier in P0-deficient myelin mutants. *Molecular and cellular neurosciences* 25, 83-94.
- Vulchanova, L., Riedl, M.S., Shuster, S.J., Stone, L.S., Hargreaves, K.M., Buell, G., Surprenant, A., North, R.A., and Elde, R.** (1998). P2X3 is expressed by DRG neurons that terminate in inner lamina II. *The European journal of neuroscience* 10, 3470-3478.
- Wang, H.B., Zhao, B., Zhong, Y.Q., Li, K.C., Li, Z.Y., Wang, Q., Lu, Y.J., Zhang, Z.N., He, S.Q., Zheng, H.C., et al.** (2010). Coexpression of delta- and mu-opioid receptors in nociceptive sensory neurons. *Proceedings of the National Academy of Sciences of the United States of America* 107, 13117-13122.
- Waxman, S.G., Dib-Hajj, S., Cummins, T.R., and Black, J.A.** (1999). Sodium channels and pain. *Proceedings of the National Academy of Sciences of the United States of America* 96, 7635-7639.
- Welte, M., Haimerl, E., Groh, J., Briegel, J., Sunder-Plassmann, L., Herz, A., Peter, K., and Stein, C.** (1992). Effect of interpleural morphine on postoperative pain and pulmonary function after thoracotomy. *British journal of anaesthesia* 69, 637-639.
- Werz, M.A., and MacDonald, R.L.** (1983a). Opioid peptides selective for mu- and delta-opiate receptors reduce calcium-dependent action potential duration by increasing potassium conductance. *Neuroscience letters* 42, 173-178.
- Werz, M.A., and Macdonald, R.L.** (1983b). Opioid peptides with differential affinity for mu and delta receptors decrease sensory neuron calcium-dependent action potentials. *The Journal of pharmacology and experimental therapeutics* 227, 394-402.
- Whiteside, G.T., Adedoyin, A., and Leventhal, L.** (2008). Predictive validity of animal pain models? A comparison of the pharmacokinetic-pharmacodynamic relationship for pain drugs in rats and humans. *Neuropharmacology* 54, 767-775.
- Williams, J.T., Egan, T.M., and North, R.A.** (1982). Enkephalin opens potassium channels on mammalian central neurones. *Nature* 299, 74-77.
- Wilson, S.G., and Mogil, J.S.** (2001). Measuring pain in the (knockout) mouse: big challenges in a small mammal. *Behavioural brain research* 125, 65-73.
- Woolf, C.J.** (2010). Overcoming obstacles to developing new analgesics. *Nature medicine* 16, 1241-1247.
- Xu, H., Cui, N., Yang, Z., Wu, J., Giwa, L.R., Abdulkadir, L., Sharma, P., and Jiang, C.** (2001). Direct activation of cloned K(atp) channels by intracellular acidosis. *The Journal of biological chemistry* 276, 12898-12902.
- Xu, Y., Gu, Y., Xu, G.Y., Wu, P., Li, G.W., and Huang, L.Y.** (2003). Adeno-associated viral transfer of opioid receptor gene to primary sensory neurons: a strategy to increase opioid antinociception. *Proceedings of the National Academy of Sciences of the United States of America* 100, 6204-6209.

- Yamamoto, J., Kawamata, T., Niiyama, Y., Omote, K., and Namiki, A.** (2008). Down-regulation of mu opioid receptor expression within distinct subpopulations of dorsal root ganglion neurons in a murine model of bone cancer pain. *Neuroscience* *151*, 843-853.
- Yang, X.W., and Gong, S.** (2005). An overview on the generation of BAC transgenic mice for neuroscience research. *Current protocols in neuroscience / editorial board, Jacqueline N Crawley [et al]* *Chapter 5*, Unit 5 20.
- Yasuda, K., Raynor, K., Kong, H., Breder, C.D., Takeda, J., Reisine, T., and Bell, G.I.** (1993). Cloning and functional comparison of kappa and delta opioid receptors from mouse brain. *Proceedings of the National Academy of Sciences of the United States of America* *90*, 6736-6740.
- Yoshimura, M., and North, R.A.** (1983). Substantia gelatinosa neurones hyperpolarized in vitro by enkephalin. *Nature* *305*, 529-530.
- Yu, Y.Q., Zhao, F., Guan, S.M., and Chen, J.** (2011). Antisense-mediated knockdown of Na(V)1.8, but not Na(V)1.9, generates inhibitory effects on complete Freund's adjuvant-induced inflammatory pain in rat. *PloS one* *6*, e19865.
- Zhang, G., Mohammad, H., Peper, B.D., Raja, S., Wilson, S.P., and Sweitzer, S.M.** (2008). Enhanced peripheral analgesia using virally mediated gene transfer of the mu-opioid receptor in mice. *Anesthesiology* *108*, 305-313.
- Zhou, L., Nepote, V., Rowley, D.L., Levacher, B., Zvara, A., Santha, M., Mi, Q.S., Simonneau, M., and Donovan, D.M.** (2002). Murine peripherin gene sequences direct Cre recombinase expression to peripheral neurons in transgenic mice. *FEBS letters* *523*, 68-72.
- Zimmermann, K., Leffler, A., Babes, A., Cendan, C.M., Carr, R.W., Kobayashi, J., Nau, C., Wood, J.N., and Reeh, P.W.** (2007). Sensory neuron sodium channel Nav1.8 is essential for pain at low temperatures. *Nature* *447*, 855-858.
- Zimmermann, M.** (1983). Ethical guidelines for investigations of experimental pain in conscious animals. *Pain* *16*, 109-110.
- Zollner, C., Shaqura, M.A., Bopaiyah, C.P., Mousa, S., Stein, C., and Schafer, M.** (2003). Painful inflammation-induced increase in mu-opioid receptor binding and G-protein coupling in primary afferent neurons. *Molecular pharmacology* *64*, 202-210.
- Zurborg, S., Piszczek, A., Martinez, C., Hublitz, P., Al Banchaabouchi, M., Moreira, P., Perlas, E., and Heppenstall, P.A.** (2011). Generation and characterization of an Advillin-Cre driver mouse line. *Molecular pain* *7*, 66.

Appendix

The specificity of all antibodies used for immunostaining was confirmed by omission of primary antibodies and a subsequent loss of immunoreactivity if only secondary antibodies were used (Figs. 33, 34, 35 and 36). Furthermore, specificity of GIRK2 and Flag antibodies was shown by immunoreactivity detected in DRGs and sciatic nerve from $\text{Na}_v1.8$ -GIRK2 mice, whereas no immunoreactivity was apparent in tissue from wildtype animals (Figs. 23, 24 and 26).

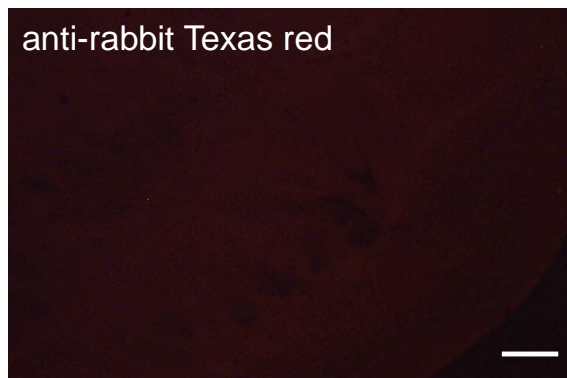


Figure 33 Test for specificity of anti-GIRK1 and anti-GIRK2 antibodies in mouse cerebellum. No immunoreactivity was detected if the secondary antibody (anti-rabbit conjugated with Texas red) was used without primary antibodies (anti-GIRK1 or anti-GIRK2). The bar represents 50 μm .



Figure 34 Test for specificity of anti-GIRK1, anti-NF200 and IB4 in rat DRGs. No immunoreactivity was observed by omission of primary antibodies and incubation with secondary antibodies (anti-rabbit conjugated with Texas red or anti-mouse conjugated with FITC) only. The bar represents 50 μm .

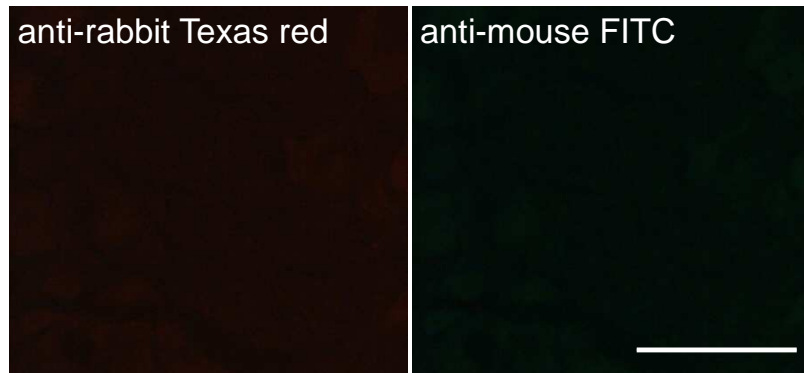


Figure 35 Test for specificity of anti-GIRK2, anti-NF200 and IB4 in rat DRGs. Omission of the primary antibodies and incubation with secondary antibodies only (anti-rabbit conjugated with Texas red or anti-mouse conjugated with FITC) resulted in a loss of immunoreactivity. The bar represents 50 μ m.

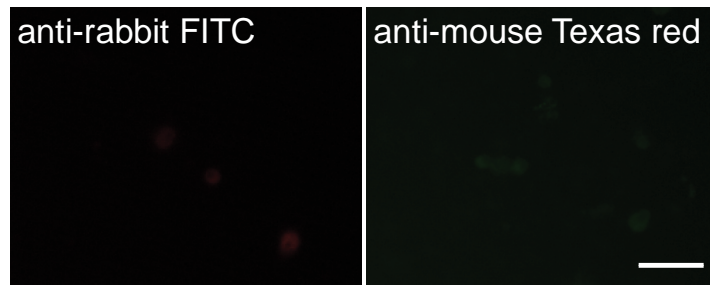


Figure 36 Test for specificity of anti-GIRK2, anti-Flag, anti-CGRP, anti-MOR and IB4 in cultured mouse DRG neurons isolated from $\text{Na}_v1.8\text{-GIRK2}$ mice. Omission of the primary antibodies and incubation with secondary antibodies only (anti-rabbit conjugated with FITC or anti-mouse conjugated with Texas red) resulted in a loss of immunoreactivity. In addition, specificity of GIRK2 and Flag antibodies was shown by immunoreactivity in DRGs and sciatic nerve from $\text{Na}_v1.8\text{-GIRK2}$ mice. No immunoreactivity was detected in tissue from wildtype animals (Figs. 23, 24 and 26). Scale bar represents 50 μ m.

Der Lebenslauf ist in der Online-Version aus Gründen des Datenschutzes nicht enthalten.

9 Publications and conferences

Publications

Nockemann D, Rouault M, Labuz D, Hublitz P, McKnelly K, Reis F.C, Stein C and Heppenstall PA. The K⁺ channel GIRQ2 is both necessary and sufficient for peripheral opioid-mediated analgesia. Accepted by *EMBO Mol Med*.

Posters

D. Nockemann, C. Stein and P.A. Heppenstall. Characterization of GIRQ channels and opioid receptor coupling in peripheral sensory neurons. 13th World Congress On Pain, 28th August - 3rd September, 2010, Montréal, Canada

D. Nockemann, C. Stein and P.A. Heppenstall. GIRQ channels are not involved in peripheral analgesia in mice. 6th Congress of European Federation of IASP Chapters (EFIC). September 9-12, 2009, Lisbon, Portugal

D. Nockemann, C. Stein and P.A. Heppenstall. Analysis of Opioid receptor/K⁺ channel coupling in sensory neurons. 38th annual meeting of the Society for Neuroscience, November 15-19, 2008 Washington D.C., USA

D. Nockemann, C. Stein and P.A. Heppenstall. Analysis of opioid receptor/K⁺ channel coupling in sensory neurons. Development and function of somatosensation and pain. 14-17 May 2008, Berlin

Presentations

“Characterization of GIRQ channels in peripheral sensory neurons of mice and rats”. 6th International Ph.D. Symposium. Berlin Brain Days, December 9-11, 2009, Berlin

10 Erklärung

Gemäß § 7 Abs. 4 der Promotionsordnung vom 04.09.2007 des Fachbereichs Biologie, Chemie, Pharmazie der Freien Universität Berlin

Hiermit versichere ich, dass ich die vorliegende Dissertationsschrift mit dem Titel “Coupling between opioid receptors and potassium channels in pain reduction: relevance for species differences and efficacy” selbstständig und ohne unerlaubte Hilfe angefertigt habe.

Dinah Nockemann

Berlin, den 01.03.2012